

MECHANISM AND USE OF PAIRED ION ELECTROSPRAY IONIZATION (PIESI) IN
HIGH-PERFORMANCE LIQUID CHROMATOGRAPHY-MASS SPECTROMETRY
(HPLC-MS) FOR SENSITIVE ANALYSIS OF ANIONIC COMPOUNDS

by

HONGYUE GUO

Presented to the Faculty of the Graduate School of
The University of Texas at Arlington in Partial Fulfillment
of the Requirements
for the Degree of

DOCTOR OF PHILOSOPHY

THE UNIVERSITY OF TEXAS AT ARLINGTON

MAY 2016

Copyright © by Hongyue Guo 2016

All Rights Reserved



This dissertation is dedicated to those whom I love and those who love me.

Acknowledgements

I would like to gratefully acknowledge all of the people who supported me throughout my graduate training. First and foremost, I owe my deepest gratitude to my mentor, Dr. Daniel W. Armstrong, for his invaluable guidance, encouragement and mentorship throughout my doctoral studies. He gave me the freedom to explore on my own and at the same time the guidance to recover when my steps faltered. He inspired me how to question thoughts and express ideas. I hope one day I can become a person of wisdom like him.

Dr. Kevin A. Schug has always been there to listen and give informed advice and constructive criticism, which greatly improved my research work. I enjoyed the collaborating project with him and his student Ines Santos, which was a great experience. I would also like to express my appreciation to Dr. Saiful Chowdhury for his advice on my research projects. I am fortunate to be educated by him in the field of Mass Spectrometry. I am truly thankful to Dr. Peter Kroll for his constant patience and support in my Ph.D. program.

I also sincerely thank Dr. Leah S. Riter, Dr. Chad E. Wujcik and Xiaohong Feng for their kind help and valuable assistance during my Co-op in Monsanto.

I would like to thank my current and previous group members: Yang Shu, Momin, Lily, Edra, Eva, Choyce, Jason, Eduardo, Yadi, Zach, J.T., Farooq, Darshan, Currran, John, Siqi, Rasangji, Jeongjae, Dr. He and Dr. Ryoo. It is an enjoyable experience to working with them in such a friendly environment. A special thank you should go to Dr. Armstrong's assistant Barbara Smith and the chemistry department staff Jill, Debbie, Brian, and Maciej.

Lastly, I owe my heart-felt and everlasting gratefulness to my family: mother, Qiong Gao; father, Hua Ruan; and brother, Hongchao for their unconditional love and

support. I owe my deepest gratitude to my beloved Lu for her understanding, innumerable love and support.

April 12th, 2016

Abstract

MECHANISM AND USE OF PAIRED ION ELECTROSPRAY IONIZATION (PIESI) IN HIGH-PERFORMANCE LIQUID CHROMATOGRAPHY-MASS SPECTROMETRY (HPLC-MS) FOR SENSITIVE ANALYSIS OF ANIONIC COMPOUNDS

Hongyue Guo, Ph.D.

The University of Texas at Arlington, 2016

Supervising Professor: Daniel W. Armstrong

In recent years, the paired ion electrospray ionization (PIESI) technique has been emerged as a promising alternative to overcome the inherent low sensitivity of negative ESI-MS. This research has focused on further understanding the mechanism of PIESI-MS and how it leads to signal enhancement and is affected by sample matrices. Additional novel applications of PIESI-MS in sensitive and selective analysis of challenging anionic compounds were considered.

Specifically, this dissertation describes research in two areas:

1) A further investigation into the mechanism of PIESI-MS by which the detection of anions is enhanced. This was done using two rational designed surface-active ion-pairing reagents. As compared to their corresponding non-surface-active ion-pairing reagents, the detection sensitivities obtained with surface-active ion-pairing reagents were further enhanced. It was found that surface activity plays a critical role in the detection sensitivity for anions with PIESI-MS.

2) Novel applications of PIESI-MS in trace analysis of anionic sugars, metabolites of abused drug and dicamba residues were demonstrated in Chapter 3, 4 and 5 respectively. Chapter 3 demonstrates that PIESI provided LODs for anionic sugars

one to two orders of magnitude lower than negative ESI-MS. Chapter 4 describes the development of a HPLC-MS/MS method based on PIESI for trace analysis of abused drugs by detecting their glucuronate and sulfate conjugates in urine. As compared to other reported negative ESI based methods, one to three orders of magnitude improvement in detection sensitivity was obtained. Chapter 5 describes the application of PIESI-MS for analysis of dicamba residues in complex raw agricultural commodities with enhanced sensitivity and selectivity. The performance of PIESI in reduction of matrix effects was demonstrated in Chapter 6. As compared to negative ion mode, PIESI-MS was less susceptible to matrix effects in groundwater and urine. Overall, the PIESI strategy should be widely used for trace analysis of other types of anionic compounds and samples.

Table of Contents

Acknowledgements	iv
Abstract	vi
List of Illustrations	xiii
List of Tables	xviii
Chapter 1 Introduction.....	1
1.1 Trace analysis of anionic compounds	1
1.2 Paired Ion Electrospray Ionization (PIESI)	2
1.3 Development of Ion-Pairing Reagents Used for PIEESI Technique	3
1.3.1 Dicationic Ion-Pairing Reagent.....	4
1.3.2 Tricationic Ion-Pairing Reagents	6
1.3.3 Tetracationic Ion-Pairing Reagents	7
1.4 Application of PIEESI in Sensitive Analysis of Anionic Compounds	7
1.5 Application of PIEESI in Sensitive Analysis of Metal Cations.....	9
1.6 Mechanism of PIEESI	9
1.7 Research Objectives and Organization of the Dissertation.....	11
Chapter 2	14
Mechanism and Sensitivity of Anion Detection Using Rationally Designed Unsymmetrical Dications in Paired Ion Electrospray Ionization (PIESI) Mass Spectrometry.....	14
2.1 Introduction	14
2.2 Experimental.....	18
2.2.1 Dicationic Ion-Pairing Reagents	18
2.2.2 PIEESI-MS Analyses	21
2.2.3 Surface Tension Measurements.	22

2.3 Results and Discussion	22
2.3.1 Unsymmetrical Dicationic Ion-Pairing Reagents	22
2.3.2 A Comparison of the LODs Obtained by Using Unsymmetrical Dications and Symmetrical Dications	23
2.3.3 Surface Tension Measurements	24
2.3.4 Partitioning Behavior of the Species in the Aerosol Droplet	35
2.3.5 LODs Determined with the Use of Unsymmetrical Dications in the SRM Mode.....	40
2.4 Conclusions	41
Chapter 3 Sensitive Detection of Anionic Sugars with Paired Ion Electrospray Ionization Mass Spectrometry.....	
3.1 Introduction.....	43
3.2 Experimental.....	46
3.2.1 Materials	46
3.2.2 Instrumental.....	50
3.2.3 LOD Measurements	50
3.2.4 Chromatographic Separation Conditions	51
3.3 Results and Discussion	52
3.3.1 Detection Limits (LOD)	52
3.3.2 Chromatographic Separation	57
3.4 Conclusions	61
Chapter 4	
Sensitive Detection of Anionic Metabolites of Drugs by Positive Ion Mode HPLC-PIESI-MS.....	
4.1 Introduction.....	62

4.2 Experimental.....	64
4.2.1 Reagents and Chemicals	64
4.2.2 Instrumental.....	69
4.2.3 Preparation of Standards	70
4.2.4 PIESI-MS Detection	70
4.2.5 Separation and Detection of Glucuro- and Sulfoconjugated Drug Metabolites by HPLC-PIESI-MS.....	71
4.2.6 Sample Preparation.....	71
4.2.7 Recovery Study	72
4.3 Results and Discussion	72
4.3.1 Ion-Pairing Reagents and Drug Metabolites	72
4.3.2 PIESI-MS Detection of Drug Metabolites with the Use of Symmetrical Ion-Pairing Reagents.....	73
4.3.3 PIESI-MS Detection of Drug Metabolites with the Use of Unsymmetrical Ion-Pairing Reagents.....	75
4.3.4 Chromatographic Separation of the Drug Metabolites.....	78
4.3.5 Urine Sample Analysis	78
4.3.5.1 Recovery Study.....	78
4.3.5.2 A Comparison in Detection Sensitivity between PIESI- MS and Other HPLC-MS Methodologies.....	83
4.4 Conclusions	83
Chapter 5	85
Quantitative Analysis of Dicamba Residues in Raw Agricultural Commodities with the Use of Ion-Pairing Reagents in LC-ESI-MS/MS.....	85
5.1 Introduction.....	85

5.2 Experimental.....	88
5.2.1 Chemicals and Solvents.....	88
5.2.2 Matrices Tested.....	89
5.2.3 Sample Preparation.....	89
5.2.4 Matrices Tested.....	91
5.2.5 Sample Preparation.....	91
5.2.6 HPLC-ESI-MS/MS.....	91
5.2.7 Method Validation Study.....	93
5.2.8 Ionization Effects Evaluation.....	94
5.2.9 Data Evaluation.....	94
5.3 Results and discussion.....	95
5.3.1 Optimization of ESI-MS/MS.....	95
5.3.2 Optimization of Chromatographic Separation Conditions.....	96
5.3.3 Method Validation.....	97
5.3.3.1 Selectivity.....	97
5.3.3.2 Linearity and Sensitivity.....	99
5.3.3.3 Accuracy and Precision.....	99
5.3.3.4 Ionization Effects Evaluation.....	101
5.4 Conclusions.....	103
Chapter 6.....	105
Reduced Matrix Effects for Anionic Compounds with Paired Ion Electrospray Ionization Mass Spectrometry.....	105
6.1 Introduction.....	105
6.2 Experimental.....	108
6.2.1 Reagents and Standards.....	108

6.2.2 Synthetic Matrix Preparation	110
6.2.3 Sample Preparation.....	111
6.2.4 PIESI-MS Analysis	112
6.2.5 LIT-MS Conditions.....	113
6.2.6 QqQ-MS Conditions	113
6.2.7 Optimization of Ion-Pairing Reagent Concentration.....	113
6.2.8 Sample Analysis and Assessment of Matrix Effect.....	115
6.3 Results and Discussion	116
6.3.1 Matrix Effects with PIESI	116
6.3.2 Groundwater Matrix Effects Using LIT-MS.....	117
6.3.3 Groundwater Matrix Effects Using QqQ-MS	121
6.3.4 Urine Matrix Effects Using LIT-MS.....	122
6.3.5 Urine Matrix Effects Using QqQ-MS	127
6.4 Conclusion.....	129
Chapter 7 General Summary	130
7.1 Part one (Chapter 2).....	130
7.2 Part Two (Chapter 3 to 6).....	131
Appendix A Publication Information and Contributing Authors.....	134
Appendix B Copyright and Permissions.....	136
References.....	144
Biographical Information	152

List of Illustrations

Figure 1-1 Instrumental setup of HPLC-PIESI-MS	3
Figure 2-1 Synthesis of 1-butyl-1-[5-(1-tetradecyl-1-pyrrolidiniumyl)pentyl]pyrrolidinium dibromide (UDC I, 3) and N1-dodecyl-N1,N1,N5,N5,N5-pentamethyl-1,5-pentanediaminium dibromide (UDC II, 4).....	20
Figure 2-2 PIEESI mass spectra of iodide by using SDC I and UDC I. Concentration of I ⁻ was 1 μM and the molar ratio of dication to I ⁻ was 20:1. [SDC I + I] ⁺ m/z: 451.3; [UDC I + I] ⁺ m/z: 591.5. The spectra were recorded separately in the single ion monitoring mode.	32
Figure 2-3 Surface tension measurements when titrating SDC I and UDC I with SCN ⁻ . Concentration of SDC I and UDC I was 0.1 M. The data points at [SCN ⁻] = 0 M represent surface tension of neat water (blank line), 0.1 M aqueous solution of SDC I (blue line) and 0.1 M aqueous solution of SDC I (blue line) and 0.1 M aqueous solution of UDC I (red line), respectively. The vertical arrows denote [SCN ⁻] of 0.02 M. It is noted that the amount of dication used for PIEESI was always in large excess to the anion.	33
Figure 2-4 Schematic showing the partitioning of an analyte anion between the surface of an aerosol droplet and the bulk interior. When the concentration of the dicationic surfactant is low ("A" above), it resides mainly at the surface of the droplet as will any associated anions. When the concentration of surface of the dicationic surfactant is high ("B" above), monolayer can be formed and all additional surfactant resides in the interior bulk solution. Thus the anionic analyte has increased partitions to the interior bulk solution.	34
Figure 2-5 ESI-MS response to the dication/SCN ⁻ complex ion (in black) and ESI-MS response to the protonated methanol ion (in red) for solutions containing UDC I and SCN ⁻ (UDC I : SCN ⁻ = 10 : 1) as the dication concentration increased from 1 × 10 ⁻⁶ to 5 × 10 ⁻⁴	

M. The intensity of the dication/ SCN^- complex ion and the protonated methanol ion were recorded by monitoring the +1 dication/ SCN^- complex ion ($[\text{UDC I} + \text{SCN}]^+$ m/z : 522.5) and the solvent ion $(\text{MeOH})_6\text{H}^+$ (m/z : 193.1) respectively in the SIM mode. Samples were directly infused at 10 $\mu\text{L}/\text{min}$ 37

Figure 2-6 ESI-MS response to the ThrH^+ ion as the concentration of threonine solution increased from 3×10^{-6} to 1×10^{-3} M. The ion intensity was recorded by monitoring the ThrH^+ ion (m/z : 120.1) in the SIM mode. 38

Figure 2-7 (A) ESI-MS response to the dications for equimolar solutions of SDC I and UDC I as the concentration increased from 2×10^{-7} to 2.5×10^{-3} M. The ion intensity was recorded by simultaneously monitoring the +2 charged dications ($[\text{SDC I}]^{2+}$ m/z : 162.2; $[\text{UDC I}]^{2+}$ m/z : 232.2) in SIM mode. (B) ESI-MS response to the dication/ SCN^- complex ion for solutions containing 10^{-4} M of SDC I and UDC I as the concentration of SCN^- added increased from 1×10^{-6} M to 2×10^{-4} M. The ion intensity was recorded by simultaneously monitoring the +1 charged dication/ SCN^- complex ion ($[\text{SDC I} + \text{SCN}]^+$ m/z : 382.3; $[\text{UDC I} + \text{SCN}]^+$ m/z : 522.5) in SIM mode. 40

Figure 3-1 Chromatographic separation of selected anionic sugars and MS detection based on PIESI. The chromatographic and MS conditions were shown in section 3.2.2 and section 3.2.4 respectively. The concentration of each injected standard was 100 ng/mL. The MS was operated in positive SIM mode with the use of the optimal ion-pairing reagent Tet 3. The m/z values detected for each analyte in PIESI mode were listed as follow: GLA/GAA (345.5); DANA (377.4); G-6-P and G-1-P (367.3) and R-5-P (357.4). 60

Figure 4-1 Total ion chromatography of separation of eleven drug metabolites by HPLC-PIESI-MS. Column: Ascentis™ C18 (2.7 μm , 2.1 x 150 mm); mobile phase A: 0.1% formic acid in water (pH=2.7), B: 0.1% formic acid in methanol; gradient elution

conditions: 0-5 min, 3% B, 5-6min, 3%-30% B, 6-22 min, 30% -80% B; MS pump flow rate: 300 μ L/min; injection volume: 5 μ L. The separation was carried out with the outperformed ion-pairing reagent, $C_5(\text{bpyr})_2$ monitored in SIM mode with three sections. 80

Figure 4-2 Extracted ion chromatography of OxaG by HPLC-PIESI-MS. Column: AscentisTM C18 (2.7 μ m, 2.1 x 150 mm); mobile phase A: 0.1% formic acid in water (pH=2.7), B: 0.1% formic acid in methanol; isocratic elution condition: 60% B; MS pump flow rate: 300 μ L/min; injection volume: 5 μ L; ion-pairing reagent: $C_5(\text{bpyr})_2$. The *m/z* of fragment of the OxaG/ $C_5(\text{bpyr})_2$ complex at 658.3 was monitored in SRM mode in section 1 (0 - 5 min). The final concentrations of OxaG in urine samples prior to injection were 40 ng/mL and 500 ng/mL respectively. 81

Figure 4-3 Extracted ion chromatography of AS and internal standard by HPLC-PIESI-MS. Column: AscentisTM C18 (2.7 μ m, 2.1 x 150 mm); mobile phase A: 0.1% formic acid in water (pH=2.7), B: 0.1% formic acid in methanol; isocratic elution condition: 60% B; MS pump flow rate: 300 μ L/min; injection volume: 5 μ L; ion-pairing reagent: $C_5(\text{bpyr})_2$. The *m/z* of fragment of the AS/ $C_5(\text{bpyr})_2$ and internal standard/ $C_5(\text{bpyr})_2$ were monitored (both were 294.3) in SRM mode in section 2 (5 - 12 min) and section 3 (12 - 22 min) respectively. The final concentrations of AS in urine samples prior to injection were 50 ng/mL and 400 ng/mL respectively. The final concentrations of internal standard were all 100 ng/mL in all these samples. 82

Figure 5-1 Instrumental setup of HPLC-ESI-MS/MS. The dotted lines represent the position where the standard solution was infused into the system in the matrix effects evaluation experiments. 88

Figure 5-2 Extracted ion chromatograms (EIC) for separation of the three analytes in a standard mixture. The standard solution was injected into the HPLC-MS/MS system

using the developed method. The injection volume of the method was 25 μ L. The chromatographic and MS/MS conditions are shown in section 5.2.4. Compound identification: 1, 5-OH dicamba; 2, DCSA; 3, dicamba. 97

Figure 5-3 Extracted ion chromatograms (EIC) of extracted corn stover blank (left three chromatograms) and soybean forage blank (right three chromatograms). The EICs of the extracted matrix blank, the extracted matrix blank fortified with 10 ppb of the analyte, and the EIC of its associated internal standard were shown in each individual graph. The top two graphs show the selectivity of dicamba in the two extracted matrix blank. The middle two graphs were for 5-OH dicamba, and the graphs for DCSA were shown in the bottom. The chromatographic and MS/MS conditions were the same as Figure 5-2, and were described in section 5.2.4. 99

Figure 5-4 Matrix effects evaluation chromatograms of extracted corn stover blank (green colored curve) and the solvent blank (0.2% formic acid in 10:90 methanol/H₂O, red colored curve). For this experiment, 10 ppb of standard solution (without internal standard) was continuously infused into the HPLC-ESI-MS/MS system at post-connector position (see instrumental in Figure 5-1, dotted lines and section 5.2.6). The chromatographic and MS/MS conditions used in this experiment were identical to those described in section 5.2.4. The chromatogram of the mixed standard solution shown here (blue color) was identical to that in Figure 5-2 and was used as reference chromatogram. 102

Figure 5-5 Matrix effects evaluation chromatograms of extracted soybean forage blank (green colored curve) and solvent blank (0.2% formic acid in 10:90 methanol/H₂O, red colored curve). For this experiment, 10 ppb of standard solution (without internal standard) was continuously infused into the HPLC-ESI-MS/MS system at post-connector position (see instrumental in section 5.2.6 and Figure 5-1, dotted lines). The

chromatographic and MS/MS conditions used in this experiment were identical to those described in section 5.2.4. The chromatogram of the mixed standard solution shown here (blue color) was identical to that in Figure 5-2 and was used as reference chromatogram. 103

Figure 6-1 Comparison of the effect of concentration of ion-pairing reagent on matrix effects as indicated by signal intensities. Perchlorate standard and perchlorate spiked in diluted artificial urine matrices (total concentrations of perchlorate in solvent (50/50, v/v, methanol and water) and in the three different diluted artificial urine matrices were all the same at 100 ng mL⁻¹) were determined in PIESI-SIM and PIES-SRM modes using the linear ion trap MS analyzer (see section 6.2.7). 115

Figure 6-2 Calibration curves of perchlorate in solvent (50/50, v/v, methanol and water) and in the 50% diluted artificial groundwater matrix determined in negative-SIM and PIESI-SRM modes using the linear ion trap MS analyzer 121

Figure 6-3 Overlaid peaks of the standard addition plots of perchlorate in the 50% diluted artificial urine. Analyses were done in both PIESI-SRM and negative-SIM modes using linear ion trap MS analyzer. Samples at the same concentration were labeled with the same color..... 125

Figure 6-4 Calibration curves of 2,4-D in solvent (50/50, v/v, methanol and water) and in the 90% diluted artificial urine determined in the negative-SRM and PIESI-SRM modes using the linear ion trap MS analyzer..... 126

Figure 6-5 Calibration curves of clofibric acid in solvent (50/50, v/v, methanol and water) and in the 99% diluted artificial urine, as determined in the PIESI-SRM and negative-SRM modes using the triple quadrupole MS analyzer..... 126

List of Tables

Table 1-1 Structures, abbreviations, and exact masses of the four best ion-pairing reagents	5
Table 2-1 Names, abbreviations and structures of dications and anions used in this study.....	19
Table 2-2 Elemental Analysis Data of UDC I and UDC II	21
Table 2-3 Comparison of limits of detection (LOD) of anions obtained with the use of unsymmetrical dications (UDC I and UDC II) and symmetrical dications (SDC I and SDC II) in the SIM mode by PIESI-MS	31
Table 2-4 Comparison of limits of detection (LOD) of anions obtained with the use of unsymmetrical dications (UDC I and UDC II) and symmetrical dications (SDC I and SDC II) in the SRM mode by PIESI-MS. The concentration of the dication used was 10 μ M.	41
Table 3-1 Names, abbreviations, structures and exact masses of the studied anionic sugars.....	47
Table 3-2 Structures of ion-pairing reagents used in this study with their abbreviations, exact masses and charges	49
Table 3-3 Limits of detection (LODs) of anionic sugars obtained in negative ion mode without using ion-pairing reagents	54
Table 3-4 Limits of detection (LODs) of anionic sugars obtained in PIESI mode with the use of ion-pairing reagents	55
Table 3-5 Comparison of detection limits of anionic sugars between PIESI and negative ion mode	56
Table 3-6 Comparison of detection limits of anionic sugars obtained in PIESI mode with other negative ESI based HPLC-MS methods reported in the literature	57

Table 4-1 Structures, abbreviations, and exact masses of the symmetrical and unsymmetrical ion-pairing reagents used in this study.	66
Table 4-2 Structures, abbreviations, and exact masses of the drug metabolites used in this study	67
Table 4-3 LODs of the drug metabolites detected in the positive ion mode using symmetrical ion-pairing reagents and in the negative ion mode without using ion-pairing reagents ^a	76
Table 4-4 LODs of the drug metabolites detected in the positive ion mode using unsymmetrical ion-pairing reagents ^a	77
Table 4-5 Recovery results of standard drug metabolites from urine spiked at two concentration levels	79
Table 4-6 Comparison of instrumental LOD (pg) of steroid glucuronides and sulfates measured by PIESI-MS method as to other HPLC-MS methodologies performed in the negative ion mode ^a	84
Table 5-1 Chemical names, structures and atomic mass units of analytes and ion-pairing reagent used in this study	90
Table 5-2 Optimized MS/MS parameters for both quantitative and confirmatory transitions of the three analytes.....	93
Table 5-3 Accuracy and precision values for all analytes.....	100
Table 6-1 Structures, abbreviations, names and exact masses of the test compounds	109
Table 6-2 Structures, abbreviations, and exact masses of the ion-pairing reagents used.....	110
Table 6-3 The ME% values and slopes of the calibration curves for the analyzed standards in solvent and in diluted artificial groundwater obtained with linear ion trap MS analyzer ^a	119

Table 6-4 The ME% values and slopes of the calibration curves for the analyzed standards in solvent and in diluted artificial groundwater obtained with triple quadrupole MS analyzer ^a	120
Table 6-5 The ME% values and calibration slopes for the analyte standards in solvent and in artificial urine with different dilution factors obtained with the linear ion trap MS analyzer ^a	124
Table 6-6 The ME% values and calibration slopes for the analyzed standards in solvent and in diluted artificial urine matrixes obtained with the triple quadrupole MS analyzer ^a	128

Chapter 1

Introduction

1.1 Trace analysis of anionic compounds

Trace-level analysis of inorganic and organic anions is essential in a variety of scientific and technical fields. Most commonly it is utilized in the analysis of samples such as environmental pollutants,¹⁻³ biological intermediates,^{4,5} drug metabolites,^{6,7} food and beverage ingredients,^{8,9} as well as surfactants.¹⁰⁻¹² Due to their anionic nature, trace analysis of these compounds sometimes can be a challenging task.¹² The polarity and high water solubility of most anionic compounds make their selective extraction (particularly at trace-level) and chromatographic resolution from potentially interfering components in complex matrices very difficult. The often low retention of many anionic compounds on conventionally used reversed-phase liquid chromatography (RPLC) stationary phases, such as C18, make their analyses complicated. The most commonly used methods for anionic compound analysis include ion chromatography,¹³⁻¹⁶ flow injection analysis,¹⁷⁻¹⁹ ion pair chromatography^{4,20,21} and capillary electrophoresis²²⁻²⁴ coupled with UV, conductivity, MS, ICP-MS (inductively coupled plasma mass spectrometry) or more recently, ion mobility spectrometry.²⁵ However, none of these techniques are completely satisfactory because they are either not universal or lack sensitivity. Indirect methods such as gas chromatography have also been used for anionic compound analysis. However, additional sample preparation steps (at low concentrations) often introduce various impurities, irreproducible yields and increased analysis times.²⁶

Currently, HPLC-MS equipped with electrospray ionization (ESI) interface has become the preferred platform for trace analysis due to advantages of improved

throughput, selectivity and sensitivity.^{4,27} The negative ion mode ESI-MS is the most common way for the detection of anionic compounds. However, the detection sensitivities provided in the negative ion mode are more moderate and sometimes inadequate for trace analysis.^{28,29} Compared to the positive ion mode, corona discharge and arcing are more prevalent in negative ion mode, which may lead to an unstable Taylor cone and consequently reduced detection sensitivity and signal instability.^{27,30,31} Other limitations of detection in negative ion mode are that small, polar anionic compounds tend to be less efficiently ionized and produce signals in a higher noise background region of the spectrometer.^{27,28,32}

1.2 Paired Ion Electrospray Ionization (PIESI)

A novel technique named paired ion electrospray ionization (PIESI), was developed by the Armstrong group for the enhancement of detection sensitivity of anionic compounds at trace levels.^{12,28,31} Briefly, it utilizes a very small amount (μM) of a multiply charged (positive) ion-pairing reagent to associate with anionic compounds by infusion of a dilute solution at a post-column position but before the ESI interface. Therein, positively charged analyte/ion-pairing reagent complex ions are formed. These complex ions are vaporized, detected and quantitated in positive ESI. With the use of optimal ion-pairing reagents, sub-picogram (pg) levels of limits of detection (LOD) were achieved for inorganic and organic anions, which were from one to four orders of magnitude more sensitive as compared to other methods reported in the literature.^{12,28,31,33-36} Several factors contribute to this high sensitivity: a) the detection is performed in the sensitive positive ion mode; b) the detection of the analyte is moved from the low mass-to-charge (m/z) region where the noise background in MS is higher, to a higher m/z region where the noise background is lower; c) the surface-activity of the analyte/ion-pairing reagent

complex is significantly higher than either the analyte or the ion-pairing reagent alone, resulting in improved ionization efficiency and further enhanced sensitivity.^{37,38}

Figure 1-1 shows the typical instrumental configuration of HPLC-PIESI-MS. A Secondary LC pump was employed to introduce the ion-pairing reagent solution (dissolved in methanol or water) into the sample stream at a post-column position. The ion-pairing reagent was then mixed with the HPLC mobile phases at the center of the Y-type mixing tee (low dead volume), and the newly formed analyte/ion-pairing reagent complex ions were then monitored in the positive scan, single ion monitoring (SIM) or selected reaction monitoring (SRM) mode.

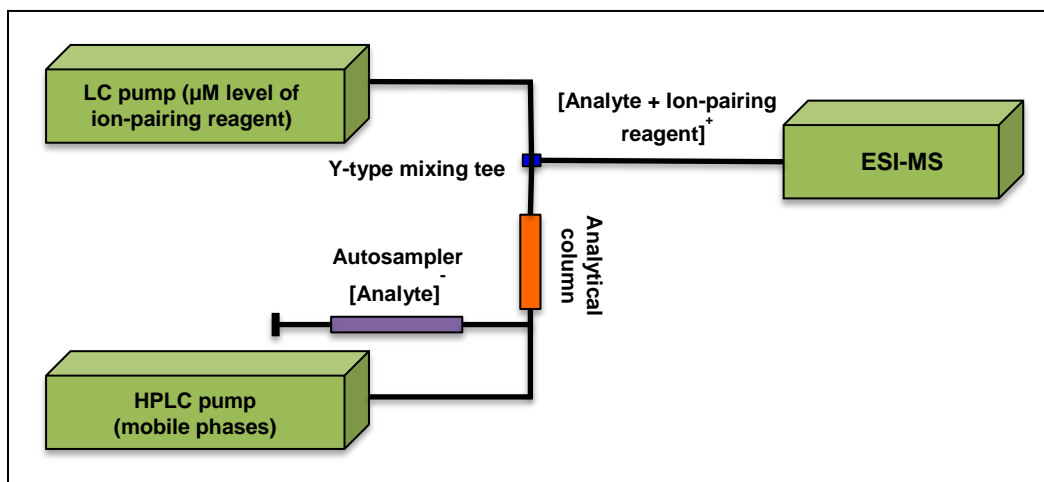


Figure 1-1 Instrumental setup of HPLC-PIESI-MS

1.3 Development of Ion-Pairing Reagents Used for PIESI Technique

Conventional ion-pairing reagents are often used as mobile phase additives in ion pair chromatography to promote the formation of ion pairs with charged analytes.³⁹ These reagents are comprised of an alkyl chain with an ionizable terminus (such as ammonium and sulfonate). When used with standard RPLC stationary phases, these ion-

pairing reagents can sometimes selectively increase the retention and separation of charged analytes. However, the high concentrations of these conventional ion-pairing reagents used in HPLC-MS (mM level) often causes severe ion suppression and ion source contamination.^{4,20,21,40} The ion-pairing reagents used in PIESI were initially synthesized for use as high-stability ionic liquids.⁴¹ These novel ion-pairing reagents often have two or more charged moieties (i.e., tetraalkylammonium, substituted imidazolium, substituted pyrrolidinium or substituted phosphonium groups) that were separated by one or several alkyl linkage chains. Another distinction from traditional ion-pairing reagents is that it is introduced into the sample stream at a post-column position with concentrations at the μM level, which can avoid MS source contamination and column deterioration. Furthermore it results in an enhanced signal rather than a suppressed signal.

1.3.1 Dicationic Ion-Pairing Reagent

The initially used ion-pairing reagents were tetraalkylammonium, methylimidazole and butylpyrrolidinium based symmetrical and dicationic ion-pairing reagents, in which the charged moieties were joined by a long alkyl chain.^{2,42} These ion-pairing reagents were synthesized in their bromide and iodide form, and were ion-exchanged to their fluoride form to maximize complexation with other anions, according to the procedure reported previously.² An early use of these ion-pairing reagents was for the improvement of detection sensitivity and selectivity of perchlorate and iodide in breast milk, urine and environmental water samples with the use of ion chromatography (IC) coupled with ESI-MS.^{2,42,43} Limits of detection as low as 25 parts per billion (ppb) were obtained for perchlorate with these ion-pairing reagents.² In 2007, Martinelango et al. further investigated the effect of factors such as the alkyl chain length, concentration and anionic form of the ion-pairing reagent, $\text{Me}_3\text{N}^+(\text{CH}_2)_n\text{-NMe}_3^+$ on detection sensitivity of perchlorate. It was found that LOD of perchlorate at 20 ppb was obtained with the

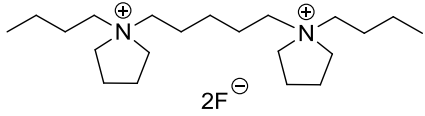
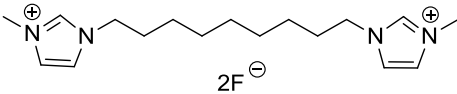
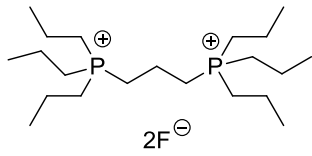
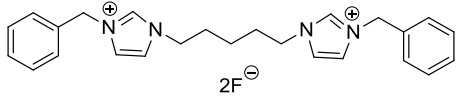
optimized conditions (the alkyl chain length n=6, concentration at 5 μ M and in the fluoride form) of the tetramethylammonium based dication.⁴⁴ In 2007, the PIESI technique was combined with a HPLC system for the sensitive analysis of 34 singly charged inorganic and organic anions. These anions were monitored in both positive SIM and SRM mode with the use of an imidazolium based dicationic ion-pairing reagent. The fragmentation pathways of the analyte/ion-pairing reagent complex ions in SRM mode were also identified in this study.²⁸

Remsburg et al. extended the dicationic ion-pairing reagents into 23 structurally different ion-pairing reagents (21 linear and 2 cyclic ion-pairing reagents).²⁹ LODs at ppb and ppt levels were able to be obtained with the use of the structurally optimized dicationic reagents. Compared to some of the rigid dicationic ion-pairing reagents, the ion-pairing reagents composed of two charged moieties that are separated by an alkyl linkage chain have relatively flexible geometries, which enable them to bend around and more tightly associate with some anions. It was also found that the detection sensitivities for the representative inorganic and organic anions (differing in mass, size-to-charge ratio, chaotropic nature, and overall complexity) were highly dependent on the structure of the ion-pairing reagent used. Overall, four ion-pairing reagents (shown in Table 1-1) were identified as most effective for the sensitive detection of inorganic and organic anions and are now commercially available in Sigma-Aldrich.

Table 1-1 Structures, abbreviations, and exact masses of the four best ion-pairing reagents

Ion-pairing reagent	Abbreviation	Structure	Exact mass of the dication
---------------------	--------------	-----------	----------------------------

Table 1-1—Continued

1, 5-pentanediy-bis-(1-butylpyrrolidinium) difluoride	C ₅ (bpyr) ₂		324.4
1, 9-Nonanediy-bis(3-methylimidazolium) difluoride	C ₉ (mim) ₂		290.3
1,3-Propanediyl-bis(triethylphosphonium) difluoride	C ₃ (triprp) ₂		362.3
1, 5-Pentanediy-bis(3-benzylimidazolium) difluoride	C ₅ (benzim) ₂		386.3

1.3.2 Tricationic Ion-Pairing Reagents

Encouraged by the success of using dicationic ion-pairing reagents in sensitive detection of singly charged anions in the positive ion mode, similar approaches of using tricationic ion-pairing reagents to detect doubly charged anions were developed in 2008.^{33,34,45} A total of thirty three linear and trigonal tricationic ion-pairing reagents were newly synthesized for the assay. These studied showed that flexible linear trications generally provided better detection sensitivities for divalent anions than rigid trigonal tricationic ion-pairing reagents.⁴⁵ However, trigonal ion-pairing reagents provided complementary performance to the linear trications in some cases. Further enhanced sensitivities by one to three orders of magnitude were achieved in SRM mode when compared to those obtained in SIM mode.^{33,45}

1.3.3 Tetracationic Ion-Pairing Reagents

In 2010, Zhang et al. successively developed eighteen novel tetracationic salts with diverse structures as ion-pairing reagents for the detection of trivalent anions in positive ion mode ESI-MS.⁴⁶ Compared to the LODs obtained in the negative ion mode, one to four orders of magnitude enhanced detection sensitivity for these trivalent anions. It was also indicated from this study that the overall geometry and structure of the cationic moieties of the ion-pairing reagents are critical factors in their effectiveness for sensitive detection of anions.⁴⁶

1.4 Application of PIESI in Sensitive Analysis of Anionic Compounds

It was found from previous studies that chaotropic anions had the lowest detection limits, with some analytes such as PFOA detected down to femtograms (fg) levels^{2,29,34,44}. PIESI was also employed for the sensitive analysis of arsenic species in a tap water sample both with and without chromatographic separation.²⁸

From 2008 to 2010, small divalent and trivalent inorganic and organic anions with diverse masses, size-to-charge ratios, chaotropic nature and different degrees of complexity were sensitively detected in positive ESI-MS with newly synthesized tricationic and tetracationic ion-pairing reagents.^{33,34,45,46} Detection limits down to pg levels were obtained with the use of the optimized ion-pairing reagents in PIESI-SIM or PIESI-SRM mode.⁴⁵ For the analysis of the challenging bisphosphonate based compounds (lack of chromophores, multiple charge states in solutions and polar), ion-pairing reagents were also pre-column introduced into mobile phases to improve both the detection sensitivity (in positive ESI-MS) and retention for these bisphosphonates on reversed-phase C18 stationary phase.³³

Analysis of biologically important compounds often is a big challenge in analytical chemistry due to their very low concentrations and complex matrices such as blood,

plasma and tissue. Many of these biological metabolites and intermediates are anionic or can be negatively charged (e.g. nucleotides and phospholipids). Due to their inherently low detection sensitivities in negative ESI-MS, PIESI can be the method of choice. In 2010, Dodbiba, et al. evaluated the feasibility of using the PIESI approach for the sensitive analysis of nucleotides, including nucleotide mono-, di-, and tri-phosphates; di- and tri-nucleotides and cyclic nucleotides.³⁵ When compared to the detection limits obtained in the negative ion mode, the results showed that up to 750 times LOD improvement were obtained with the use of optimal dicationic, tricationic and tetracationic ion-pairing reagents.^{29,33,34,45,46} In the following year, Dodbiba, et al. further applied PIESI to the sensitive analysis of zwitterionic phospholipids combined with hydrophilic interaction liquid chromatographic (HILIC) and RPLC separations.³⁶ The detection limits of the selected phospholipids were improved by one to six orders of magnitude as compared to the LOD values obtained in negative ion mode without the use of ion-pairing reagents.³⁶

Although the PIESI technique has been used since 2005,² the name “paired ion electrospray ionization (PIESI)” was firstly appeared in a 2013 publication by Armstrong and co-workers, when the technique was applied for the sensitive analysis of acidic pesticides in environmental water samples.³¹ Four now commercially available dicationic ion-pairing reagents were used for the detection (see Table 1-1). The LOD values of the nineteen selected acidic pesticides ranged from 0.6 pg to 19 pg with the use of the optimal ion-pairing reagent. Notably, the developed method was one to three orders of magnitude more sensitive than other reported HPLC-MS methods with different ionization interfaces and negative ion mode operation.³¹ Most recently, the PIESI approach was used for the trace analysis of sphingolipids and anionic surfactants.^{12,47}

1.5 Application of PIESI in Sensitive Analysis of Metal Cations

Metal cations have poor detection sensitivity in positive ion mode ESI-MS, because metal cations have small m/z values, which make them reside in high noise background region.^{2,27} These highly solvated metal cations also have relatively low ionization efficiency in ESI-MS.^{28,48} The most common ESI-MS approach for sensitive detection of metal cations involves the use of chelating agents with the metal ions and detecting the organometallic complex in negative ion mode. However, the negative ion mode is generally less sensitive than the positive ion mode. Dodbiba and Xu, et al. reported a novel strategy for the ultra-sensitive detection of metal cations in the positive ion mode based on PIESI.^{48,49} Briefly, the ion-pairing reagent was introduced to associate further with the chelated metal cations, and subsequently positively charged ternary complex ions were formed and were ultimately detected via positive ESI-MS.^{48,49} With the use of optimal ion-pairing reagents and chelating agents, the detection sensitivity were from one to three orders of magnitude better than negative ion mode (with LODs down to sub-pg levels). The nature of ion-pairing reagents and chelating agents both affected the detection sensitivities of the selected metal cations. Therefore, it was recommended to optimize ion-pairing reagents and chelating agents for certain metal cations prior to sample analysis. Also, the optimum sample solution pH was found to be between 5 to 7.^{48,49}

1.6 Mechanism of PIESI

In ESI-MS, the ionization of analyte from solution phase to gas phase often involves the following process. First of all, charge separation is produced at the surface of the sample liquid with the high applied capillary voltage (2-5 kV), and subsequently a "Taylor Cone" is formed.⁵⁰ When the solution that comprises the Taylor Cone reaches the point at which coulombic repulsion of the surface charge is equal to the surface tension of

the solution (known as the Rayleigh limit⁵¹), droplets that contain an excess charge was dispersed from its tip. For small molecules, the generation of the charged analyte ions from droplets is described in the ion evaporation model (IEM). In IEM, ions are directly ejected from the droplet surface resulting from the solvent evaporation, which causes coulombic repulsion to overcome the liquid's surface tension.⁵² The charge residue model (CRM) is suitable for the explanation of the mechanism of large molecules' ionization from the liquid phase to gas phase ions. This model assumes that large droplets are divided into smaller and smaller droplets due to solvent evaporation and thus increased charge density. Eventually, the charge of the vanishing droplet is transferred to the analyte.⁵³ The final step is that analyte ions in the gas phase are selectively transferred from atmospheric pressure to the mass analyzer.

ESI responses can vary significantly among different analytes that have identical concentrations.²⁷ A classic example is that the ESI response of decyltrimethylammonium (DTMA) was more than ten times higher than cesium (Cs^+) using the equimolar mixture solution (both in their bromide form).⁵⁴ This difference arises from the higher surface-activity of DTMA ions.²⁷ Several other studies also found that analytes with high surface-activity had higher ESI response.⁵⁴⁻⁶⁰ Cech et al. proposed the equilibrium-partitioning model (EPM) to rationalize the effect of surface-activity on ESI response.⁶¹⁻⁶³ The EPM was developed based on competition among the ions in the solution for the limited number of excess charge sites on the surface of the ESI droplet.⁶³ Briefly, the interior of the droplets was assumed electrically neutral, and consisted of cations and anions that balance each other in charge. The neutralized analytes or ion-paired analytes would not be observed mass spectrometrically because they would evaporate to form neutral salts. Only analytes that could become part of this excess charge phase on the surface of the ESI droplet would be responsive to ESI. Therefore, the more surface-active an analyte,

the higher its capability to transfer to the surface of the ESI droplet, resulting in out-competing other ions for the limited excess charge sites on the ESI droplet surface.^{27,63} Tang et al. provided an experimental verification of the EPM by photographing the colored surfactant deposition on a grounded metal plate after electrospray.⁶⁰

Recently, the mechanism for the significantly enhanced sensitivity for anions obtained by PIESI was investigated by our group.³⁷ Since the system involves a process of anion/ion-pairing reagent complexation and the partitioning of ions in the aerosol droplets, both the binding constant of anion/ion-pairing reagent and the surface activity of the complex were considered. Experimental results showed that the binding constant obtained in the gas phase was approximately two orders of magnitude greater than the solution phase. The surface activity of anion/ion-pairing reagent complex was substantially increased over that of either the anion or the ion-pairing reagent alone. According to EPM, the enhanced surface activity is the driven force for the ultra-high sensitivities of PIESI. As the complexes form and the droplet shrink, the anion/ion-pairing reagent has a large affinity for the droplet surface which enhances ionization efficiency. When the binding equilibrium in the center of the droplet is disrupted by the continuous partitioning of the complex to the surface, more complex is formed in the center of the droplet to maintain the equilibrium constant. The surface-active nature of the anion/ion-pairing reagent complex ions helps the analyte outcompete other ions for the limited space of the droplet surface, and thus the ionization efficiency of the analyte is enhanced.^{37,64}

1.7 Research Objectives and Organization of the Dissertation

The dissertation is focused on the mechanism and the novel application of PIESI in HPLC-MS for sensitive analysis of biologically clinically, and environmentally challenging anionic species. The first portion of the dissertation (Chapter 2) concentrates

on the development of unsymmetrical ion-pairing reagents for ultra-sensitive detection of anions and further discussion of the mechanism of PIESI. Since the surface-activity was a critical factor affecting the ionization efficiency of anions as well as the effectiveness of PIESI based on the previous mechanism study,³⁷ it was logical to design more surface-active ion-pairing reagents to further enhance the detection sensitivities of anions. Thus, a long alkyl chain was introduced into the structure of symmetrical ion-pairing reagents. The effectiveness of these newly synthesized unsymmetrical ion-pairing reagents in detection sensitivity was evaluated and compared to two closely related symmetrical ion-pairing reagents. The mechanism of PIESI was further discussed in this chapter.

The second portion of the dissertation (Chapters 3 to 6) focuses on the development of HPLC-MS methodologies based on PIESI for the sensitive analysis of biologically, clinically and environmentally challenging anionic compounds. Chapter 3 describes the application of PIESI in sensitive detection of anionic sugars. Compared to conventionally used negative ESI, one to two orders of magnitude lower LODs were obtained with the utilization of the PIESI approach. A HPLC-PIESI-MS method was developed for the separation of the selected anionic sugars particularly the isomeric sugar phosphates. Chapter 4 describes the development of HPLC-PIESI-MS method for ultra-sensitive analysis of abused drugs including performance-enhancing drugs in urine by detecting their glucuronide and sulfate conjugates. It was found that detection limits down to sub-pg levels were obtained with the use of the optimal ion-pairing reagents. As compared to other reported methods, the detection sensitivities for steroid metabolites were up to three orders of magnitude better. Chapter 5 describes the application of PIESI in sensitive and selective determination of dicamba residues in raw agricultural commodities (RACs). The developed HPLC-MS method based on PIESI provided enhanced detection sensitivity and selectivity for dicamba residue analysis with excellent

quantitative linearity, accuracy and precision. Further investigation of ionization effects indicated that minimal matrix effects were present in RACs with the use of the developed HPLC-PIESI-MS/MS method.

When comparing PIESI and conventional approaches for analysis of actual biological and/or environmental samples, PIESI often appeared to be less subject to matrix effects. No studies have examined whether or not the PIESI approach mitigates matrix effects. Consequently, a controlled study was done using easily reproduced synthetic groundwater and urine matrices to evaluate the effectiveness of PIESI in reduction of matrix effects (Chapter 6). As compared to the negative ion mode, PIESI provided less ionization suppression in both matrices when examined on two MS platforms, a Thermo LXQ linear ion trap and a Shimadzu triple quadrupole MS. Using PIESI-MS, less dilution of the sample is needed to eliminate ionization suppression which, in turn, permits lower limits of detection and quantitation. Finally, a general summary is presented in Chapter 7.

Chapter 2

Mechanism and Sensitivity of Anion Detection Using Rationally Designed Unsymmetrical Dications in Paired Ion Electrospray Ionization (PIESI) Mass Spectrometry

Abstract

Paired ion electrospray ionization (PIESI) mass spectrometry was developed as a useful technique that provides sensitive detection for anions in the positive ion mode. The ion-pairing reagent utilized plays an essential role affecting the detection limits. This work describes the design and synthesis of two novel dications with unsymmetrical structures and their utilization for anion detection and mechanistic insights. The performance of dications was evaluated for seven selected anions in both single ion monitoring (SIM) mode and selected reaction monitoring (SRM) mode. The unsymmetrical dications allowed sensitive detection for these anions with down to sub-picogram limits of detection (LOD), and an improved sensitivity from 1.5 to 12 times as compared to the corresponding symmetrical dications. The enhanced sensitivity could be attributed to the surface activity of the unsymmetrical dications, which results in a concurrent strong partitioning of the anion to the aerosol droplet surface. Surface activity measurements of the anion/ion-pairing reagent complex were conducted and a correlation between the observed ESI responses and the surface activity of the complex was found. The mechanism was further explored and explained based on the concepts of the equilibrium partitioning model (EPM).

2.1 Introduction

The use of electrospray ionization (ESI), introduced by Fenn et al.,⁶⁵⁻⁶⁸ with mass spectrometry (MS) has grown tremendously in the last few decades. The power and broad applicability of ESI-MS has been demonstrated in the analysis of different classes

of molecules, ranging from extremely large molecules, such as proteins,⁶⁸⁻⁷⁰ polymers,^{71,72} and oligonucleotides,⁷³ to small molecules, such as lipids,^{74,75} and amino acids.^{76,77} The majority of ESI-MS analyses are conducted in the positive ion mode, where the analyte cation produced from protonation/adduct formation is measured, whereas the detection of analyte anions is less preferable.⁷⁸ Anion detection by ESI-MS, which is not as extensively explored as the detection of cations, was primarily hampered by the low sensitivity and signal instability in the negative ion mode, resulting from the increased tendency toward electrical (corona) discharge and the inherent chemical noise.^{30,79,80}

Previously, we investigated the possibility of sensitive detection of anions in the positive ion mode by ESI-MS,^{2,28,29,31,36,45,48,49} and introduced an innovative approach named paired ion electrospray ionization (PIESI) mass spectrometry. This technique involves adding very low concentrations of multiple charged ion-pairing reagents into the sample stream, thereby allowing the anionic molecules to be measured with extremely high sensitivity in the positive ion mode as the anion/ion-pairing reagent associated complexes. With the use of optimal ion-pairing reagents, limits of detection (LOD) have been pushed down to sub-picogram for small organic anions,^{29,31} and to low picogram for inorganic anions.^{28,45} This technique was recently reviewed by Breitbach et al.⁸¹ The advantages of PIESI were particularly notable when detecting inorganic ions (such as the halides), since they were previously hardly detectable in negative ion mode ESI-MS. Compared to the more common analytical anion detection techniques, such as ion selective electrodes, ion chromatography with conductivity detection, or atomic spectroscopy,⁸²⁻⁸⁶ PIESI-MS has shown superior performance in terms of both specificity and sensitivity. PIESI-MS also has been shown to be highly advantageous for the analysis of moderately size lipophilic molecules such as anionic and zwitterionic

phospholipids.³⁶ The reported LODs were from 3 to 6 orders of magnitude better than those of other known methods. It is important to note that this approach is already being successfully employed in a number of actual applications involving naturally occurring samples and matrices.^{2,28,31,87}

While these results have been impressive and of potential value, the use of polycationic ion-pairing agents is highly structurally dependant. For example, diquat difluoride (dication XXII in ref.29) performed more than 500 times worse than structurally optimized dications used to detect singly charged anions.²⁹ Some common features of these “unsuccessful” ion-pairing reagents usually include a relatively rigid structure and/or not containing any flexible linkage chain between the cationic moieties.^{29,37} This dichotomy of highly sensitive and insensitive detection by using structurally different dications indicates the need for a more comprehensive understanding of the characteristics of the ion-pairing reagents, as well as the formation and ionization mechanism of the ion-pairing reagent/anion complex, which could affect the observed sensitivity of this methodology.

Surface activity has been considered one of the important properties that affect all aerosol-based analytical methodologies including ESI-MS. Early on the role of surfactants and surface tension were noted for aerosol-based analytical techniques of atomic absorption and flame emission spectroscopy.⁸⁸ Subsequently similar effects were observed for ESI-MS.^{54,57,60-63,89-92} Tang and Kebarle observed that tetraalkylammonium ions, which are known to be surface active, give much higher ESI ion signals than alkali metal cations.⁵⁷ While the higher sensitivity of tetraalkylammonium ions can be attributed to their lower solvation energy (less solvated) and a consequent higher ion evaporation rate compared to alkali metal cations, they also suggested that the surface activity of the analytes may play an important role. The surface-active analyte ions, which are expected

to be enriched on aerosol droplet surfaces, should leave the droplets and become gas-phase ions more readily and thus have a higher ESI response, according to the ion evaporation model (IEM) proposed by Iribarne and Thomson.^{52,58,93} Subsequently the mechanistic interpretation was also extended to capillary electrophoresis (CE) with ESI-MS detection. Rundlett and Armstrong addressed a modified aerosol ionic redistribution (AIR) mode and qualitatively explained the analyte signal quenching when using modest concentrations of anionic surfactants in CE-ESI-MS.⁸⁹ Enke's equilibrium partitioning model (EPM) provided insight regarding the effect of analyte/solvent characteristics on the ESI response.⁶¹⁻⁶³ They proposed that the ionic species in the ESI droplet partition between two phases: an interior phase which is solvated and electrically neutral and a surface phase which carries the excess charge determining the observed ion response. The higher response of the surface active ion species can be therefore quantitatively explained by their higher equilibrium partition coefficients (K), which allow them to favorably complete the excess charge sites on the droplet surface as was previously outlined by Rundlett and Armstrong.⁸⁹ Tang and Smith photographed the colored surfactant deposition on a grounded metal plate after electrospray, and observed both the satellite and the progeny droplets generated during the ESI fissioning process are significantly surfactant-enriched.⁶⁰ This provided an experimental verification of the assumption that surface-active species preferentially reside on the droplet surface during the electrospray process. Brodbelt et al. extended the equilibrium partitioning model to host-guest complexation systems, and accurately modeled the ESI response to the host-guest complexation interactions.^{91,92} Recently, we investigated the mechanism for the greatly enhanced sensitivity obtained for anions by PIESI with consideration of both the binding behavior between anion and ion-pairing reagent and the surface activity of the anion/ion-pairing reagent complex.³⁷ Since the system involves the process of anion/ion-

pairing reagent complexation and the partitioning of ions in the aerosol droplets, both the binding constant of anion/ion-pairing reagent and the surface activity of the complex were considered. It was found that an appropriate binding constant in both the solution phase and gas phase was necessary but not sufficient for high detection sensitivity. Interestingly, the surface activity of anion/ion-pairing reagent complex, which was greatly increased compared to either the anion or ion-pairing reagent alone, seems to be the most crucial factor leading to improved sensitivity.³⁷

Based on the aforementioned proposed mechanism and model,³⁷ we attempted, for the first time, to rationally design two novel dicationic species with unsymmetrical structures, with the purpose of further improving the sensitivity for anion detection in the positive ion mode by PIESI-MS. The performances of the unsymmetrical dicationic species were evaluated in terms of limits of detection, which were determined for seven selected anions in both single ion monitoring (SIM) mode and selected reaction monitoring (SRM) mode. A comparison of structurally related symmetrical and unsymmetrical dicationic species was made. The surface activity of the anion/ion-pairing reagent complex and its correlation to the observed ESI responses were evaluated, which provides support for the proposed mechanism.³⁷ The results from this work may also provide a basis for the design of future PIESI reagents.

2.2 Experimental

2.2.1 Dicationic Ion-Pairing Reagents

Names, abbreviations and structures of the dicationic species are listed in Table 2-1. 1-butyl-1-[5-(1-butyl-1-pyrrolidiniumyl)pentyl]pyrrolidinium difluoride (SDC I) and N¹,N¹,N¹,N⁵,N⁵,N⁵-hexamethyl-1,5-pentanediaminium diiodide (SDC II) were commercially available from Sigma-Aldrich (St. Louis, MO). Materials, synthetic procedures and elemental analysis for 1-butyl-1-[5-(1-tetradecyl-1-

pyrrolidiniumyl)pentyl]pyrrolidinium dibromide (UDC I) and N¹-dodecyl-N¹,N¹,N⁵,N⁵,N⁵-pentamethyl-1,5-pentanediaminium dibromide (UDC II) are described in Figure 2-1 and Table 2-2 respectively. To maximize the production of dication/anion complex in the solution phase, the bromide and iodide dications were converted to fluoride form by using the anion-exchange resin. The procedure for anion-exchange was described previously² and was provided as following. An 1.5 cm x 5cm (diameter x length) anion exchange column was packed with Amberlite® IRA-400 chloride anion exchange resin (Sigma-Aldrich , St. Louis, MO). The column was first wet with deionized (DI) water, and was then rinsed with 10 times column volume of 1M NaOH converting the resin from chloride form to hydroxide form. The resin column was then washed with 10 times column volume of DI water. Then, 10 times column volume of 0.5 M NaF was added to the column so that the OH⁻ ion on the resin was exchanged to F⁻ ion. The column was again equilibrated with 10 times column volume of DI water. The dication bromide salt, which was completely dried in vacuum oven, was carefully weighed and made to 0.1 M solution in water. The above 1 mL of dication bromide salt solution was added dropwise to the resin bed, and the dication was then eluted with MS water into a 10 mL volumetric flask. The final solution will be 10 mM solution of ion-pairing reagent in F⁻ form. Anionic analytes were purchased as the sodium/potassium salt or as the free acid from Sigma-Aldrich (St. Louis, MO, USA). These structures are shown in Table 2-1.

Table 2-1 Names, abbreviations and structures of dications and anions used in this study

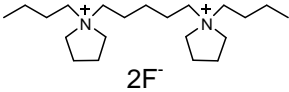
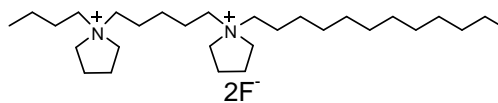
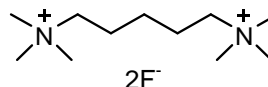
Dication Name (Abbreviation)	Structure
symmetrical dication I (SDC I)	

Table 2-1—Continued

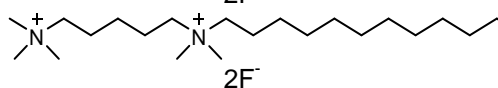
unsymmetrical dication I (UDC I)
(Surfactant)



symmetrical dication II (SDC II)



unsymmetrical dication II (UDC II)
(Surfactant)



Analyte Anion Name (Abbreviation)	Structure
benzenesulfonate (BZSN ⁻)	
iodide (I ⁻)	I ⁻
benzoate (BZO ⁻)	
arsenate monobasic (ASN ⁻)	H ₂ AsO ₄ ⁻
monochloroacetate (MCA ⁻)	
thiocyanate (SCN ⁻)	⁻ S-C≡N
etidronate (HEDP ⁻)	

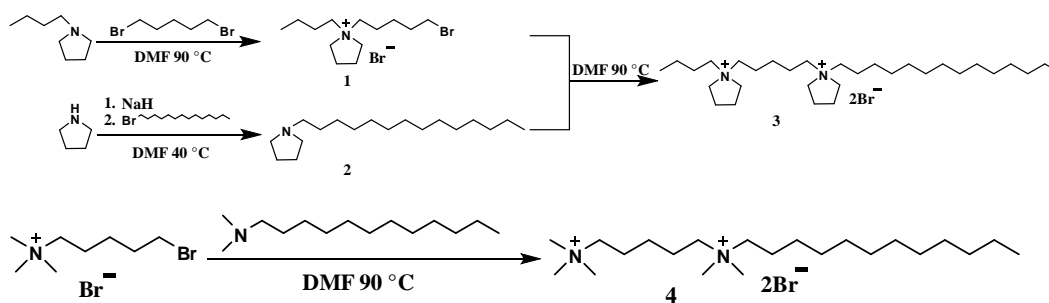


Figure 2-1 Synthesis of 1-butyl-1-[5-(1-tetradecyl-1-pyrrolidinium)pentyl]pyrrolidinium dibromide (UDC I, 3) and N1-dodecyl-N1,N1,N5,N5,N5-pentamethyl-1,5-pentanediaminium dibromide (UDC II, 4)

Table 2-2 Elemental Analysis Data of UDC I and UDC II

Dication	Empirical formula	Calculated (%)				Found (%)			
		C	H	N	Br	C	H	N	Br
UDC I	C ₃₁ H ₆₄ Br ₂ N ₂	59.61	10.33	4.48	25.58	57.15	10.1	4.38	24.89
UDC II	C ₂₂ H ₅₀ Br ₂ N ₂	52.59	10.03	5.58	31.81	52.54	10.47	5.46	28.33

2.2.2 PIESI-MS Analyses

Studies were performed using a Finnigan LXQ (Thermo Fisher Scientific, San Jose, CA) mass spectrometer in the positive ion mode with Xcalibur 2.0 as data analysis software. They were carried out at a spray voltage of 3 kV and a capillary voltage of 11 V. The temperature of the ion transfer capillary was held at 350 °C. Normalized collision energy in the selected reaction monitoring (SRM) mode was set at 30, the activation time was set at 30 ms, and the Q value was set at 0.25. PIESI-MS analysis was performed by using the above ESI-MS system and with an additional HPLC pump which was used for post-column reagent addition of the cationic ion-pairing reagent. A schematic and description of the instrumental configuration of PIESI-MS has been given in Figure 1-1 and in detail in our previous publications.^{31,49} Except as otherwise noted, a Surveyor MS pump (Thermo Fisher Scientific, San Jose, CA) provided a 300 µL/min (33% H₂O/67% MeOH, by volume) carrier stream into the mass spectrometer, which was merged with a flow of 40 µM aqueous dicationic ion-pairing reagent solution delivered by a Shimadzu LC-6A pump (Shimadzu, Columbia, MD) at rate of 100 µL/min. The sample was injected into the carrier stream through a six-port injection valve prior to the mixing tee. This setting results in an overall solvent composition of 50% H₂O/50% MeOH containing 10 µM of dicationic ion-pairing reagent flowing into the mass spectrometer (400 µL/min). Detection limits were taken to be a signal-to-noise ratio of 3 using a Genesis Peak

Detection Algorithm with 5 replicate injections. Monoisotopic masses were used to monitor the dication/ion-pairing reagent complex ions in both SIM and SRM mode, which will result in the isotope of highest abundance being selected.

2.2.3 Surface Tension Measurements.

The surface tensions were measured with a Fisher Model 20 tensiometer (Fisher Scientific, Fair Lawn, NJ) by the duNouy ring technique. The platinum ring used has a ring/wire radius ratio of 53.21 and a mean circumference of 5.940 cm. Measurements were taken at 23 ± 0.1 °C. The surface tension measurement for the dication/ion-pairing reagent solution were performed through a titration experiment where the sodium thiocyanate was successively added into the bulk solution of SDC I and UDC I resulting in 0.1 M dication solutions containing a concentration of thiocyanate anion from 0.02 to 0.2 M being measured. Deionized water was titrated with thiocyanate anion as a blank. Each data point represents the average value of triplicate measurements.

2.3 Results and Discussion

2.3.1 Unsymmetrical Dicationic Ion-pairing Reagents

Previous empirical observations have suggested that the performance of symmetrical dications could be greatly influenced both by the length of the alkyl linkage chain and the nature of the cationic moieties. In this study, identical, five carbon (methylene groups) linkage chains were used for all of the dicationic agents (Table 2-1). This spacing between cationic moieties avoided the formation of bolaform surfactants, which may spontaneously fold in solution and therefore result in an unpredictable surface activity.^{94,95} SDC I and SDC II have pyrrolidinium or ammonium charged moieties respectively (Table 2-1). The structures of the unsymmetrical dications were specifically designed to be surface active versions of the corresponding symmetrical dications, and thus a definitive comparison between the two types of dications can be made. The

increased surface activity was achieved by attaching a long alkyl chain on one end of the symmetrical dication. The positively charged polar portion of these pairing agents was necessary to enable the association with the anion analytes of interest, while the hydrophobic portion was included to increase the fraction of the complex that preferably resides at the gas-solvent interface of the aerosol.

2.3.2 A Comparison of the LODs Obtained by Using Unsymmetrical Dications and Symmetrical Dications

The analytes selected represent a cross section of anion types that include both inorganic and small organic anions. The detection limits for the seven selected anions with the use of unsymmetrical dications and symmetrical dications in the single ion monitoring mode are given in Table 2-2. The results indicate that the LOD improved for six out of seven anions, using 1 μM UDC I (1.5 to 5 times) compared to using same concentration of SDC I. The LODs for six out of seven anions (using UDC II) improved 1.6 to 7.5 times. Note that the symmetrical dications are already known to improve the sensitivity of anion detection in the positive ion mode mass spectrometry (compared to the negative ion mode) often by orders of magnitude. However, the symmetrical dications are not surface active until paired with an appropriate anion.³⁷ These observations (Table 2-2) tend to support the concept of the equilibrium partitioning model. Since the unsymmetrical dications are known to have greater surface activity than symmetrical cations, the anion/ion-pairing reagent complex formed from unsymmetrical dications should also be more surface active, and thus the anion would partition to the droplet surface more efficiently resulting in a higher signal response. To investigate the effect of dication concentration on detection limit of anions, the LODs of seven anions were evaluated at a higher concentration level of dication (Table 2-3). It is shown that the LOD for five out of seven anions, using 10 μM UDC I, were 2.5 to 7.3 times better than using

same concentration of SDC I. The LODs of four out of seven anions, using UDC II, were 2.5 to 12 times improved compared to SDC II. Further increases in the concentration of the unsymmetrical pairing agent resulted in significant decreases in the LODs. For example, the LODs of BZSN^- , I^- , and SCN^- obtained when using 200 μM UDC I were found to be 320 pg, 60 pg, and 35 pg respectively, which were 27 times, 40 times, and 44 times worse compared to those obtained by using 1 μM UDC I respectively (Table 2-3). This observation also is in accordance with what would be expected with the equilibrium partitioning model, as will be explained in subsequent paragraphs.

In this study, it is clear that having the concentration of pairing reagents between 1 μM to 10 μM is an appropriate range for enhanced detection without causing significant suppression the analyte ion signal. Figure 2-2 shows the PIESI mass spectra of iodide by using SDC I and UDC I, where the ion signal observed for iodide by using the UDC I was approximately 3.6 times higher as compared to using SDC I indicating the improved performance of the unsymmetrical dications.

2.3.3 Surface Tension Measurements

To further investigate the surface activity of the anion/ion-pairing reagent complex and to better explain the aforementioned results, surface tension measurements of the anion/ion-pairing reagent complex were performed (Figure 2-3). It was observed that the surface tension of neat water dropped only slightly (by a $\Delta\gamma$ less than 1.5 dynes/cm (where $\Delta\gamma$ is the change in the surface tension)) upon addition of SCN^- , while the surface tension of the symmetrical dication solution dramatically decreased as SCN^- was added. This behavior was noted previously and formed the basis of the proposed mechanism of PIESI-MS signal enhancement.³⁷ As shown in Figure 2-2, at 0.02 M of SCN^- added (the molar ratio of the anion and ion-pairing reagent was 1:5), the surface tension for neat water was 73.1 dynes/cm while the surface tension for the

Table 2-3 Comparison of limits of detection (LOD) of anions obtained with the use of unsymmetrical dications (UDC I and UDC II) and symmetrical dications (SDC I and SDC II) in the SIM mode by PIESI-MS

Anion	1 μM of Dication ^a						10 μM of Dication ^a									
	UDC I		SDC I		UDC II		SDC II		UDC I		SDC I		UDC II		SDC II	
	LOD ^b (pg)	LOD ^b (pg)	Improvement ^c		LOD ^b (pg)	LOD ^b (pg)	Improvement ^c		LOD ^b (pg)	LOD ^b (pg)	Improvement ^c		LOD ^b (pg)	LOD ^b (pg)	Improvement ^c	
BZSN ⁻	12	24	2.0	+	12	30	2.5	+	8.0	20	2.5	+	6.0	28	4.7	+
I ⁻	1.5	6.5	4.3	+	4.0	5.0	1.3	○	15	110	7.3	+	50	45	0.9	○
BZO ⁻	40	200	5.0	+	60	450	7.5	+	30	18	0.6	○	33	84	2.5	+
ASN ⁻	2400	4000	1.7	+	4000	21000	5.3	+	480	1800	3.8	+	100	1200	12	+
MCA ⁻	16	24	1.5	+	9.0	40	4.4	+	7.2	20	2.8	+	9.0	12	1.3	○
SCN ⁻	0.80	1.6	2.0	+	5.0	8.0	1.6	+	4.0	12	3.0	+	200	160	0.8	○
HEDP ⁻	8000	4000	0.5	-	17000	35000	2.1	+	4000	4800	1.2	○	1600	13000	8.1	+

^aThe concentration refers to the final dication concentration that flowed in into the MS.

^bLOD was defined as the lowest analyte amount in picograms (pg) yielding a S/N = 3.

^cFactor of improvement of LOD of unsymmetrical dication vs. LOD of symmetrical dication. "+": better; "-": worse; "○": similar.

symmetrical dication was 56.4 dynes/cm. This indicates that the presence of the symmetrical dication leads to a 16.7 dynes/cm surface tension decrease ($\Delta\gamma_1$) for the anion solutions. The increased surface activity achieved through complexation allows for an enhanced partitioning of the anion/dication complex to the aerosol droplet surface, which results in improved detection sensitivity. The surface tension of purely aqueous unsymmetrical solution of the dication (Figure 2-2 at $[\text{SCN}^-] = 0 \text{ M}$) was observed to be lower than that of the symmetrical dication (by 17.7 dynes/cm between SDC I and UDC I) as expected.

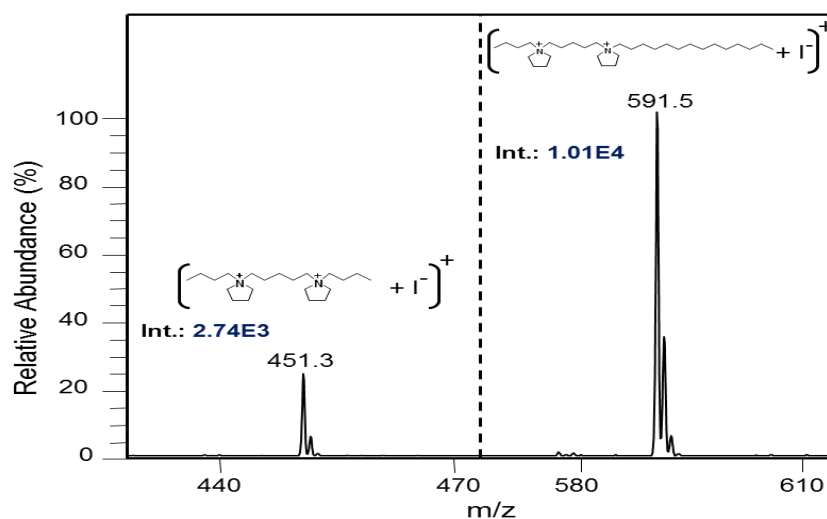


Figure 2-2 PIEESI mass spectra of iodide by using SDC I and UDC I. Concentration of I^- was $1 \mu\text{M}$ and the molar ratio of dication to I^- was 20:1. $[\text{SDC I} + \text{I}^+]^+$ m/z: 451.3; $[\text{UDC I} + \text{I}^+]^+$ m/z: 591.5. The spectra were recorded separately in the single ion monitoring mode.

It is interesting that the addition of SCN^- did not cause a rapid decrease in the surface tension for the unsymmetrical dication as it did for the symmetrical dication (Figure 2-3). The surface tension of the unsymmetrical dication solution decreased by 5.4

dynes/cm over the entire titration range with SCN^- . Nonetheless, it is shown that the unsymmetrical dication still has a greater effect on lowering the surface tension of a solution containing the anionic analyte (SCN^-). The surface tension of the solution containing both the unsymmetrical cation and 0.02 M SCN^- was 25.3 dynes/cm lower than neat water and was 8.6 dynes/cm ($\Delta\gamma_2$) lower compared to the analogous symmetrical dication solution (Figure 2-3). Consequently, it is expected that the presence of the unsymmetrical dication would lead to an increased concentration of the anion/dication complex at the aerosol droplet surface (Figure 2-4A). This would lead to better detection sensitivity.

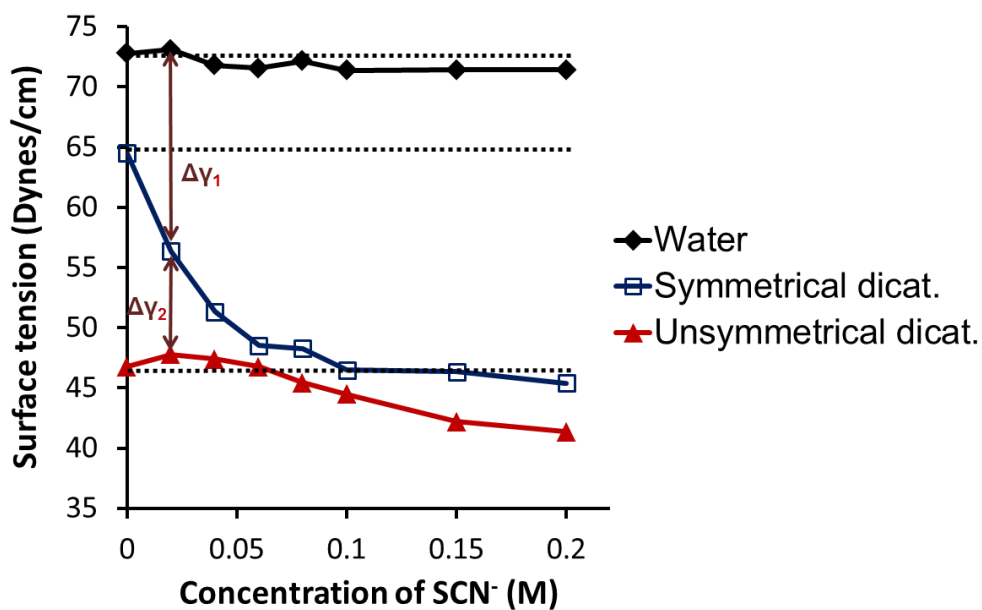


Figure 2-3 Surface tension measurements when titrating SDC I and UDC I with SCN^- . Concentration of SDC I and UDC I was 0.1 M. The data points at $[\text{SCN}^-] = 0$ M represent surface tension of neat water (blank line), 0.1 M aqueous solution of SDC I (blue line) and 0.1 M aqueous solution of SDC I (blue line) and 0.1 M aqueous solution of UDC I (red line), respectively. The vertical arrows denote $[\text{SCN}^-]$ of 0.02 M. It is noted that the amount of dication used for PIESI was always in large excess to the anion.

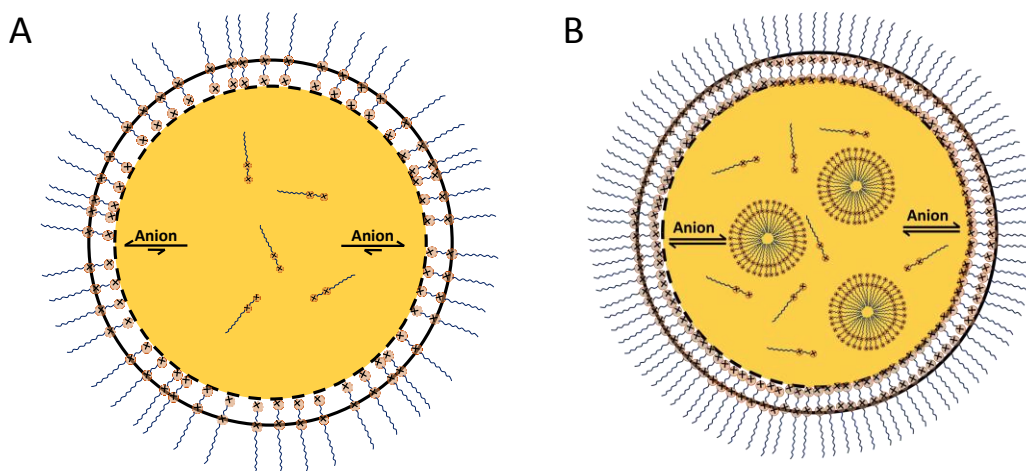


Figure 2-4 Schematic showing the partitioning of an analyte anion between the surface of an aerosol droplet and the bulk interior. When the concentration of the dicationic surfactant is low (“A” above), it resides mainly at the surface of the droplet as will any associated anions. When the concentration of surface of the dicationic surfactant is high (“B” above), monolayer can be formed and all additional surfactant resides in the interior bulk solution. Thus the anionic analyte has increased partitions to the interior bulk solution.

It should be noted that another scenario is possible with this system. Since the unsymmetrical dication is an excellent surfactant even in the absence of an anionic analyte, it is initially enriched at the aerosol droplet surface. This is somewhat different from the case of the symmetrical dicationic reagent that is not surface active until it binds an anion.³⁷ Only then does the symmetrical dication/anion complex partition to the aerosol surface. Therefore, in the case of the unsymmetrical dicationic reagent, there is a competition between the two highly surface active ionic species (i.e., one paired with the anionic analyte and the other unpaired). Once the surface of the aerosol droplet in

saturated (monolayer) with the unsymmetrical dicationic surfactant, additional material can only be solubilized in the interior of the droplet (Figure 2-4B). These “inner solution” dications will compete for any anionic analytes. Note that micelle formation in the inner solution would even more effectively compete for anions. In this case, some signal suppression could occur because of surface dilution of the anion/dication complex. Ultimately this limits the advantage of having increasingly surface active ion-pairing agents.

2.3.4 Partitioning Behavior of the Species in the Aerosol Droplet

The partitioning behaviors of the dications and anion/ion-pairing reagent complexes were evaluated. In this experiment, the ESI responses of thiocyanate/UDC I complexes were measured by infusing (10 $\mu\text{L}/\text{min}$) increasing concentrations of solutions containing 10:1 UDC I:SCN⁻ (Figure 2-5, black line). It is shown that the response of the thiocyanate/UDC I complex initially increases linearly ($R^2 = 0.970$) in the concentration range from 1×10^{-6} M to 5×10^{-5} M. However, signal saturation occurs when the concentration of the solution reaches approximately 5×10^{-5} M. This saturation behavior indicates the equilibrium for the ionic species partitioning between droplet surface and droplet interior is different at dication concentrations before and after 5×10^{-5} M. When the concentration of dication is greater than 5×10^{-5} M, where uncomplexed UDC I strongly competes with other paired ion species for the limited number of surface positions, the equilibrium for the thiocyanate/UDC I complex shifts to the droplet interior and consequently leads to a decrease in the amount of thiocyanate/UDC I complex that resides on the surface (a suppressed signal). This observation indicates that in the previous experiments, where 200 μM (2×10^{-4} M) ion-pairing reagent was used, surface saturation of the aerosol droplets by the surfactant had occurred. The methanol molecules in the solvent were easily protonated and initially carry the majority of

charges.⁶¹ The ESI response of the protonated methanol ions was shown to be suppressed when the concentrations of thiocyanate/UDC I solution exceeded 2×10^{-5} M, at approximately the same concentration when curvature and leveling off of the ESI responses of thiocyanate/UDC I complex occurs (Figure 2-5, red line). This signal suppression behavior is a result of the thiocyanate/UDC I complex ions outcompeting the solvent ions for limited numbers of excess charges on the droplet surface. According to Enke's equilibrium partitioning theory, the concentration of excess charge [Q] can be expressed as

$$[Q] = \frac{I}{F\Gamma} \quad (1)$$

in which [Q] is the excess charge in molar concentration, I is the total droplet current in amperes, F is the Faraday's constant (96,485 coulomb/mol), and Γ is the flow rate of sample solution in L/s.⁶³ The value of [Q] determined by using Equation 1 was equal to 5.1×10^{-5} M, which means that the total charge ([Q]) will run out when the analyte concentration reaches 5.1×10^{-5} M. This suggests that there would be a charge limitation to the analyte response at higher concentration levels. Notably, the concentration at this charge limitation (5.1×10^{-5} M) is consistent with the concentration at which signal saturation of the thiocyanate/UDC I complex ion occurs (5×10^{-5} M). To prove that the leveling off of the ESI response observed is due to the lack of any more available surface area and/or the charges on ESI droplet rather than due to a saturation of detector response, a calibration curve of threonine, which is not a surface active species, was made (Figure 2-6). The ESI response of the ThrH^+ was linear over a concentration range of 3×10^{-6} to 1×10^{-3} M. Since the discontinuity with our "ion-pairing surfactants" occurs at 5×10^{-5} M (well below that of the threonine saturation) this can only

be due to the surface activity of the reagent causing it to saturate the droplet surface at the lower concentration.

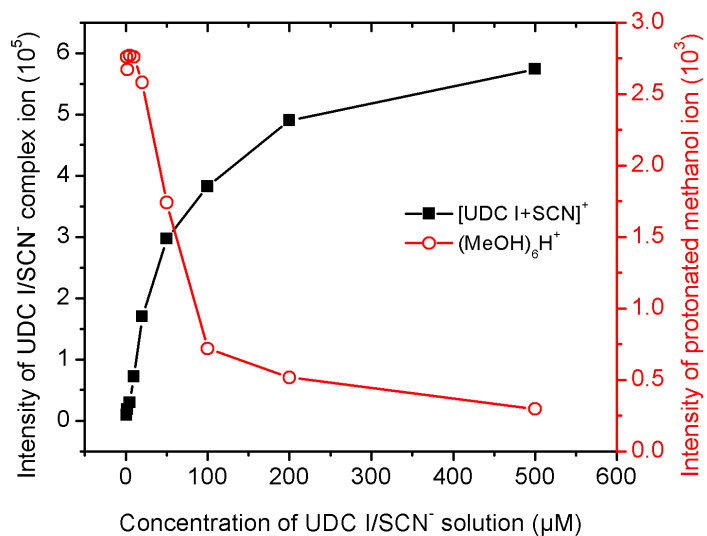


Figure 2-5 ESI-MS response to the dication/SCN⁻ complex ion (in black) and ESI-MS response to the protonated methanol ion (in red) for solutions containing UDC I and SCN⁻ (UDC I : SCN⁻ = 10 : 1) as the dication concentration increased from 1 × 10⁻⁶ to 5 × 10⁻⁴ M. The intensity of the dication/SCN⁻ complex ion and the protonated methanol ion were recorded by monitoring the +1 dication/SCN⁻ complex ion ([UDC I + SCN]⁺ m/z: 522.5) and the solvent ion (MeOH)₆H⁺ (m/z: 193.1) respectively in the SIM mode. Samples were directly infused at 10 μL/min.

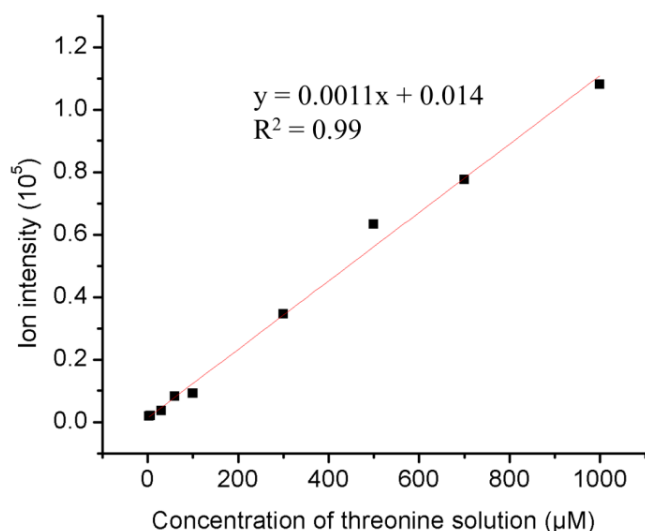


Figure 2-6 ESI-MS response to the ThrH⁺ ion as the concentration of threonine solution increased from 3×10^{-6} to 1×10^{-3} M. The ion intensity was recorded by monitoring the ThrH⁺ ion (m/z : 120.1) in the SIM mode.

The competition behavior of the unsymmetrical and symmetrical dications also was evaluated by simultaneously measuring the ESI responses of SDC I and UDC I (by direct infusion (10 µL/min)) as a function of their concentrations (Figure 2-7A). It is shown that the response curve was fairly linear at concentrations from 2×10^{-7} M to 10^{-4} M with $R^2 = 0.999$ for UDC I and $R^2 = 0.986$ for SDC I, and saturation behavior clearly occurs at a concentration of 10^{-4} M. Also, it was observed that the responses of the two dications were similar at the low concentration region from 2×10^{-7} M to 2×10^{-5} M. However, at higher concentrations the response of UDC I was significantly higher than that of SDC I (at concentrations greater than 2×10^{-5} M). This behavior could be explained by the competition between unsymmetrical and symmetrical dications for the limited number of charge positions on the droplet surface at higher concentrations. Since the partitioning of

UDC I (the surface active reagent) is more favorable, signal suppression occurs for SDC I leading to a gradually decreased response at its higher concentrations. These observations are in agreement with Enke's prediction using the equilibrium partitioning model for analytes with different equilibrium partition coefficients⁶³ as well as Kebarle and Tang's experimental data.⁵⁷ It should be noted that the discontinuous "jump" in response factor exhibited at concentrations between 10^{-5} to 10^{-4} M is not constant with the theoretical predictions and the experimental observations in Kebarle and Tang's study.⁵⁷ This is likely due to the high surface activity of the unsymmetrical dications used in this study and also the symmetrical dication/anion associated complexes. The symmetrical ions used in Kebarle and Tang's study⁵⁷ did not have such pronounced surface activity. The highly surface active species (i.e., the unsymmetrical dications used in this study) would rapidly form a monolayer at the droplet surface and then exhibit further behaviors such as aggregate/micelle formation in the interior of the aerosol droplet. This would result in a change in the ion distribution in the droplet and in turn affect the surface concentration of the analyte.

Ion responses of the anion/ion-pairing reagent complexes were examined for increasing concentrations of SCN^- , in the presence of equimolar amounts of UDC I and SDC I (Figure 2-7B). It was shown that increasing the concentration of SCN^- led to a concomitantly linear increase in ion response for both the thiocyanate/UDC I complex and thiocyanate/SDC I complex. This suggests that the addition of SCN^- has little effect on the relative partitioning of each complex to the droplet surface. The response of the thiocyanate/UDC complex started to exhibit a saturation behavior when the concentration SCN^- reached 1×10^{-4} M, while the response of the thiocyanate/SDC complex did not. The early surface saturation of thiocyanate/UDC complex results in a smaller difference between response of the thiocyanate/UDC complex and the response of the

thiocyanate/SDC complex at higher concentrations (difference in response is 6.3 times at $[\text{SCN}^-] = 10^{-6}$ M while 3.4 times at $[\text{SCN}^-] = 2 \times 10^{-4}$ M).

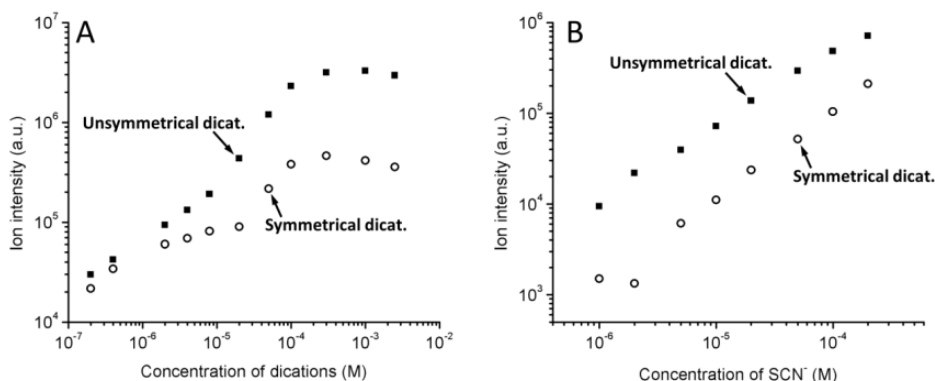


Figure 2-7 (A) ESI-MS response to the dications for equimolar solutions of SDC I and UDC I as the concentration increased from 2×10^{-7} to 2.5×10^{-3} M. The ion intensity was recorded by simultaneously monitoring the +2 charged dications ($[\text{SDC I}]^{2+}$ m/z: 162.2; $[\text{UDC I}]^{2+}$ m/z: 232.2) in SIM mode. (B) ESI-MS response to the dication/SCN⁻ complex ion for solutions containing 10^{-4} M of SDC I and UDC I as the concentration of SCN⁻ added increased from 1×10^{-6} M to 2×10^{-4} M. The ion intensity was recorded by simultaneously monitoring the +1 charged dication/SCN⁻ complex ion ($[\text{SDC I} + \text{SCN}^-]^+$ m/z: 382.3; $[\text{UDC I} + \text{SCN}^-]^+$ m/z: 522.5) in SIM mode.

2.3.5 LODs Determined with the Use of Unsymmetrical Dications in the SRM Mode

SRM experiments were performed for the same anions with the use of the same unsymmetrical dications and symmetrical dications (Table 2-4). It was observed that the SRM mode usually provided somewhat better sensitivity (1.2 to 9 times) than the SIM mode. This is understandably due to the enhanced analytical specificity and reduction in the chemical noise. It should be noted that these SRM experiments utilized collision

induced dissociation (CID) and monitored a fragment of the anion/ion-pairing reagent complex, and therefore the observed LODs are hardly correlated to the properties of the analytes without considering other factors involved, such as efficiency of fragmentation and ion transmission.

Table 2-4 Comparison of limits of detection (LOD) of anions obtained with the use of unsymmetrical dications (UDC I and UDC II) and symmetrical dications (SDC I and SDC II) in the SRM mode by PIESI-MS. The concentration of the dication used was 10 μ M.

Anion	UDC I	SDC I	Improvement ^b		UDC II	SDC II	Improvement ^b	
	LOD ^a (pg)	LOD (pg)			LOD (pg)	LOD (pg)		
BZSN ⁻	2.3	3.5	1.5	○	10	28	2.8	+
I ⁻	3.2	0.72	0.2	-	1.2	3.4	2.8	+
BZO ⁻	1.5	3.2	2.1	+	2.0	4.0	2.0	+
ASN ⁻	100	320	3.2	+	16	600	38	+
MCA ⁻	0.16	3.2	20	+	1.8	2.4	1.3	+
SCN ⁻	— ^c	—			—	—		
HEDP ⁻	30000	660	0.02	-	500	2700	5.4	+

^aLOD was defined as the lowest analyte amount in picogram yielding a S/N = 3.

^bFactor of improvement of LOD of unsymmetrical dications vs. LOD of symmetrical dications. "+": better; "-": worse; "○": similar.

^cNot detected.

2.4 Conclusions

The two unique unsymmetrical dications that were synthesized and evaluated proved useful for enhancing and understanding paired ion electrospray ionization mass spectrometry (PIESI-MS). The use of surface active ion-pairing agents provides lower detection limits for anions (from 1.5 to 12 times) than symmetrical ion-pairing agents (which are not surface active species). This bias in the performance of anion detection between unsymmetrical and symmetrical dications confirms that the surface activity is

one crucial factor for sensitivity enhancement in PIESI-MS. The effective concentration range was shown to be 1 μM to 10 μM . Further increases in the concentration of the unsymmetrical pairing agent resulted in a decrease in the LODs of all anions. It was proposed that this limitation of sensitivity at high dication concentration was attributed to the enrichment of surface active ion-pairing agents in the interior of the aerosol droplet, which compete for the anions on the droplet surface leading to a surface dilution of the anion/dication complex. This study further sheds light on the PIESI-MS signal enhancement mechanism. It is proposed that the use of unsymmetrical dicationic ion-pairing reagents results in the formation of highly surface active anion/dication complex and thus an enhanced partitioning of the anion to the droplet surface. This assumption was further experimentally supported by the results of surface tension titration studies and the correlation between surface activity of the unsymmetrical dication and the ESI response of the anion/dication complexes. In addition, a discontinuity in the ion response versus dication concentration was found. The reason for the discontinuity in response factor exhibited at concentrations region between 10^{-5} to 10^{-4} M is likely due to the formation of surfactant aggregates/micelles in the bulk interior solution of the aerosol droplets in the electrospray process. This would influence the ion partitioning/distribution. Future studies will be focused on quantitative prediction of the ESI responses of the anion and symmetrical/unsymmetrical dication complexes.

Chapter 3

Sensitive Detection of Anionic Sugars with Paired Ion Electrospray Ionization Mass Spectrometry (PIESI)

Abstract

The analysis of anionic sugars is of primary importance in understanding biological regulatory mechanisms and diagnosis of health related diseases. However, traditional analytical methods face challenges regarding detection sensitivity and selectivity. In this study, paired ion electrospray ionization mass spectrometry (PIESI) was employed for the ultra-sensitive detection of anionic sugars. The detection limits (LODs) for the selected anionic sugars ranged from 15 to 200 picograms (pg) with the use of the optimal ion-pairing reagent. Compared to the negative ESI, the LODs were improved from 2 to 167 fold in the PIESI mode. A mixed-mode vancomycin stationary phase was employed for the separation of anionic sugars especially the isomeric sugar phosphates. The separated analytes were sensitively detected in the PIESI mode.

3.1 Introduction

Of all the relevant metabolites involved in various intracellular metabolic pathways in all biological organisms, anionic sugars are among the most fundamental and abundant compounds.⁴ Their structures consist simply of carbohydrate moieties and one or several acidic terminal groups such as phosphate and/or carboxylate. As key intermediates, anionic sugars play essential roles in biological systems as communication media,⁵ energy sources (such as ATP), and bio-synthesis precursors. In addition to these functions, their concentration and distribution induced by environmental or naturally occurring genetic variability in the cell pool can serve as indicators of the metabolic state.⁴ Further, their reliable analytical measurement is of prime significance in

quantitative metabolomics,⁹⁶⁻⁹⁸ and in the diagnosis of metabolic defect related diseases such as RPI (ribose-5-phosphate isomerase) and TALDO (transketolase and transaldolase) deficiency.^{21,99-102}

Due to their hydrophilicity, low in vivo concentrations (pM ~ nM), poor UV absorbance, low volatility and thermal stability, the quantitative analysis of anionic sugars can be challenging. Further, these analytes exist in complicated biological matrices, and exist as various structural isomers with similar fragmentation patterns in MS/MS.¹⁰³ In the past, anionic sugars had been analyzed by enzyme-based methods.¹⁰⁴⁻¹⁰⁶ However, these approaches have inherent drawbacks such as interferences by other sample components and their time-consuming, low throughput nature. These methods also are limited by the availability of enzymes.⁵ Derivatization is often required to analyze these non-volatile compounds when using gas chromatography (GC). The main disadvantages associated with derivatization protocols are the time, labor, sample loss, incomplete derivatization and thermal instability of target compounds such as sugar phosphates in the GC oven.^{96,107,108} Capillary electrophoresis (CE) is a promising tool for these ionic sugar metabolites analyses, but it has the disadvantages of insensitivity and irreproducibility.^{24,109,110} Conventionally used reversed-phase liquid chromatography (RPLC) has poor retention of these polar compounds. While anion-exchange chromatography (AEC) might be a good candidate for the analysis of anionic sugars, which has been routinely used for the analysis of sugar phosphates and carboxylic sugars with pulsed amperometric,¹¹¹ potentiometric¹¹² or conductometric detector.^{113,114} Although AEC in past approaches showed improved separation resolution and efficiency, considerable concentration of samples are required to complement the moderate sensitivity of AEC based methods. When coupled with MS detection, the high ionic strength required to elute the analytes from AEC column often causes deposition of non-

volatile salts at the ion source inlet, which can lead to contamination of MS components.^{4,24}

To date, LC combined with MS detection has become one of the core techniques for the analysis of biological samples, due to the excellent figures of merit such as universality, high throughput, two dimensional resolution, and sensitivity.¹¹⁵ MS with an electrospray ionization (ESI) interface is ideally suited to biochemical analysis, because it allows for large, non-volatile molecules to be analyzed directly from the liquid phase, and thus can be coupled to separation techniques such as high performance liquid chromatography.²⁷ There are two modes used for the ionization process, the positive and negative ion mode. Most reported LC-ESI-MS based methods routinely utilized the negative ion mode to detect anionic sugars due to their anionic nature.^{4,5,21,24,99,116} However, the negative ion mode often is not preferred as it can produce higher background noise and lower electrospray stability compared to the positive ion mode due to possible corona discharge and arcing in the negative ion mode.^{27,117} Paired ion electrospray ionization (PIESI), which was developed by Armstrong and co-workers in recent years, has been applied for ultrasensitive detection of anionic compounds including acidic pesticides,^{26,31} anionic and zwitterionic phospholipids,³⁶ nucleotides,³⁵ anionic surfactant¹² and performance-enhancing drugs.¹¹⁸ Sub-pg levels of detection limits for these compounds were obtained with PIEESI, which were often one to four orders of magnitude more sensitive as compared to other reported methods.^{31,36,118} Briefly, this approach utilizes the introduction of a small amount (tens of μM) of chaotropic and multiply charged ion-pairing reagents to associate with anionic compounds in the sample stream. Thus positively charged complexes can be formed and be detected in the positive ion mode. PIEESI improves sensitivity in several ways. First, it avoids detection in the negative ion mode. Second, it moves the detection of the analyte to a higher mass-to-

charge ratio (m/z) region, where the background noise is lower. In addition, the surface activity of anion/ion-pairing reagent complex ions in the aerosol droplets is often greatly increased compared to either the anion or the ion-pairing reagent alone, which results in enhanced ionization efficiency of the anion/ion-pairing reagent complex and further leads to higher sensitivity.^{37,119} In this study, the feasibility of using PIESI to enhance the detection sensitivity of representative anionic sugars was evaluated. The lack of a chromophore for optical detection as well as the poor chromatographic selectivity of these anionic sugar compounds, make the development of an HPLC-MS method for simultaneous separation and sensitive detection of these selected anionic sugars with the PIESI approach quite attractive.

3.2 Experimental

3.2.1 Materials

A list of the studied anionic sugars is given in Table 3-1. All of them were purchased from Sigma Aldrich (St. Louis, MO, USA), either in their acid, or sodium form. Acetonitrile (ACN), methanol (MeOH) and water of HPLC grade (Honeywell Burdick and Jackson, Morristown, NJ, USA), ACS grade formic acid (88%, J. T. Baker. Inc., Mallinckrodt Baker, UK) were used for the preparation of the mobile phases and standard solutions. The Astec Chirobiotic V column was supplied by Supelco (column size: 250 mm length \times 2.1 mm i. d.; particle size: 5 μm ; pore size: 100 \AA ; Supelco, St. Bellefonte, PA, USA), which is prepared by covalently bonding the amphoteric glycopeptide vancomycin to the surface of silica gel.^{120,121} The unique structure of vancomycin provides stereoselective and hydrophilic/ion exchange mixed-mode properties in chromatographic separations. The structure of the ion-pairing reagents used in this study is shown in Table 3-2. They were originally synthesized in their bromide form in our

laboratories^{29,46} and were anion-exchanged to their fluoride form to maximize the complexation formation between the ion-pairing reagent and the anions.^{2,28}

Table 3-1 Names, abbreviations, structures and exact masses of the studied anionic sugars

Analyte ¹	Abbreviation	Structure	Exact Mass ²
N-Acetyl neuraminic acid	NANA		308.1
N-Acetyl-2,3-dehydro-2-deoxyneuraminic acid	DANA		290.1
D-Glucuronic acid	GLA		193.0
D-Galacturonic acid	GAA		193.0
D-Saccharic acid potassium salt	SCA		209.0
α-D-Glucose 1-phosphate disodium salt hydrate	G-1-P		258.0

Table 3-1—Continued

<p>α-D-Glucose 6-phosphate sodium salt</p>	<p>G-6-P</p>		<p>259.0</p>
<p>D-Ribose 5-phosphate disodium salt hydrate</p>	<p>R-5-P</p>		<p>228.0</p>
<p>D-Fructose 6-phosphate disodium salt hydrate</p>	<p>F-6-P</p>		<p>258.0</p>
<p>D-Fructose-1,6-bisphosphate trisodium salt</p>	<p>F-1,6-BP</p>		<p>337.0</p>

¹The anionic sugars were bought either in their acid or sodium salt form

²The exact masses of the structures of sugar anions

Table 3-2 Structures of ion-pairing reagents used in this study with their abbreviations, exact masses and charges

Ion-pairing reagent	Structure	Exact mass	Charge
C ₅ (bpyr) ₂		324.3	+2
C ₃ (triprp) ₂		362.3	+2
C ₅ (benzim) ₂		386.3	+2
C ₉ (mim) ₂		290.3	+2
Tet 1		1062.5	+4
Tet 2		910.5	+4
Tet 3		842.5	+4

3.2.2 Instrumental

All experiments were carried out on a Thermo Finnigan HPLC-MS system, which consisted of an electrospray ionization source of a LXQ linear ion trap MS (Thermo Fisher Scientific, San Jose, CA, USA). The system was controlled by X-calibur 2.0 software (Thermo Fisher). The ion-pairing reagent solution was introduced by an independent LC pump (Shimadzu, Columbia, MD, USA), and post-column mixed with the sample stream via a Y-type mixing device. The schematic of the instrumental configuration was shown in Figure 1-1. The MS parameters were optimized by the standard tuning method provided in the instrument handbook. The values were set as follows: ionization voltage, 3 kV; capillary voltage, 11 V; capillary temperature, 350 °C; sheath gas flow, 37 arbitrary units (AU); and the auxiliary gas flow, 6 AU. In selective reaction monitoring (SRM) mode, the normalized collision energy, Q value and activation time were set at 30 V, 0.25 and 30 ms respectively. The six-port switching valve served as an injector valve for both LOD measurement and chromatographic separation experiments. The volume of the injection loop was 5 μ L.

3.2.3 LOD Measurements

As can be observed in Figure 1-1, a carrier flow consisting of a 2:1 volume ratio of MeOH and water at 300 μ L/min was transferred by the HPLC pump to the mixing device. Meanwhile, a 40 μ M ion-pairing reagent aqueous solution was directed by the independent LC pump at a speed of 100 μ L/min and was mixed with the carrier flow at the center of the device, resulting a total flow rate of 400 μ L/min with the final solvent composition of 50% MeOH and 50% water and with the final concentration of the ion-pairing reagent at 10 μ M. The MS was operated in both the positive and negative SIM and SRM modes. The m/z peak width monitored for each analyte was set 5. Serial dilution of stock solutions of each standard with HPLC grade water was performed to

obtain the desired concentration that gives an averaged signal-to-noise ratio (S/N) of three with five replicate injections of each standard. The data was processed based on Genesis Peak Detection Algorithm provided by X-calibur 2.0 software. The LODs obtained in the negative ion mode was used for comparison to the positive ion mode PIESI results. To have equal LC conditions as PIESI mode, a direct mobile phase consisting of 50/50 MeOH/water (v/v) at a flow rate of 400 μ L/min was used for the determination. The optimized MS parameters in the negative ion mode were as following: spray voltage, 4.5 kV; capillary voltage, -30 V; capillary temperature, 400 $^{\circ}$ C; sheath gas flow, 40 arbitrary units (AU); and the auxiliary gas flow, 5 AU. Due to multiple charges of some selected anionic sugars, the most intensive m/z of the analyte/ion-pairing reagent complex ion and MS/MS fragment ion were selected as the precursor and the daughter ion respectively.

3.2.4 Chromatographic Separation Conditions

The chromatographic separations were carried out on a Chirobiotic V column (Supelco, Sigma-Aldrich) with eluent A (0.5% formic acid in ACN) and eluent B (0.5% formic acid in water). The gradient profile was displayed as follows: 0-10 min, 50 % A, 10-20 min, 50% A to 40% A. HPLC mobile phases at a flow rate of 300 μ L/min were introduced into the mixing device, and mixed with the ion-pairing reagent solution which was pumped at 100 μ L/min. The best ion-pairing reagent obtained from the LOD measurement experiment was used for the MS detection in PIESI mode. The selected ion-pairing reagent was dissolved in MeOH to increase the ionization efficiency. Each analyte/ion-pairing reagents was monitored in PIESI-SIM mode with m/z peak width set at 3. The concentration of each standard in the mixture solution was 100 ng/mL.

3.3 Results and Discussion

3.3.1 Detection Limits (LOD)

Three types of anionic sugars were selected for the evaluation (see Table 3-1). N-acetyl neuramic acid (NANA) and N-acetyl-2,3-dehydro-2-deoxyneuraminic acid (DANA) are important sialic acids and are frequently used for screening sialic acid storage diseases.¹²² Sugar carboxylic acids including glucuronic acid (GLA), galacturonic acid (GAA) and saccharic acid (SCA), as well as sugar phosphates including glucose 1-phosphate (G-1-P), glucose 6-phosphate (G-6P), ribose 5-phosphate (R-5-P), fructose 6-phosphate (F-6-P) and fructose 1,6-bisphosphate (F-1,6-BP) are key intermediates in multiple intracellular metabolic pathways such as glycolysis, tricarboxylic acid cycle and the pentose phosphate pathway.⁴ Sugar phosphates are often used for diagnosis of metabolic defect related diseases such as ribulose-5-phosphate epimerase and ribos-5-phosphate isomerase (RPI) deficiency, as well as transketolase and transaldolase (TALDO) deficiency.^{21,101,102} The four dicationic and the three tetracationic ion-pairing reagents (see Table 3-2) were selected based on previous studies: the four dicationic ion-pairing reagents out-performed other developed reagents in sensitive detection of anions containing carboxylic group.^{28,29,31} and the three tetra-cationic ion-pairing reagents gave the lowest LODs for phosphorylated compounds such as nucleotides and phospholipids.^{35,36,46} Since sugar phosphates are multiply charged, the complex ions of sugar phosphate/ion-pairing reagent are also multiply charged. The most abundant complex ion was selectively detected in both the SIM and SRM mode. In PIESI-SRM mode, the most sensitive fragment of analyte/ion-pairing reagent complex was used as the daughter ion for the detection of the analyte.

The LODs obtained in the negative ion mode are shown in Table 3-3. The detection limits for these anionic sugars ranged from 500 to 12500 pg. The SRM mode is

often thought to provide improved sensitivity due to its selectivity. However, the SRM mode was not advantageous in improving the sensitivity for many of these highly polar and hydrophilic anionic sugars (see Table 3-3).

With the use of ion-pairing reagents, the detection limits of these anionic sugars were improved in the positive ion mode (see Table 3-4). Overall, the tetra-cationic ion-pairing reagent Tet 3 gave the lowest LOD values for all these anionic sugars. The LOD values ranged from 15 to 200 pg obtained with Tet 3. As is observed in Table 3-4, the LODs for the same analyte differed when other ion-pairing reagents were used, indicating that the structure of ion-pairing reagents is a critical factor affecting the PIESI effectiveness. Further the LODs among these ten anionic sugars were different from each other with the use of the same ion-pairing reagent, which suggests that the nature of the analyte also plays a role in detection sensitivity. Therefore, it is useful to optimize ion-pairing reagents for a particular type of analyte before analysis.

Table 3-5 compares the LODs obtained with PIESI to those obtained in the negative ion mode without the use of ion-pairing reagents. The LODs obtained with the use of the best ion-pairing reagent, Tet 3 ranged from 2.5 to 167 fold lower as compared to the LODs obtained in negative ion mode. These improvements demonstrate the high sensitivity of PIESI for the detection of anionic sugars.

Compared to other LC-ESI-MS methods reported in the literature,^{4,21,123-125} the absolute LOD values of the anionic sugars obtained in PIESI mode (15 to 200 pg) were one to three orders of magnitude lower, further indicating the high sensitivity of the PIESI-MS approach (see Table 3-6)

Table 3-3 Limits of detection (LODs) of anionic sugars obtained in negative ion mode
without using ion-pairing reagents

Analyte	LOD (pg) ³	
	SIM ¹	SRM ¹
NANA	1500	NA ²
DANA	500	NA ²
GLA	1500	1500
GAA	4000	500
SCA	1500	NA ²
G-1-P	2500	2500
G-6-P	12000	4000
R-5-P	2500	NA ²
F-6-P	3000	1000
F-1,6-BP	12500	NA ²

¹For the multiply charged anionic sugar, the most sensitive m/z of the analyte was used as the precursor ion in both negative SIM and SRM mode.

²Not detectable due to weak background noise

³The limits of detection (LODs) were reported in absolute values (pg)

Table 3-4 Limits of detection (LODs) of anionic sugars obtained in PIESI mode with the use of ion-pairing reagents

Analyte	C ₉ (mim) ₂		C ₃ (tprp) ₂		C ₅ (benz) ₂		C ₅ (bpyr) ₂		Tet 1		Tet 2		Tet 3 ³	
	SIM ¹	SRM	SIM ¹	SRM	SIM ¹	SRM	SIM ¹	SRM	SIM ¹	SRM	SIM ¹	SRM	SIM ¹	SRM
NANA	750	500	500	2000	200	800	1750	200	500	2500	450	450	300	50
DANA	525	350	250	625	310	155	400	100	655	1000	310	310	150	45
GLA	250	400	125	250	150	200	500	40	750	1250	1000	225	15	35
GAA	500	700	200	325	300	500	500	75	1000	1500	1000	500	250	200
SCA	1250	2000	350	450	900	2250	500	2500	600	1000	400	60	650	25
G-1-P	1000	1750	500	600	650	750	3000	600	1750	750	3750	NA	250	100
G-6-P	1000	1000	350	350	375	500	1750	1250	1250	625	1000	500	25	60
F-6-P	900	1200	350	350	400	500	2100	1250	2000	240	1000	225	175	20
F-1,6-BP	1650	3000	1500	NA ⁴	2000	5000	NA ⁴	NA ⁴	7500	2000	>2500	2500	75	75
R-5-P	450	1250	500	350	400	750	20000	500	2500	75	>500	250	375	20

¹The most sensitive m/z of the analyte/ion-pairing reagent complex ion was selected as the precursor ion in PIESI-SIM mode.

²The most abundant fragment of the precursor ion used in PIES-SIM mode was selected as the daughter ion in PIESI-SRM mode

³The ion-pairing reagent that gave the best detection sensitivities for these selected anionic sugars were highlighted in bold font.

⁴Not detectable due to weak background noise

Table 3-5 Comparison of detection limits of anionic sugars between PIESI and negative ion mode

Analyte	LOD (pg)				Improvement factor ¹
	Negative ion mode		PIESI-MS (Tet 3)		
	SIM	SRM	SIM	SRM	PIESI vs. Negative
NANA	1500	NA ²	300	50	30
DANA	500	NA ²	150	45	11
GLA	1500	1500	15	35	100
GAA	4000	500	250	200	2.5
SCA	1500	NA ²	650	25	60
G-1-P	2500	2500	250	100	25
G-6-P	12000	4000	25	60	160
R-5-P	2500	NA ²	375	20	125
F-6-P	3000	1000	175	20	50
F-1,6-BP	12500	NA ²	75	75	167

¹LOD obtained in negative ion mode divide by LOD value obtained in PIESI mode with the use of the best performed ion-pairing reagent Tet 3.

²Not detectable due to weak noise background

Table 3-6 Comparison of detection limits of anionic sugars obtained in PIESI mode with other negative ESI based HPLC-MS methods reported in the literature

Method	Mode	Related compounds	Importance of analysis	Absolute LOD (pg)	Reference No.
IP-HPLC-ESI-MS ¹	Negative SRM	Sugar phosphate (F-6-P, R-5-P, G-6-P)	Disease signaling	100-400	[4]
HILIC-ESI-MS/MS ²	Negative SRM	G-6-P, F-6-P, F-1,6-BP, R-5-P	Metabolomics	50-1000	[120]
IP-RPLC-ESI-MS/MS ¹	Negative SRM	G-6-P, F-6-P, F-1,6-BP, R-5-P	Metabolomics	300-1000	[26]
HPLC-ESI-MS/MS	Negative SRM	NANA	Disease signaling	>1350	[113]
IP-RPLC-ESI-QQQ ^{1,3}	Negative-SRM	F-6-P, R-5-P, G-1-P, G-6-P, F-1,6-BP	Metabolomics	240 - 15000	[96]
D-HPLC-ESI-QTOF ⁴	Positive full scan	F-6-P, R-5-P, G-6-P, F-1,6-BP	Disease signaling	1200 -100000	[122]
Current method	Positive SIM/SRM	The ten selected anionic sugars ⁵	Disease signaling and metabolomics	15-200	

¹IP: Ion-pairing reversed phase liquid chromatography; ²HILIC: hydrophilic interaction liquid chromatography; ³QQQ: Triple-quadrupole; ⁴QTOF: quadrupole coupled with time of flight mass analyzer;

3.3.2 Chromatographic Separation

Chromatographic selectivity is a major problem for the analysis of anionic sugars due to similarities in their weight, charge and structure. Recently, ion pairing-reversed phase liquid chromatography (IP-RPLC), utilizing hydrophobic stationary phases (mostly C18) and MS compatible solvents were used to separate ionic compounds. Addition of oppositely charged volatile ammonium salts into the mobile phase was necessary and

appeared to be an alternative to the analysis of such anionic metabolites. It has been shown to provide robust and versatile separations with good selectivity for metabolites in several biological matrices.^{4,21,99,126} However, severe ion suppression occurred when these hydrophobic reagents (often added into mobile phases at mM levels) were introduced into the ESI-MS, rendering these methods suitable only for negative ESI. Moreover, those additives have a high propensity to adhere to the components of LC-MS instrumentation, and are thus responsible for the long term contamination of the chromatographic and MS system. To ensure a robust and reproducible chromatographic separation, a substantial number of injections of samples and longer time in conditioning columns are often required.⁴⁰

In this study, hydrophilic interaction chromatography (HILIC) stationary phases such as aminopropyl, ZIC-HILIC, β -cyclodextrin and cyclofructan were tested. However, the resolution and selectivity toward isomeric and isobaric anionic sugars were not satisfactory. Porous graphitic carbon (PGC) was also tested for the separation. Despite the exceptional stability of PGC over the entire pH range and quite different chromatographic behavior in contrast to other RP and HILIC stationary phases, the resolution of sugar isomers was still not improved. It was shown that this stationary phase had very strong retention for sugars phosphates. In recent years, several types of mixed-mode stationary phases have emerged which show good selectivity for hydrophilic compounds. The mixed mode stationary phase Primesep SB, packed with reversed phase material carrying strong embedded basic ion-pairing groups, was first used for the separation of Calvin cycle intermediates (mostly anionic sugars) with the combination of MS detection.¹²⁷ Better selectivity for anionic sugar isomers was achieved on a 3-aminoquinuclidine-derived reversed phase/weak anion exchange based stationary phase.¹⁰³ However, the elution conditions used for the separation were not MS

compatible. Consequently a less sensitive charged aerosol detector had to be used instead.

The vancomycin based Chirobiotic stationary phase is widely used in chiral separations due to its excellent separation efficiency and selectivity. These advantages of chirobiotic V stems from its unique structure, which can provide π - π , weak anion/cation exchange, hydrogen bonding, hydrophilic and inclusion complex interactions.¹²⁸ This multiple-mode property proved to be beneficial and to give unique selectivities for isomeric compounds. Thus the mixed-mode Chirobiotic V stationary phase was utilized for the improvement of the selectivity of isomeric and anomeric anionic sugar compounds in this study. MS-friendly mobile phases (0.5% formic acid in methanol and water) were employed for the separation. The best performing ion-pairing reagent, Tet 3, was used for PIESI detection. As shown in Fig. 2, sialic acids and carboxylic sugars were separated from sugar phosphates on the chirobiotic V column. GAA and GLA were partially separated with each other. Notably, the isomeric sugar phosphates, G-1-P and G-6-P that could not be separated by most stationary phases were baseline separated by the column. Additionally, the column showed high separation efficiency for DANA. Other compounds were resolved by LC-MS due to their different m/z values.

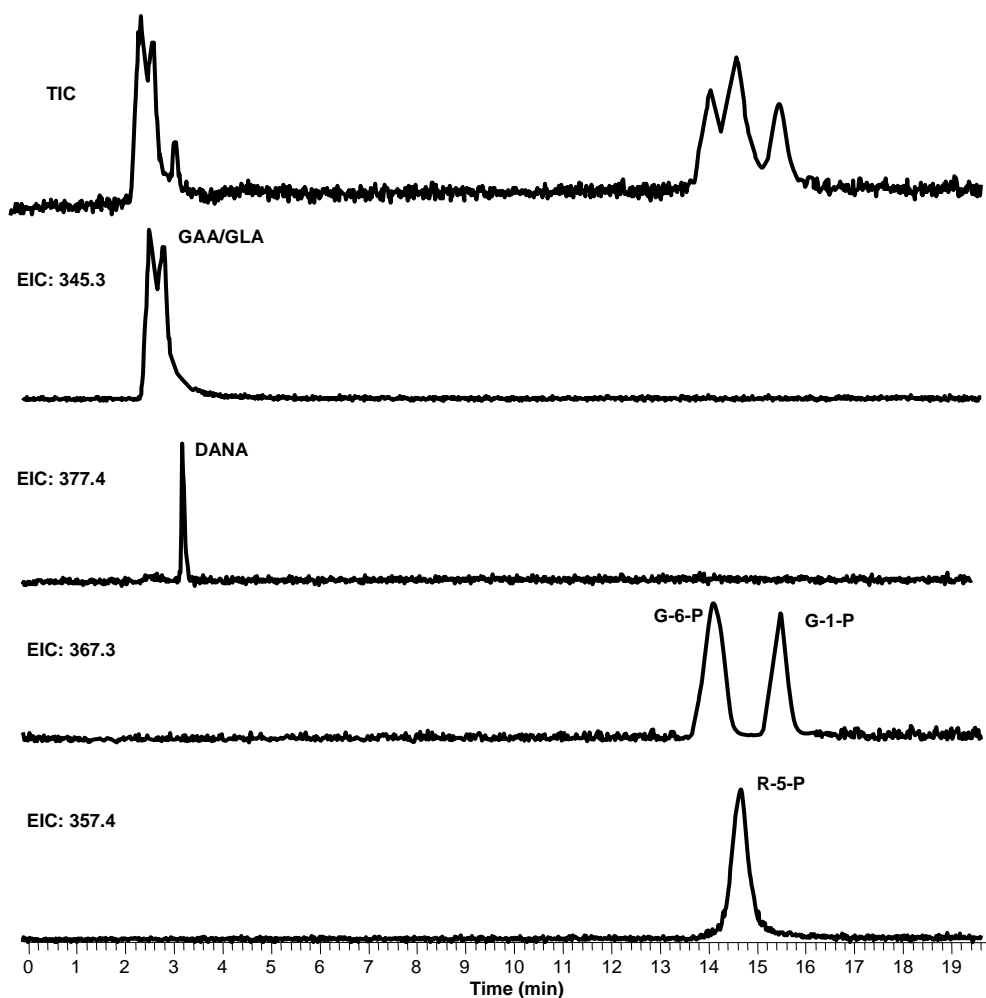


Figure 3-1 Chromatographic separation of selected anionic sugars and MS detection based on PIESI. The chromatographic and MS conditions were shown in section 3.2.2 and section 3.2.4 respectively. The concentration of each injected standard was 100 ng/mL. The MS was operated in positive SIM mode with the use of the optimal ion-pairing reagent Tet 3. The m/z values detected for each analyte in PIESI mode were listed as follow: GLA/GAA (345.5); DANA (377.4); G-6-P and G-1-P (367.3) and R-5-P (357.4).

3.4 Conclusions

The PIESI approach was successfully applied for the sensitive detection of anionic sugars. Instead of detecting these anionic compounds in the less sensitive negative ESI, they were detected in positive ESI with the use of multiple charged ion-pairing reagents. LODs ranging from 15 to 200 pg were obtained with the optimal ion-pairing reagent Tet 3, which were 2 to 167 fold lower as compared to those obtained in negative ESI. Compared to other reported LC- ESI-MS based methods, the detection sensitivities for these selected sugar acids and sugar phosphates were one to three orders of magnitude better with the PIESI approach. It was also observed that the nature of analyte and ion-pairing reagent both affect the detection sensitivity. A HPLC-PIESI-MS method was developed for simultaneous analysis of anionic sugars in a single run. The separation was based on a mixed-mode vancomycin based stationary phase with MS-friendly LC mobile phases. The isomeric sugar phosphates, G-1-P and G-6-P, which could not be separated by most other HPLC columns, were baseline separated on the vancomycin column, and were sensitively detected with the optimized ion-pairing reagent, Tet 3 in PIESI mode. Overall, the PIESI approach was suitable for sensitive analysis of anionic sugars and should be applied for real sample analysis.

Chapter 4

Sensitive Detection of Anionic Metabolites of Drugs by Positive Ion Mode

HPLC-PIESI-MS

Abstract

The detection window for drugs of abuse, including performance-enhancing drugs is limited by the sensitivity of analytical methodologies. Herein, paired ion electrospray ionization mass spectrometry (PIESI-MS) was employed for sensitive analysis of performance-enhancing drugs and drugs of abuse by detecting their glucuronide and sulfate conjugates. The proposed approach provides enhanced sensitivity for these drug metabolites, and overcomes the drawbacks of the less sensitive negative ion mode ESI-MS by detecting the anionic metabolites in the positive ion mode at higher m/z where the background noise is less. Absolute LODs down to sub-pg levels were obtained with the use of the optimal symmetrical or unsymmetrical ion-pairing reagents. One to three orders of magnitude improvement were obtained compared to other reported methods performed in the negative ion mode. Structurally similar steroid conjugates were chromatographically separated and detected by HPLC coupled with PIEESI-MS. Finally, an off-line solid phase extraction (SPE) protocol was successfully developed to eliminate any matrix effects in the analysis of human urine samples.

4.1 Introduction

Detection times and elimination times of drugs and their metabolites in humans are of clinical and forensic interest.^{129,130} In the case of performance-enhancing drugs; the “detection window” subsequent to the administration or consumption of such drugs is particularly relevant and can vary considerably. The pharmacokinetics and pharmacodynamics of most drugs are known, but these are usually for highly controlled

single dose experiments.¹³¹⁻¹³⁵ Further, it is well known that different classes of drugs and even different drugs within a class can have unique metabolic pathways and therefore very different elimination half-lives.¹³⁵⁻¹³⁹ In the case of performance-enhancing drugs, several mitigating factors can affect individual drug-metabolite elimination/lifetimes/detection times. These include: an individual's duration of use, the dosage, the form of the drug (e.g., salt, neutral molecule, crystal structure if solid, particle size, diluents or excipients present), the nature of administration, inter-individual differences and the matrix to be analyzed (e.g., urine, blood, saliva).^{129,130} The analyst has no control over any of these factors except perhaps, in limited cases, the latter. However, the analyst does control one important factor that profoundly affects drug detection, the analytical methodology.

In general the detection time of a drug is increased if the analysis is performed on: a) the most persistent metabolite, b) the optimal biological fluid and c) using the most sensitive method of analysis. Therefore, it is not surprising that the plethora of papers published on drug detection often involve new and improved instrumental approaches. These are often accompanied by sample pre-concentration and/or pre-treatment steps such as enzymatic hydrolysis and derivatization.^{6,140-160} Indeed the quest for more sensitive and reliable methods continues unabated, usually with a focus on hyphenated separations and mass spectrometric approaches.¹⁶¹⁻¹⁷⁶ While many recent papers have focused on glucuronide and sulfate conjugates of steroids, these types of metabolites are relevant for most performance-enhancing drugs, and drugs of abuse, even ethanol.^{6,141,171,175,177}

A study of anabolic steroid glucuronides concluded that chemical background noise and fragmentation are less with electrospray ionization mass spectrometry (ESI-MS) than with atmospheric-pressure chemical ionization (APCI).¹⁴⁴ In addition to being

more sensitive, the positive ion mode produced more abundant and diagnostic fragment ions than the negative ion.^{144,154} In this work we focus on mass spectrometry (MS) and MS/MS detection methods that use very small amounts of specifically designed and synthesized agents for the ultra-sensitive detection of anionic metabolites in the positive ion mode. This approach is known as “paired ion electrospray ionization” (PIESI).^{2,12,28,29,31,34-37,45,119} PIESI provides a facile approach for doing ESI-MS and ESI-MS/MS of negatively charged analytes in the positive ion mode. Further it moves the detection of analytes away from a higher noise, low m/z region to a relatively lower noise, high m/z region.^{2,29} The ionization efficiency also appears to be enhanced in PIESI.^{37,119} However, an anion’s response can be quite different when using different cationic pairing agents. Thus choosing the optimal agent is important.

The goal of this work was to examine the feasibility of adapting the PIESI approach for the sensitive detection and quantitation of drug metabolites, specifically, glucuronide and sulfate conjugates. This is compared to direct MS and MS/MS analysis of these anionic metabolites in the negative ion mode, as well as the commonly used HPLC-MS methodologies previously reported in the literature. The optimized PIESI approach was then coupled to HPLC for the analysis of selected metabolites in urine samples.

4.2 Experimental

4.2.1 Reagents and Chemicals

Acetonitrile (ACN), methanol and water were of HPLC-MS grade and purchased from Honeywell Burdick and Jackson (Morristown, NJ, USA). The chemical structures and abbreviations of the symmetrical and unsymmetrical ion-pairing reagents used in this study are shown in Table 4-1. These ion-pairing reagents were originally synthesized in our laboratories,^{29,31} and were anion exchanged from bromide to their fluoride salt form

prior to analysis to maximize ion-pairing reagent/anion complex formation.² Notably, four of our symmetrical ion-pairing reagents have become commercially available from Sigma-Aldrich. The more recently developed unsymmetrical ion-pairing reagents were selected as they provided enhanced detection sensitivity for some anions.¹¹⁹ Ethyl- β -D-glucuronide (EtG), ethyl sulfate (ES), morphine-3 β -D-glucuronide (M3G), oxazepam glucuronide (OxaG) and 5-androsten-3 β -ol-17-one sulfate (dehydroepiandrosterone sulfate, DHEAS) were gifts from Cerilliant (Round Rock, TX, USA). 5 α -androstan-3 α -ol-17-one sulfate (androsterone sulfate, AS), androstadiene-3-one-17 β -ol (boldenone sulfate, BS), 5 α -androstane-17 β -diol (17 β -dihydroepiandrosterone sulfate, 17 β -DHEAS), 5-androsten-3 β -ol-17-one glucuronide (dehydroepiandrosterone glucuronide, DHEAG), 4-androsten-17 β -ol-3-one glucosiduronate (testosterone glucuronide, TG) and 4-androsten-17 β -ol-3-one sulfate (testosterone sulfate, NTS) were purchased from Steraloids, Inc. (Newport, RI, USA). Their structures are listed in Table 4-2. The internal standard, d6-dehydroepiandrosterone-3-sulphate (d6-DHEAS) was obtained from Sigma Aldrich (St. Louis, MO, USA). ACS grade formic acid (88%, w/w, J. T. Baker. Inc., Mallinckrodt Baker, UK) was used as the additive for the chromatographic separations.

Table 4-1 Structures, abbreviations, and exact masses of the symmetrical and unsymmetrical ion-pairing reagents used in this study.

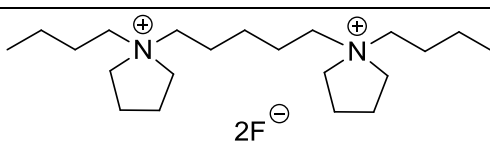
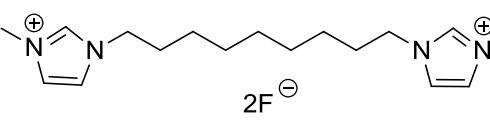
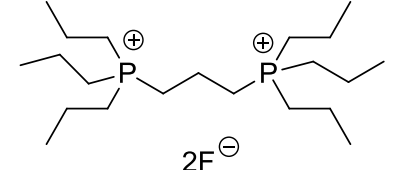
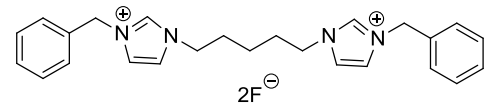
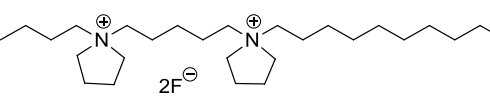
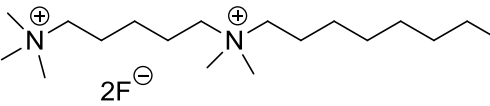
Ion-pairing reagent	Abbreviation	Structure	Exact mass of the dication
1, 5-pentanediy-bis-(1-butylpyrrolidinium) difluoride	C ₅ (bpyr) ₂		324.4
1, 9-Nonanediy-bis(3-methylimidazolium) difluoride	C ₉ (mim) ₂		290.3
1,3-Propanediy-bis(triethylphosphonium) difluoride	C ₃ (triprp) ₂		362.3
1, 5-Pentanediy-bis(3-benzylimidazolium) difluoride	C ₅ (benzim) ₂		386.3
1-butyl-1-[5-(1-tetradecyl-1-pyrrolidiniumyl)pentyl]pyrrolidinium difluoride	UDC1		464.5
N1-dodecyl-N1,N1,N5,N5,N5-pentamethyl-1,5-pentanediaminium difluoride	UDC2		342.4

Table 4-2 Structures, abbreviations, and exact masses of the drug metabolites used in this study

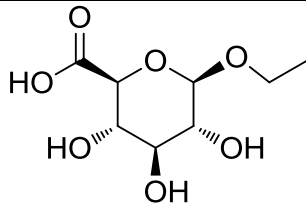
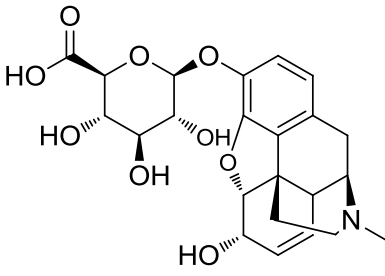
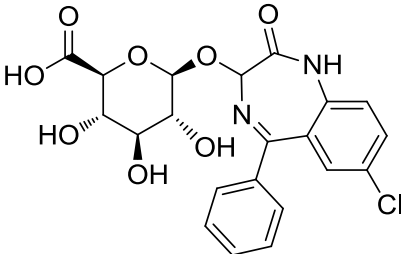
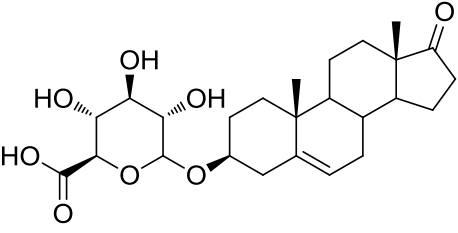
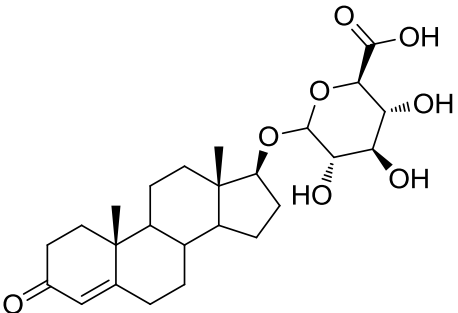
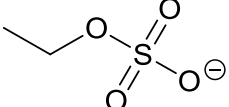
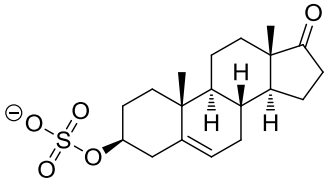
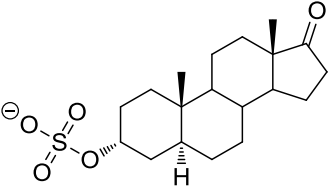
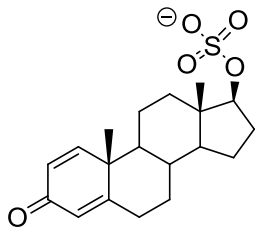
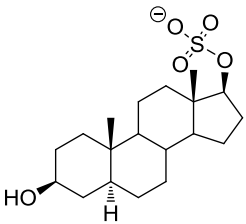
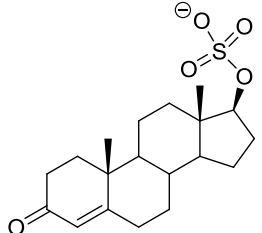
Analyte	Abbreviation	Structure	Exact mass
Ethyl- β -D-Glucuronide	EtG		222.1
Morphine-3- β -D-Glucuronide	M3G		461.2
Oxazepam Glucuronide	OxaG		462.1
Dehydroepiandrosterone Glucuronide	DHEAG		464.2
Testosterone Glucuronide	TG		464.2

Table 4-2—Continued

Ethyl Sulfate	EtS		125.0
Dehydroepiandrosterone Sulfate	DHEAS		367.2
Androsterone* Sulfate	AS		369.2
Boldenone Sulfate	BS		365.1
17β-Dihydroepiandrosterone Sulfate	17β-DHEAS		371.2
Testosterone Sulfate	NTS		367.2

*Androsterone is an endogenous steroid hormone with an androgenic potency of ~14% that of testosterone

4.2.2 Instrumental

All experiments were performed on a Thermo Finnigan HPLC system coupled with a LXQ linear ion trap mass spectrometer (Thermo Fishier Scientific, San Jose, CA, USA). A scheme of the instrumental setup for the PIESI-MS detection study is shown in Figure 1-1. Briefly, a carrier flow consisting of methanol and water (67/33, v/v) was delivered by a binary LC pump at 300 $\mu\text{L}/\text{min}$, while a 40 μM aqueous solution of ion-pairing reagent was introduced by a secondary pump (Shimadzu LC-6A, Shimadzu, Columbia, MD, USA) at a flow rate of 100 $\mu\text{L}/\text{min}$. The two streams were combined in a low dead volume, Y-type, mixing device and subsequently a total flow of methanol/water (50/50, v/v) containing 10 μM of ion-pairing reagent was introduced into the MS at a flow rate of 400 $\mu\text{L}/\text{min}$. Samples were injected into the HPLC system through a six-port injection valve prior to the mixing device. As a result, the anionic analyte was associated with the dicationic ion-pairing reagent, to form positively charged analyte/ ion-pairing reagent complexes, which could be detected by the MS in the positive ion mode. The MS parameters in the positive ion mode were set as follows: spray voltage, 3 kV; capillary voltage, 11 V; capillary temperature, 350 $^{\circ}\text{C}$; sheath gas flow, 37 arbitrary units (AU); and the auxiliary gas flow, 6 AU. For the chromatographic separations and real sample analysis, an analytical column was inserted between the mixing device and the injection valve (see Figure 1-1). The injection volume was kept at 5 μL for all the experiments. In SRM mode, the normalized collision energy, Q value and the activation time were set at 30, 0.25, and 30 ms, respectively.

The detection limits (LODs) obtained in the negative ion mode was used for comparison to the positive ion mode PIESI results. The MS parameters in this mode were optimized as follows: spray voltage, 4.5 kV; capillary voltage, -32 V; capillary temperature, 350 $^{\circ}\text{C}$; sheath gas flow, 50 arbitrary units (AU); and the auxiliary gas flow,

6 AU. To have equal LC conditions, a carrier flow consisting of methanol and water (50/50, v/v) at 400 $\mu\text{L}/\text{min}$ was introduced into the MS directly without using ion-pairing reagent.

4.2.3 Preparation of Standards

Stock solutions used for LOD determinations were obtained by either diluting the commercial standard solutions to 10 $\mu\text{g}/\text{mL}$ (EtG, EtS, M3G, DHEAS and OxaG) or dissolving the solid material in water to make 50 $\mu\text{g}/\text{mL}$ stock solutions (TG, BS, NTS, DHEAG, AS and 17 β -DHEAS). The M3G and OxaG standards in the sample mixture used for chromatographic separation were at a concentration of 5 $\mu\text{g}/\text{mL}$, while the other metabolites were at 1 $\mu\text{g}/\text{mL}$. The working solution of the internal standard used in the recovery studies had a 50 $\mu\text{g}/\text{mL}$ stock solution. All solutions and urine samples were stored in the dark at -20 $^{\circ}\text{C}$.

4.2.4 PIESI-MS Detection

The detection limit in PIESI-MS was obtained by serial dilution of the standard solution until a signal-to-noise ratio (S/N) of three was noted in 5 replicate injections of each sample. The S/N was calculated by using a Genesis Peak Detection Algorithm with Xcalibur 2.0 software (Thermo Fisher Scientific, San Jose, CA, USA). The PIESI-MS detection was performed both in the selected ion monitoring (SIM) mode and selected reaction monitoring (SRM) mode. In the SIM mode, the m/z of the analyte/ion-pairing reagent complex ion was monitored, while in the SRM mode the most abundant MS/MS fragment ion from the collision induced dissociation (CID) was monitored. The m/z width in the LOD determination study was kept at 5 in both SIM and SRM mode.

4.2.5 Separation and Detection of Glucuro- and Sulfoconjugated Drug Metabolites by

HPLC-PIESI-MS

Separations were performed on an Ascentis Express C18 column (150 mm × 2.1mm, 2.7µm; Sigma Aldrich, St. Louis, MO, USA). The mobile phase composition was (A) 0.1 % formic acid in water, (B) 0.1 % formic acid in methanol. The gradient program was optimized as: 3% B, 0 - 5 min; 3% - 30% B, 5 - 6 min; 30% - 80% B, 6 - 22 min. The MS was operated in SIM mode and the chromatogram was recorded with three separate SIM segments (segment 1, 0 - 5 min, m/z monitored: 449.2, 545.5, 784.4; segment 2, 5 - 12 min, m/z monitored: 785.4; segment 3, 12 - 22 min, m/z monitored: 677.5, 689.4, 691.5, 693.6, 695.5, 787.5). The m/z width of the trapped parent complex was set at 1 in this study due to the close m/z of many steroid metabolites.

4.2.6 Sample Preparation

A solid phase extraction (SPE) method was developed with a Discovery DSC-18 cartridge (1 g sorbent, 50 µm particle size, Sigma Aldrich) for the analysis of these metabolites in urine. The SPE method allows for minimization of matrix effects as well as analyte pre-concentration. The loading solution was composed of 500 µL of urine (obtained from a healthy male volunteer), 20 µL of internal standard stock solution, and 1480 µL of 0.1% formic acid solution spiked with metabolite standards. The extraction protocol was as follows. The cartridges were first washed with 5 mL of ACN and 5 mL of methanol respectively, and subsequently equilibrated with 10 mL of a 0.1% of formic acid aqueous solution. The sample solution was then loaded onto the sorbent, and two steps followed. The cartridges were first washed with 5 mL of HPLC-MS grade water, and then eluted with 8 mL of methanol. The eluent was subsequently diluted with water in volumetric flask to obtain a final volume of 10 mL sample solution prior to injection. Each sample was prepared in triplicate. The final concentrations of internal standard solutions

were kept at 100 ng/mL for all samples. In this study, only a small amount of urine was needed, and it was diluted 20 times prior to injection. The SPE protocol was employed to minimize urine matrix effects.

4.2.7 Recovery Study

The extraction efficiency was investigated in terms of recovery. HPLC-PIESI-MS was employed to test the recovery of the method. The mobile phase consisted of methanol and water (60/40, v/v) containing 0.1% of formic acid. The PIESI-MS was operated in SRM mode with the use of the best ion-pairing reagent. The chromatogram was recorded with three separate segments (segment 1, 0 - 5 min, transition monitored: 785.4 → 658.3; segment 2, 5 - 10 min, transition monitored: 697.5 → 294.3; segment 3, 10 - 25 min, transition monitored: 693.6 → 294.3). In each segment, only the m/z of one daughter ion was monitored. The m/z width of each daughter ion monitored was set at 3. The two metabolites investigated in this study were OxaG and AS. OxaG does not exist in the urine of individuals who have not consumed oxazepam, while AS is present as a natural substance in the urine of all normal individuals. For quantitation, the recovery of OxaG, AS, and the internal standard from the SPE were determined and the relative response factors (HPLC-PIESI-MS) between the internal standard and the metabolites were found.

4.3 Results and Discussion

4.3.1 Ion-Pairing Reagents and Drug Metabolites

The ion-pairing reagents play an essential role in the detection limits obtained using the PIESI-MS approach. The structures for all the tested ion-pairing reagents are shown in Table 4-1. The symmetrical ion-pairing reagents tested here (Table 4-1) were selected because they gave the best performance for anion detection in previous studies.^{28,29,31} The four symmetrical ion-pairing reagents have diverse structures in their

cationic moieties, which includes pyrrolidinium ($C_5(\text{bpyr})_2$), imidazolium ($C_9(\text{mim})_2$ and $C_5(\text{benzim})_2$), and phosphonium ($C_3(\text{tripr})_2$). The two charged moieties of each ion-pairing reagent are separated by an alkyl chain with different lengths. This type of “bolaform” structure makes the ion-pairing reagents somewhat flexible, which has proven to be advantageous in PIESI-MS.^{31,37,45,119} Two unsymmetrical ion-pairing reagents, UDC 1 (unsymmetrical dication 1) and UDC 2 (unsymmetrical dication 2), were designed based on their symmetrical analogues by introducing a long alkyl chain to one end (see Table 4-1). These unique structures give higher surface activity compared to their symmetrical analogues. These surfactant like ion-pairing reagents often show superior performance for anion detection compared to the symmetrical ion-pairing reagents due to enhanced ionization efficiency.¹¹⁹

Table 4-2 gives the structures and masses of eleven tested drug metabolites, along with their abbreviations. Except Oxazepam, all of these drugs are prohibited by World Anti-Doping Agency.¹⁷⁸ These metabolites are glucuronide or sulfate conjugates of the parent drugs. Biologically, they are products of common metabolic pathways in phase II reactions to form polar water soluble conjugate products, which increases their tendency to be excreted in urine.¹⁵⁰

4.3.2 PIESI-MS Detection of Drug Metabolites with the Use of Symmetrical Ion-Pairing

Reagents

Table 4-3 summarizes the absolute LODs of eleven drug metabolites detected in the positive ion mode using symmetrical ion-pairing reagents and in the negative ion mode without using ion-pairing reagents. The best LOD for each compound is highlighted in bold font (Table 4-3). Overall, the negative ion mode was not as sensitive as the PIESI-MS. The detection limits obtained in the negative ion mode was 3 - 20 times worse. It should be noted that the SRM analyses in the negative ion mode were not successfully

conducted due to unstable fragment ion signals. Moreover, it was also observed that the analytes with small m/z ratios, such as EtS, gave worse LODs (m/z: 125.0, LOD: 100 pg) than other, higher mass, sulfated steroids (m/z: 350 ~380, LOD: 10 pg to 20 pg) in the SIM negative ion mode.

The positive ion mode was more suitable for the detection of the tested metabolites than the negative ion mode. For example, when EtS was detected in the SIM positive ion mode with the use of C₅(bpyr)₂ as the ion-pairing reagent, the LOD could be reduced from 100 pg (obtained in the SIM negative ion mode) to 5.0 pg. It was also observed that with the optimal ion-pairing reagents, the PIESI-MS approach could improve the detection limit by several folds in many cases. The performance of four ion-pairing reagents varied significantly in detecting these drug metabolites. This suggests that the structure and/or geometry of ion-pairing reagents play an important role in the observed detection sensitivity for anions. Overall, C₅(bpyr)₂ showed the best overall performance compared to the other three ion-pairing reagents, with the majority of the LODs obtained using C₅(bpyr)₂ fell below 37 pg. The chemical properties of the analytes also affected the detection sensitivity. For example, C₉(mim)₂ was considered one of the best ion-pairing reagents for detecting small organic and inorganic anions in our previous studies,^{28,29} however, it did not perform well in detection of the drug metabolites in this study. Interestingly, detection limits of the sulfated drugs (pK_a < 1) were usually better than the glucuronated drugs (pK_a ~ 4.5). This indicates that the pK_a of the analyte could also affect the observed detection limits. The lower pK_a of these sulfated conjugates results in more anions in the solution phase, which could lead to more analyte/ion-pairing reagents complex formation in solution. A similar phenomenon also was observed in the negative ion mode. Moreover, M3G and OxaG always gave poorer LODs compared to the other compounds. This could result from the presence of a tertiary amine (pK_a ~ 10)

and an imine group ($pK_a \sim 11$) respectively in their structures. These could affect the formation of analyte/ ion-pairing reagent complex.

The SRM mode often enhances analytical specificity and reduces background noise, and as a result, better sensitivity can be often achieved.³¹ However, it was observed in this study that some LODs obtained from the SRM mode were worse than that from the SIM mode. For example, the LOD of NTS detected in the SRM mode with $C_3(\text{triprp})_2$ (LOD: 1000 pg) was 400 times worse than the LOD obtained in the SIM mode (LOD: 2.5 pg). This decreased sensitivity in SRM mode might due to the fact that the product ions generated during the CID process were not stable.³¹

4.3.3 PIESI-MS Detection of Drug Metabolites with the Use of Unsymmetrical Ion-Pairing Reagents

The dicationic ion-pairing reagents with unsymmetrical structures have been recently developed by our group, with the purpose of further improving the sensitivity for anion detection by PIESI-MS.¹¹⁹ In this study, we evaluated the performance of two unsymmetrical ion-pairing reagents, UDC 1 and UDC 2, on the detection sensitivity of the drug metabolites (Table 4-4). As shown in Table 4-4, the unsymmetrical ion-pairing reagents provided improved detection sensitivity for more than half of the tested metabolites (6 out of 11) compared to the symmetrical ion-pairing reagents. The improvement in LODs from symmetrical to unsymmetrical ion-pairing reagents ranged from two to seven times. It was found that the unsymmetrical ion-pairing reagents generally provided greater detection improvements for sulfated steroids, while they gave similar detection limits for the glucuronated metabolites compared to the symmetrical ion-pairing reagents. For example, the LOD of BS was 800 fg with the use of UDC2 in the SRM mode, which was seven times better than the LOD obtained with the best symmetrical ion-pairing reagent (5.5 pg by using $C_5(\text{bpyr})_2$ in SRM mode). On the other

Table 4-3 LODs of the drug metabolites detected in the positive ion mode using symmetrical ion-pairing reagents and in the negative ion mode without using ion-pairing reagents^a

Sample	LOD (pg)										Improvement factor ^b
	C ₅ (bpyr) ₂		C ₅ (benzim) ₂		C ₃ (triprp) ₂		C ₉ (mim) ₂		Negative ion mode		
	SIM (<i>m/z</i> ^d)	SRM (<i>m/z</i> ^e)	SIM (<i>m/z</i>)	SRM (<i>m/z</i>)	SIM (<i>m/z</i>)	SRM (<i>m/z</i>)	SIM (<i>m/z</i>)	SRM (<i>m/z</i>)	SIM (<i>m/z</i>)	SRM (<i>m/z</i>)	
EtG	500 (545.5)	37 (418.3)	150 (607.3)	170 (385.3)	250 (583.4)	250 (187.2)	400 (511.3)	500 (289.3)	100 (221.1)	100 (202.9)	3
M3G	1500 (784.4)	130 (657.4)	1100 (846.4)	1100 (385.3)	10000 (822.5)	15000 (361.1)	1500 (750.4)	1500 (289.3)	800 (460.2)	NA ^c	6
OxaG	180 (785.4)	28 (658.3)	250 (847.3)	100 (385.3)	1200 (823.4)	2500 (361.1)	1200 (751.3)	880 (289.3)	250 (461.1)	NA	9
DHEAG	400 (787.5)	10 (660.5)	60 (849.3)	60 (385.3)	120 (825.6)	400 (361.1)	600 (753.5)	100 (289.3)	70 (463.2)	70 (445.3)	7
TG	190 (787.5)	6.0 (660.5)	40 (849.3)	40 (385.3)	22 (825.6)	190 (361.1)	750 (753.5)	97 (289.3)	30 (463.2)	30 (445.3)	5
EtS	6.0 (449.2)	5.0 (322.2)	75 (511.3)	18 (227.2)	17 (487.3)	17.5 (187.2)	200 (415.3)	500 (289.3)	100 (125.0)	NA	20
DHEAS	7.5 (691.5)	4.5 (214.2)	7.5 (753.6)	5.0 (227.2)	1.2 (729.5)	7.5 (459.3)	5.0 (657.5)	1.2 (387.3)	10 (367.2)	NA	8
AS	8.0 (693.6)	8.5 (294.3)	3.0 (755.6)	5.0 (483.3)	4.0 (731.5)	6.0 (459.3)	45 (659.4)	3.7 (387.3)	12 (369.2)	NA	4
BS	8.0 (689.4)	5.5 (294.3)	7.0 (751.5)	7.0 (227.2)	6.0 (729.5)	750 (459.3)	25 (655.5)	75 (289.3)	16 (367.2)	NA	3
17β-DHEAS	19 (695.5)	19 (294.3)	3.0 (757.5)	5.0 (227.2)	4.5 (733.5)	100 (459.3)	65 (661.5)	150 (289.3)	20 (371.2)	NA	7
NTS	15 (677.5)	4.2 (294.3)	3.8 (739.4)	9.5 (227.2)	2.5 (715.5)	1000 (459.3)	10 (643.4)	60 (289.3)	10 (353.1)	NA	4

^aThe best LOD for each drug metabolite obtained using symmetrical ion-pairing reagents is in bold type.

^bTimes improvement of best LODs obtained using symmetrical ion-pairing reagents vs. LODs obtained in the negative ion mode without using ion-pairing reagents

^cNot detectable

^dThe *m/z* of the analyte/ion-pairing reagent complex ion monitored in SIM mode.

^eThe *m/z* of the most abundant fragment ion generated from the analyte/ion-pairing reagent complex in SRM mode; the precursor ion was the same as the *m/z* of the complex used in SIM mode.

Table 4-4 LODs of the drug metabolites detected in the positive ion mode using unsymmetrical ion-pairing reagents^a

Sample	UDC1		UDC2		Best LODs with symmetrical ion-pairing reagents ^b	Improvement factor (unsymmetrical vs. symmetrical ion-pairing reagents) ^c	Total improvement factor (PIESI-MS vs. negative ion mode) ^d
	SIM (<i>m/z</i>)	SRM (<i>m/z</i>)	SIM (<i>m/z</i>)	SRM (<i>m/z</i>)			
EtG	450 (685.6)	250 (418.4)	150 (563.5)	150 (504.4)	37	0.25	3
	1100 (924.7)	200 (657.5)	1100 (803.6)	1000 (743.7)	130		
M3G	250 (925.7)	90 (798.6)	500 (804.6)	250 (744.7)	28	0.31	9
	75 (927.7)	5.0 (660.5)	220 (805.5)	75 (746.8)	10		
DHEAG	75 (927.7)	8.5 (660.5)	30 (805.5)	30 (746.8)	6.0	0.70	5
	9.0 (589.5)	3.0 (462.4)	2.7 (467.4)	2.1 (408.5)	5.0		
EtS	2.5 (831.7)	1.5 (354.5)	3.5 (709.6)	1.2 (380.4)	1.2	1.0	8
	5.0 (833.6)	3.0 (354.5)	5.0 (711.5)	1.5 (380.4)	3.0		
AS	3.7 (831.7)	3.7 (434.4)	4.0 (707.6)	0.80 (380.4)	5.5	7.0	20
	10 (835.7)	6.0 (434.4)	7.5 (713.6)	1.5 (380.4)	3.0		
17β-DHEAS	5.0 (817.6)	2.5 (434.4)	5.0 (695.5)	1.0 (380.4)	2.5	2.5	10

^aThe best LOD for each drug metabolite obtained using unsymmetrical ion-pairing reagents is in bold type.

^bData was obtained from Table 4-3.

^cTimes improvement of best LODs obtained using unsymmetrical ion-pairing reagents vs. LODs obtained using symmetrical ion-pairing reagents

^dTimes improvement of best LODs obtained using both symmetrical and unsymmetrical ion-pairing reagents in PIESI-MS vs. LODs obtained in the negative ion mode without using ion-pairing reagents.

^eThe *m/z* of the analyte/ion-pairing reagent complex ion monitored in SIM mode.

^fThe *m/z* of the most abundant fragment ion generated from the analyte/ion-pairing reagent complex was monitored in SRM mode. The precursor ion in SRM mode was the same as the *m/z* used in SIM mode.

hand, the LOD of TG was 8.5 pg and 6.0 pg with the best unsymmetrical and symmetrical ion-pairing reagent respectively, which shows a slightly worse detection limit when using the unsymmetrical ion-pairing reagent.

4.3.4 Chromatographic Separation of the Drug Metabolites

The simultaneous separation of drug metabolites, in particular structurally similar analytes is essential for drug testing and analysis. Therefore HPLC coupled with PIESI-MS was used to achieve the separation and highly selective detection/quantification at the same time. Gradient elution was performed in reversed phase mode within 22 min (see Figure 4-1). $C_5(\text{bpyr})_2$ was used for the HPLC-PIESI-MS, since it was shown to have superior performance on the detection of these drug metabolites and is also commercially available. The MS was operated in SIM mode with three detection segments. The drop in baseline at 5 min is caused by switching from segment 1 to segment 2 (see Figure 4-1). As shown in Figure 4-1, the selected drug metabolites were well separated except for two pairs, EtS/EtG and BS/NTS. However, because of different m/z values for each pair, a complete chromatographic resolution was not necessary.

4.3.5 Urine Sample Analysis

4.3.5.1 Recovery Study

A SPE protocol was carried out with the use of human urine matrix spiked with the drug metabolites at two different concentrations (50 ng/mL and 400 ng/mL respectively). OxaG and AS were selected as representatives of these drug metabolites. As shown in the extracted ion chromatogram (EIC) of the urine blank (Figure 4-2 and 4-3), the interference peaks in the urine blank were negligible. The amount of AS naturally existing in urine was subtracted from its total amount when calculating the concentrations of spiked AS. The results of the recovery study are shown in Table 4-5. The extraction efficiency of the internal standard was determined to be 100%, and therefore it was

directly used for the calibration of OxaG and AS. The response factors of AS and OxaG in relative to the internal standard were measured to be 1.02 ± 0.02 and 0.20 ± 0.02 respectively. These values were reasonable considering the structural similarity between the AS and the internal standard, as well as the structural difference between the OxaG and the internal standard. The recovery yields of these two standards were obtained based on their response factors. As shown in Table 4-5, the recoveries of OxaG and AS were 90% (RSD, 15%) and 107% (RSD, 7.9%) respectively at the low concentration, while they were 89% (RSD, 4.5%) and 98% (RSD, 3.5%) respectively at the high concentration. The SPE protocol is suitable to be employed for further quantitative analysis. The concentration of AS that existed naturally in this urine sample was determined to be 1.2 $\mu\text{g/mL}$. This concentration is consistent with reported AS concentrations in the urine of a healthy male ($\sim 1.3 \mu\text{g/mL}$).¹⁷⁷

Table 4-5 Recovery results of standard drug metabolites from urine spiked at two concentration levels

drug metabolite	Spiked standard			Spiked standard		
	Concentration (ng/mL)	Recovery (%)	RSD (%)	Concentration (ng/mL)	Recovery (%)	RSD (%)
OxaG*	50	90%	15%	400	89%	4.5%
AS*	50	107%	7.9%	400	98%	3.5%

*OxaG: oxazepam glucuronide; AS: androsterone sulfate

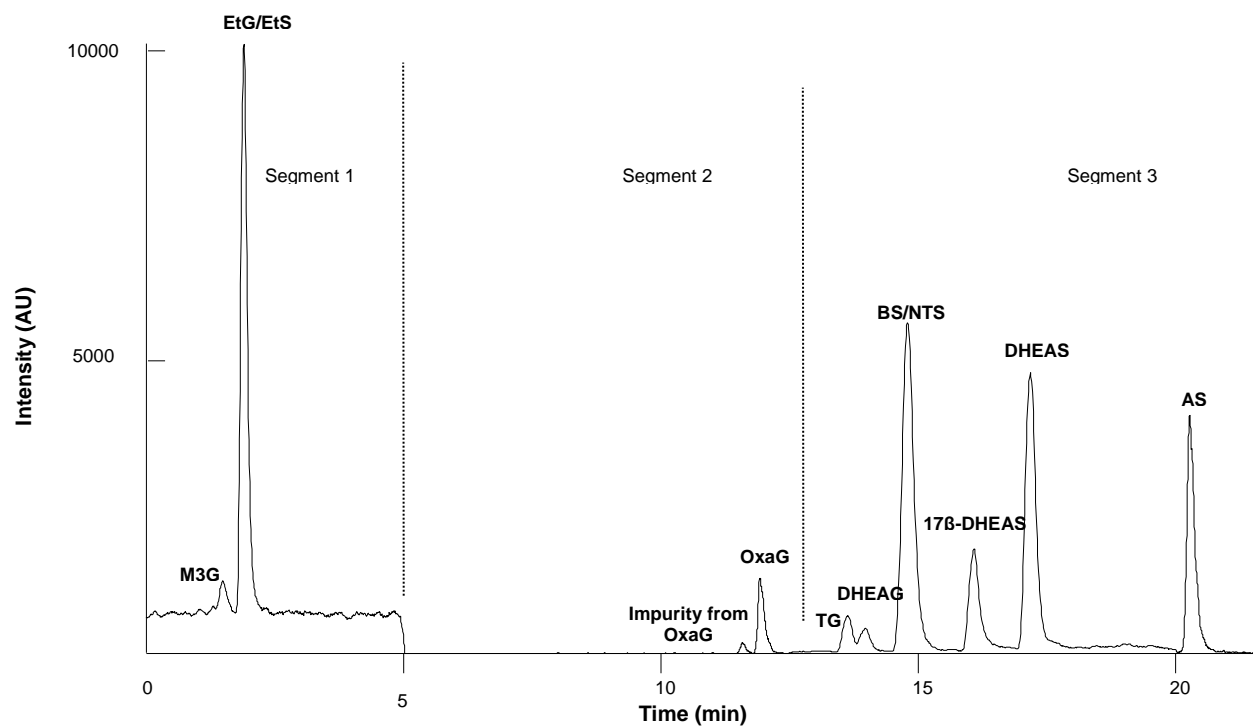


Figure 4-1 Total ion chromatography of separation of eleven drug metabolites by HPLC-PIESI-MS. Column: Ascentis™ C18 (2.7 μm, 2.1 x 150 mm); mobile phase A: 0.1% formic acid in water (pH=2.7), B: 0.1% formic acid in methanol; gradient elution conditions: 0-5 min, 3% B, 5-6min, 3%-30% B, 6-22 min, 30% -80% B; MS pump flow rate: 300 μL/min; injection volume: 5 μL. The separation was carried out with the outperformed ion-pairing reagent, C₅(bpyr)₂ monitored in SIM mode with three sections.

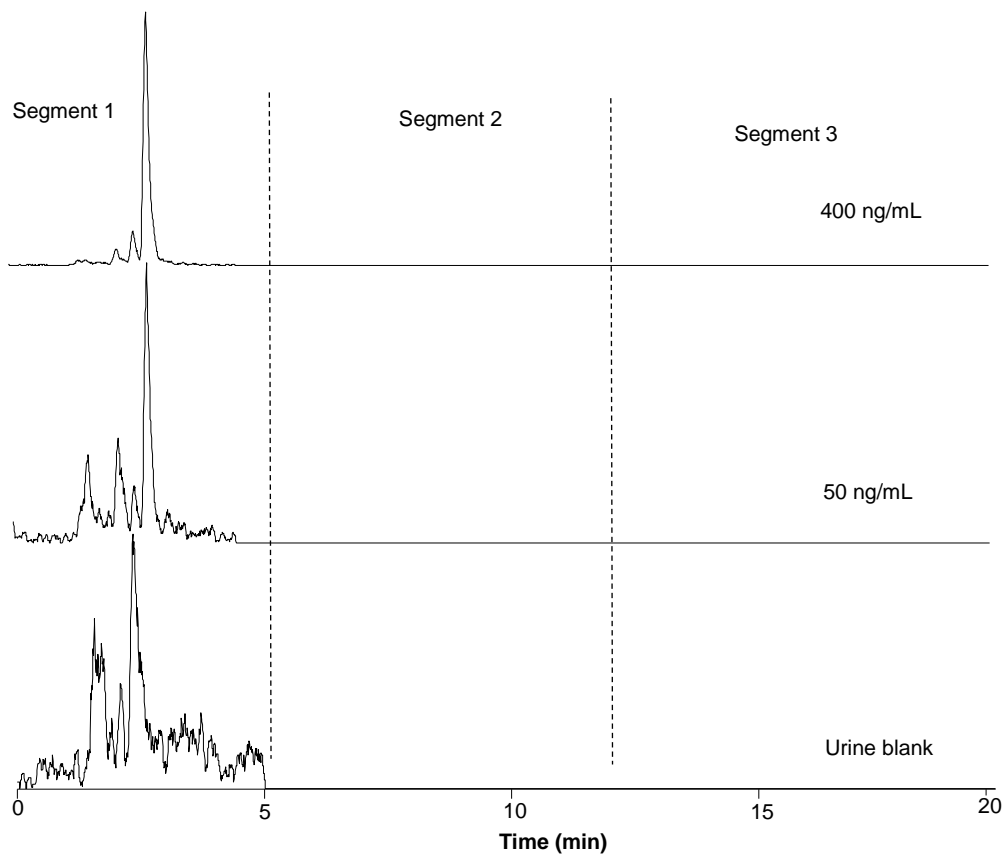


Figure 4-2 Extracted ion chromatography of OxaG by HPLC-PIESI-MS. Column: Ascentis™ C18 (2.7 μm , 2.1 x 150 mm); mobile phase A: 0.1% formic acid in water (pH=2.7), B: 0.1% formic acid in methanol; isocratic elution condition: 60% B; MS pump flow rate: 300 $\mu\text{L}/\text{min}$; injection volume: 5 μL ; ion-pairing reagent: $\text{C}_5(\text{bpyr})_2$. The m/z of fragment of the OxaG/ $\text{C}_5(\text{bpyr})_2$ complex at 658.3 was monitored in SRM mode in section 1 (0 - 5 min). The final concentrations of OxaG in urine samples prior to injection were 40 ng/mL and 500 ng/mL respectively.

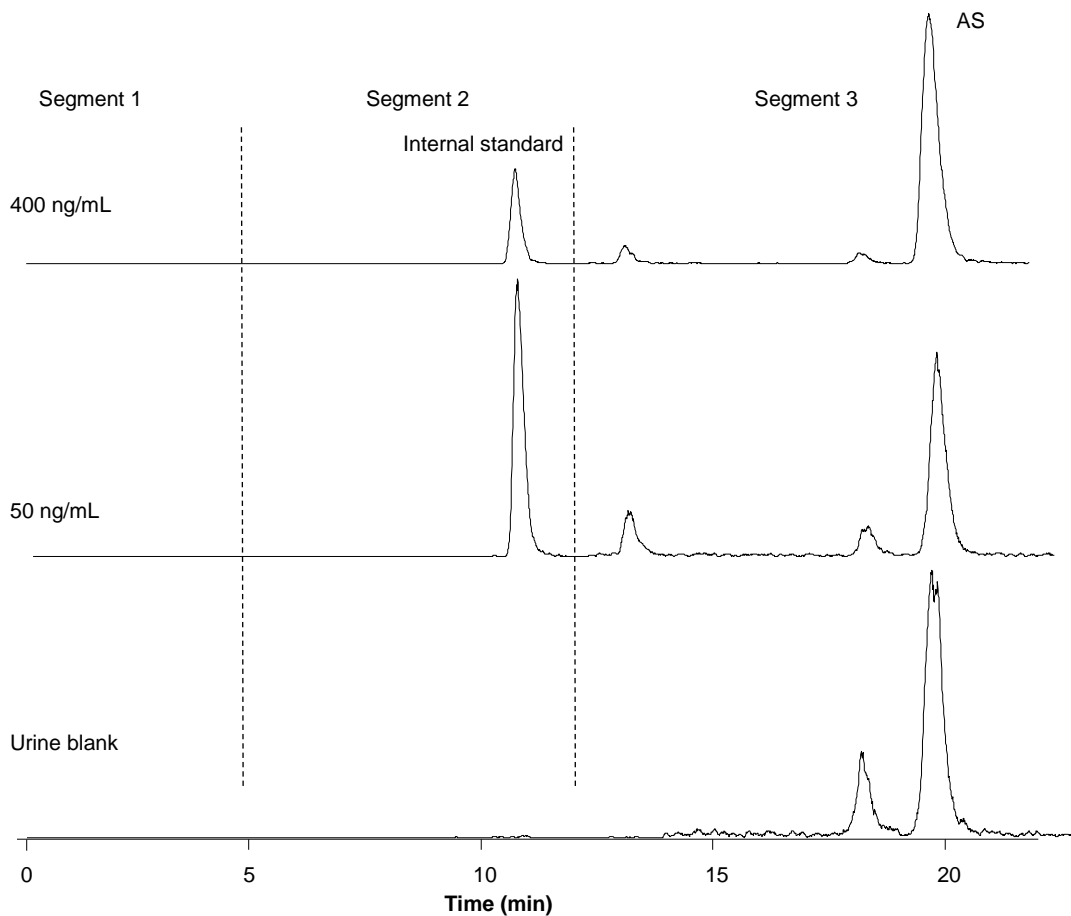


Figure 4-3 Extracted ion chromatography of AS and internal standard by HPLC-PIESI-MS. Column: Ascentis™ C18 (2.7 μm , 2.1 x 150 mm); mobile phase A: 0.1% formic acid in water (pH=2.7), B: 0.1% formic acid in methanol; isocratic elution condition: 60% B; MS pump flow rate: 300 $\mu\text{L}/\text{min}$; injection volume: 5 μL ; ion-pairing reagent: $\text{C}_5(\text{bpyr})_2$. The m/z of fragment of the AS/ $\text{C}_5(\text{bpyr})_2$ and internal standard/ $\text{C}_5(\text{bpyr})_2$ were monitored (both were 294.3) in SRM mode in section 2 (5 - 12 min) and section 3 (12 - 22 min) respectively. The final concentrations of AS in urine samples prior to injection were 50 ng/mL and 400 ng/mL respectively. The final concentrations of internal standard were all 100 ng/mL in all these samples.

4.3.5.2 A Comparison in Detection Sensitivity between PIESI-MS and Other HPLC-MS Methodologies

The determination of the detection limit of each drug metabolite in urine samples was performed in the same SPE, LC and MS conditions as these of recovery study experiments. Table 6 compares the absolute LODs (pg) of steroid metabolites obtained using the PIESI-MS approach with other reported HPLC-MS methodologies.^{155,157,160,171,177} Compared to other HPLC-MS based methods, PIESI-MS provided detection limits from one to three orders of magnitude better for the detection of steroid glucuronides and sulfates. It should be noted that most of the commonly used HPLC-MS methodologies employ sample pre-concentration to obtain a higher sensitivity. However, this technique has no effect on improving instrumental detection limits, which is the main focus of this study. Moreover, the detection limits reported in this study could be further enhanced with the use of more sensitive mass analyzers and detectors (e.g., triple quadrupole mass analyzer).

4.4 Conclusions

The method developed based on PIESI was shown to be sensitive and effective for the analysis of performance-enhancing drugs and drugs of abuse by detecting their glucuronide and sulfate conjugates. LODs in the sub-pg range were obtained for the metabolites, which were 3 to 48 times improvement compared to the negative ion mode detection. It was also found that the two unsymmetrical ion-pairing reagents provided further sensitivity enhancement and complimentary performance in detecting these drug metabolites. For further quantitative analysis, a method based on HPLC-PIESI-MS was successfully developed for the simultaneous separation of these eleven drug metabolites under the optimized conditions. A SPE protocol can be carried out to eliminate any matrix effects in the analysis of urine samples, which would provide more precise and accurate

quantification for the analysis of these drug metabolites. Overall, the developed method could be useful for drug testing in clinical laboratories.

Table 4-6 Comparison of instrumental LOD (pg) of steroid glucuronides and sulfates measured by PIESI-MS method as to other HPLC-MS methodologies performed in the negative ion mode^a

Ionization mode, MS analyzer used	Scan mode	Absolute LOD ^f (pg)	Reference
ESI, IT ^b	SRM	15-300	[153]
ESI, QTOF ^c	SRM	200-1000	[155]
ESI, QTOF	SRM	50-500	[158]
API, QqQ ^d	SRM	40000-50000	[169]
SSI ^e , IT	SIM	40-800	[175]
PIESI, IT	SIM/SRM	0.8-6.0 ^g	current method

^aLODs represent instrumental detection limits. For the methods using SPE to concentrate samples for analysis, the LODs have been corrected by the SPE concentration factors.

^bIon Trap; ^cQuadrupole coupled with Time of Flight; ^dTriple Quadrupole; ^eSonic Spray Ionization

^fOnly the LODs for steroid glucuronides and sulfates that belong to the same categories as in this study are considered in these references.

^gThe LODs for these steroid metabolites were measured in the human urine matrix under the same SPE, LC and MS conditions as the recovery study.

Chapter 5

Quantitative Analysis of Dicamba Residues in Raw Agricultural Commodities with the Use of Ion-Pairing Reagents in LC-ESI-MS/MS

Abstract

A sensitive and selective HPLC-MS/MS method was developed for the quantitative analysis of dicamba residues in raw agricultural commodities (RACs). Instead of analysis in the traditionally used negative electrospray ionization (ESI) mode, these anionic compounds were detected in positive ESI with the use of ion-pairing reagents. In this approach, only a small amount (60 μM) of a commercially available dicationic ion-pairing reagent was introduced into the post-column sample stream. This method has been validated in six different types of RACs including corn grain, corn stover, cotton seed, soybean, soy forage and orange with satisfactory quantitative accuracy and precision. The limits of quantitation (LOQ) values for these analytes were 1.0 to 3.0 $\mu\text{g}/\text{kg}$. The standard curves were linear over the range of the tested concentrations (3.0 to 500 $\mu\text{g}/\text{kg}$), with correlation coefficient (r) values ≥ 0.999 . Evaluation of ionization effects in RAC matrix extracts using diluent blanks for comparison showed no significant matrix effects were present.

5.1 Introduction

Dicamba (3,6-dichloro-2methoxybenzoic acid), a systematic broad-spectrum auxin-type herbicide, has been used for efficient control of most broadleaf weeds in a variety of crops for more than 40 years.¹⁷⁹ Due to the presence of heterogeneous crop matrix components (i.e., sugar, carbohydrate, starch, macromolecule, pigment, fat and structurally similar compounds), analysis of dicamba residues in RACs can be an extremely challenging task.¹⁸⁰ The polar nature and high water solubility of dicamba

residues make their selective extraction and chromatographic resolution from these potentially interfering components very difficult. The diversity of various RAC types and composition further complicates the extraction as each matrix can have unique properties and interfering compounds. Established methods for dicamba residue analysis are based on gas chromatography coupled with electron capture detection (GC-ECD) as adopted by Environmental Protection Agency (EPA) in 1993.¹⁸¹ These methods often require an additional sample derivatization step, which at the low concentrations normally has several limitations and often results in irreproducible yields, multiple impurities and an increased analysis time.¹⁸² A variety of other analytical methods also have been developed for the analysis of dicamba residues, including GC-MS,¹⁸³ enzyme-linked immunosorbent assay,¹⁸⁴ micellar electrokinetic capillary chromatography (MEKC),¹⁸⁵ capillary liquid chromatography with UV detection,¹⁸⁶ and HPLC coupled with UV¹⁸⁷ or MS detection.^{180,188-190} These methods generally suffered from low sensitivity, which limits their utility for trace residue analysis.

In recent years, HPLC-MS equipped with electrospray ionization (ESI) interface has become the preferred platform for the simultaneous analysis of pesticide residues without derivatization, due to advantages of improved throughput, selectivity, and sensitivity.¹⁹¹ Generally, applying tandem MS instrumentation (MS/MS) adds further selectivity to the MS detection of compounds in complex RACs. However, analytes with low molecular masses and relatively high polarities pose a general problem to LC-MS/MS sensitivity and selectivity when monitored in the conventionally used negative ESI.¹⁹² These analytes often possess poor ionization efficiency. Impacts on MS sensitivity from often abundant background noise in the low-mass range present additional challenges for low mass dicamba residues. To minimize these factors, we proposed a novel approach with the use of ion-pairing reagent for the sensitive and selective analysis of dicamba

residues in RACs. Briefly, it involves the use of specially designed and structurally optimized ion-pairing reagents to pair post-column with the negatively charged analyte.^{12,29,118} The subsequently formed positively charged complexes can be detected and quantified in positive ion mode (see Figure 5-1). This technique has several advantages over the routinely used HPLC-MS/MS with negative ESI methods. It moves the detection of analyte from a low m/z region, where the background noise is high, to a higher and more selective m/z region where the background noise is low. Further, the ionization efficiency of the paired analyte is enhanced as shown in previous mechanism studies.^{37,119} In addition, the fragmentation pattern often offers more compound-specific fragment ions for MRM, which eliminates interfering matrix compound peaks and reduces MS background noise. In this work, we evaluated the applicability of using ion-pairing reagent for the sensitive, selective and high throughput analysis of dicamba residues in different types RACs including corn grain, corn stover, cotton seed, soybean, soy forage and orange. Dicamba and its major metabolites, 2,5-dichloro-3-hydroxy-6-methoxybenzoic acid (5-OH dicamba) and 3,6-dichlorosalicylic acid (DCSA) were detected using a commercially available ion-pairing reagent. The developed HPLC-ESI - MS/MS method was validated in terms of method limit of detection (LOD), limit of quantitation (LOQ), selectivity, accuracy and precision in these six different types of RACs. The ionization effects using this method were also evaluated by infusion of a standard solution at the post-connector position and were compared to those of the diluent blank.

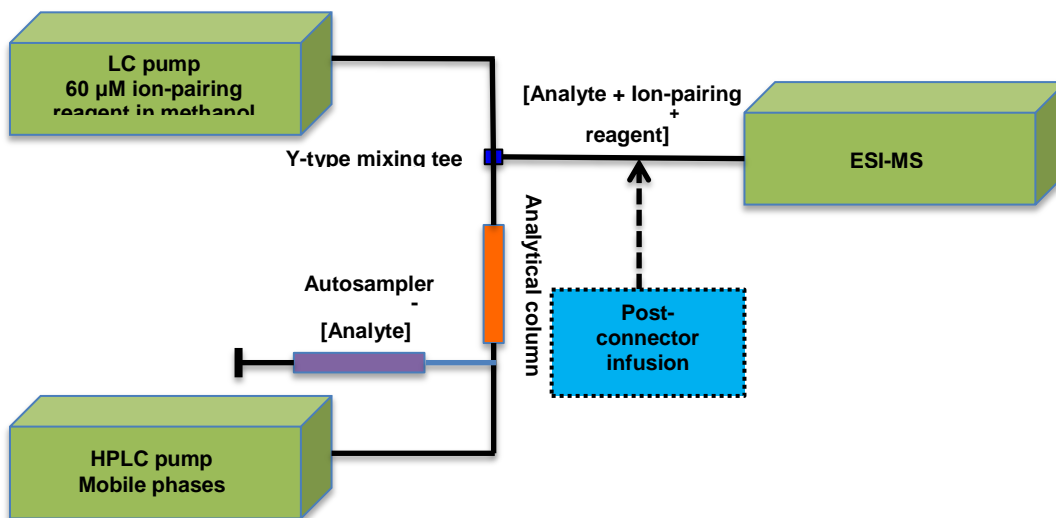


Figure 5-1 Instrumental setup of HPLC-ESI-MS/MS. The dotted lines represent the position where the standard solution was infused into the system in the matrix effects evaluation experiments.

5.2 Experimental

5.2.1 Chemicals and Solvents

Analytical standards (>95%) of dicamba, DCSA and 5-OH dicamba, along with their stable-isotope labeled internal standards: ($^{13}\text{C}_6$)dicamba, ($^{13}\text{C}_6$)5-OH dicamba and ($^{13}\text{C}_6$)DCSA were supplied by Monsanto (St. Louis, MO, USA). Their structures are shown in Table 5-1. Individual stock standard solutions of 1000 $\mu\text{g}/\text{mL}$ were prepared separately with ethanol. The mixed intermediate calibration solution of 1.0 $\mu\text{g}/\text{mL}$ was prepared by dilution of the appropriate amount of stock solutions with 1 M hydrochloric acid (HCl) in H_2O . This mixed intermediate calibration solution was used for the preparation of working calibration solutions in the range of 3 – 500 ng/mL . A mixed internal standard (IS) working solution was freshly prepared at a concentration of 12.5

ng/mL in 50% ACN in acidified water the day to be used for sample preparation. HPLC grade methanol, water and acetonitrile (ACN) were purchased from Burdick & Jackson (Muskegon, MI, USA) or J.T. Baker (Center Valley, PA, USA). Other ACS grade solvents, ethanol, isooctane and ethyl acetate were purchased from Fisher Scientific (Pittsburgh, PA, USA). LC-MS grade formic acid, as well as the ion-pairing reagent, 1,5-pentanediy-bis(1-butylpyrrolidinium) difluoride solution (2.5 mM) were purchased from Sigma-Aldrich (St. Louis, MO, USA). Optima grade HCl (32-35%) was purchased from Fisher Scientific. A 60 μ M of the C₅(bpyr)₂-2F solution was prepared by diluting the commercial solution in methanol.

5.2.2 Matrices Tested

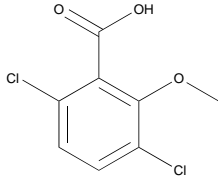
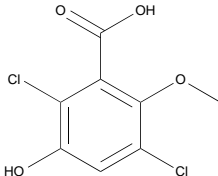
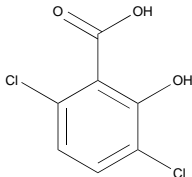
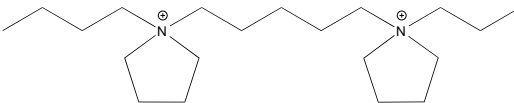
Six representative raw agricultural commodities (RACs), corn grain and stover (dry), soybean forage (wet), soybean seed and cotton seed (oily), and whole oranges (acidic) were selected to represent all matrix groups defined by the SANCO guidelines.¹⁹³ RACs were collected from residue field test plots at multiple locations using normal regional agricultural harvest practices. Oranges were purchased from a local grocery store (St. Louis, MO, USA).

5.2.3 Sample Preparation

RAC matrices were milled to appropriate homogeneity to allow reproducible measurement of 100-mg subsamples using a two-step fine milling method.¹⁹⁴ The milled matrix was weighed into 96-well format tubes followed by the addition of an acidified 40% ACN solution containing stable-labeled internal standards for all three analytes. The sample tubes were capped and agitated on a high-speed shaker for extraction. An aliquot of the extract was transferred and hydrolyzed in 1 M HCl at 95 °C. The hydrolysate was partitioned with 20:80 ethyl acetate/isooctane. The organic phase was transferred, dried

under nitrogen, and reconstituted in a 10:90 methanol/H₂O solution containing 0.2% formic acid.

Table 5-1 Chemical names, structures and atomic mass units of analytes and ion-pairing reagent used in this study

Compound name	Abbreviation	Structure*	Atomic mass units
3, 6-dichloro-2-methoxybenzoic acid	Dicamba		220
2,5-dichloro-3-hydroxy-6-methoxybenzoic acid	5-OH dicamba		236
3,6-dichlorosalicylic acid	DCSA		206
1,5-pentanediy-bis(1-butylpyrrolidinium)	C ₅ (bpyr) ₂		324.3

*Stable isotop-labeled internal standards of the three analytes have six ¹³C on the benzene ring carbons

5.2.4 Matrices Tested

Six representative raw agricultural commodities (RACs), corn grain and stover (dry), soybean forage (wet), soybean seed and cotton seed (oily), and whole oranges (acidic) were selected to represent all matrix groups defined by the SANCO guidelines.¹⁹³ RACs were collected from residue field test plots at multiple locations using normal regional agricultural harvest practices. Oranges were purchased from a local grocery store (St. Louis, MO, USA).

5.2.5 Sample Preparation

RAC matrices were milled to appropriate homogeneity to allow reproducible measurement of 100-mg subsamples using a two-step fine milling method.¹⁹⁴ The milled matrix was weighed into 96-well format tubes followed by the addition of an acidified 40% ACN solution containing stable-labeled internal standards for all three analytes. The sample tubes were capped and agitated on a high-speed shaker for extraction. An aliquot of the extract was transferred and hydrolyzed in 1 M HCl at 95 °C. The hydrolysate was partitioned with 20:80 ethyl acetate/isooctane. The organic phase was transferred, dried under nitrogen, and reconstituted in a 10:90 methanol/H₂O solution containing 0.2% formic acid.

5.2.6 HPLC-ESI-MS/MS

The system consisted of a Shimadzu Prominence™ 20A HPLC (Tokyo, Japan) with a quaternary pump, an AB Sciex API 5000 triple quadrupole mass spectrometer (Ontario, Canada) equipped with turbo-V ionization source, a HPLC switching valve (Sigma Aldrich, St. Louis, MO, USA) and a Y-type microvolume connector (Valco, Houston, TX, USA). All runs were acquired and processed using the Sciex Analyst™ software (version 1.6.2). Chromatographic separations were carried out on a Halo C8 column (50 mm x 2.1 mm x 2.7 µm, Mac-Mod, Chadds Ford, PA, USA) at 50 °C. The

following gradient profile using 0.2 % formic acid in H₂O as mobile phase A and 0.2% formic acid in methanol as mobile phase B was employed: 0-2 min, 15% B; 2-3 min, 15% - 30% B; 3-7 min, 30% - 50% B; 7-7.5 min, 50% - 90% B; followed by a 3.5-minute washing step at 90% B; then a 2-minute equilibrium step with the initial conditions. The flow rate was constantly set at 0.3 mL/min, except for the column-wash step. In this step, a flow rate of 1 mL/min was used instead. The post-column derivatization took place at the center of the Y-type connector, where a 60 μM of C₅(bpyr)₂ solution in methanol delivered by pump C was well mixed with the sample stream. The flow rate of pump C was constantly set at 0.1 mL/min. The autosampler temperature was set at 4 °C and the injection volume were 25 μL for all samples. The mass spectrometer was operated in positive ionization mode, and data were acquired in the multi-selected reaction monitoring (MRM) mode with one quantitative and one confirmatory transition per analyte. The MS data was collected in two separate periods: 5-OH dicamba in the first period with duration time of two minutes, DCSA and dicamba in the second period with duration time of three minutes. The eluent in the first two minutes was diverted into waste, and the total MS data collection time was five minutes with a 120-second delay time. The ionization source parameters were set the same in both periods: source temperature, 500 °C; voltage, 4500 V; curtain gas, 10 units; collision gas, 12 units; nebulizer gas 1, 70 units; nebulizer gas 2, 70 units; scan time, 150 milliseconds. The quantitative and confirmative ion transitions and their potentials for each analyte are shown in Table 5-2.

Table 5-2 Optimized MS/MS parameters for both quantitative and confirmatory transitions of the three analytes

Analyte ¹	Precursor ion Q1 (m/z) ²	Product ion Q3 (m/z) ²	Declustering potential (V)	Collision energy (V)
5-OH dicamba	432.3	219.0	300	45
DCSA	402.3	214.3	270	34
Dicamba	416.3	203.0	300	45
Confirmatory ions				
5-OH dicamba	434.3	204.3	300	45
DCSA	404.3	189.3	270	34
Dicamba	416.3	188.0	290	75

¹Entrance potential and collision cell exit potential for all transitions were the same, 10 V and 12 V respectively.

²Mass-to-charge ratio

5.2.7 Method Validation Study

The method validation study was carried out in accordance with SANCO guidelines.¹⁹³ Linearity of the method was evaluated by analyzing 12 standard solutions in duplicate at each concentration level. The calibration curves were constructed by plotting the peak area ratio of analytes to IS versus analyte concentrations using a 1/x weighted linear regression model. The limit of detection (LOD) is the minimal concentration from which the presence of the analyte can be deduced with reasonable statistical certainty, giving a minimum signal-to-noise ratio of 3:1 in five replicates. The limit of quantification (LOQ) is established as the lowest fortification concentration with five replicates, giving a signal-to-noise ratio of 10:1, which could be measured with a

mean recovery at or within 70-120% of the back-calculated nominal value and precision \leq 20% RSD (relative standard deviation).

The accuracy and precision of all the analytes in QC samples were evaluated by analyzing fortified blank samples at low, medium and high concentrations, and were determined in six replicates in the same day. This experiment was performed at three spiking levels: 10, 100 and 400 ng/mL in six different types of RACs. The accuracy was determined via comparison of the back-calculated concentration and the fortified concentration in percentage and the precision was defined as the RSD of the back-calculated concentration. Acceptance criteria for accuracy and precision were set at 70 - 120% recovery and \leq 20% RSD.

5.2.8 Ionization Effects Evaluation

The ionization effects were evaluated by infusing a 10 ng/mL of mixed standard solution (dissolved in 10/90 methanol:H₂O containing 0.2% formic acid) at the post-connector position (see Figure 5-1, dotted line). The standard solution was introduced by a separate pump (Shimadzu Prominence™ 20A, Tokyo, Japan) at a constant flow rate of 50 μ L/min. The chromatographic and MS/MS conditions of this experiment were identical to those described in the Experimental section. Two of the most complex RAC matrices encountered, corn stover and soybean forage, were used for this assessment. The post-extraction fortified matrix blank was compared to the fortified sample reconstitution solution, 10/90 methanol:H₂O containing 0.2% formic acid.

5.2.9 Data Evaluation

Analyte concentrations were calculated using the Analyst software, and were reported as μ g/kg of sample.

5.3 Results and discussion

5.3.1 Optimization of ESI-MS/MS

One of the best performing ion-pairing reagent, $C_5(\text{bpyr})_2 \cdot 2F$ was selected for the analysis based on previous studies.^{29,31} This reagent was originally synthesized in the bromide form, and was ion-exchanged to the fluoride form to maximize its association with anionic analytes.²

The mass spectrometric parameters (i.e., precursor and product ions used in MRM and optimized voltages) of dicamba and its two major metabolites are shown in Table 5-2. The optimization of MS/MS parameters were conducted by directly infusing a mixed solution containing the individual analyte and the ion-pairing reagent, $C_5(\text{bpyr})_2 \cdot 2F$ (molar ratio, 1:10) at a flow rate of 20 $\mu\text{L}/\text{min}$ along with the mobile phases. The dominant molecular ion of dicamba complex, $[C_5(\text{bpyr})_2 + \text{dicamba} - \text{H}]^+$ (m/z 543.3) was dissociated and gave rise to a main product ion $[C_{13}\text{H}_{26}\text{N}^+ + \text{dicamba}]^+$ (m/z 416.3), which was generated from the cleavage in in-source collision induced dissociation (CID) of the $C_\alpha\text{-N}$ bond in $C_5(\text{bpyr})_2$ part of the complex. The $[C_{13}\text{H}_{26}\text{N}^+ + \text{dicamba}]^+$ ion was selected as the precursor ion in this study because it gave better selectivity and less matrix interfering peaks in the chromatography. This precursor ion was subsequently CID fragmented to produce structurally specific product ions. The two most sensitive fragment ions, m/z 203.0 and 188.0 were selected as the quantitative and qualitative product ions for dicamba, respectively. The structures of these two product ions corresponded to $[\text{dicamba} - \text{OH}]^+$ and $[\text{dicamba} - \text{OH}^- - \text{CH}_3]^+$ ion, respectively. Similar fragmentation pattern was observed for the analogous metabolite, 5-OH dicamba. The most abundant fragment of $[C_{13}\text{H}_{26}\text{N}^+ + 5\text{-OH dicamba}]^+$, m/z 219.0 (5-OH dicamba losing a $-\text{OH}$ in carboxylic acid group) was used for the quantitative analysis. The second most sensitive fragment of $[C_{13}\text{H}_{26}\text{N}^+ + 5\text{-OH dicamba}]^+$, m/z 204.3 (5-OH dicamba losing a $-\text{OH}$ in

carboxylic acid group and a $-CH_3$ in the methoxyl group) was used for confirmation. For DCSA, the most sensitive fragment ion of $[C_{13}H_{26}N^+ + DCSA]^+$ was m/z 214.3, which was used as the quantitative ion. The production ion, m/z 214.3 was generated from the $C_{13}H_{26}N^+$ moiety from the ion-pairing reagent associating with the hydroxyl group attached to the benzene ring in DCSA and a proton. The second most sensitive fragment of $[C_{13}H_{26}N^+ + DCSA]^+$, m/z 189.3 (DCSA losing a hydroxyl groups) was used for confirmation.

5.3.2 Optimization of Chromatographic Separation Conditions

After testing several reverse phase based columns, it was found that a Halo C8 based stationary phase (50 mm x 2.1 mm x 2.7 μ m, Mac-Mod, Chadds Ford, PA, USA) provided sufficient resolution and retention for the chromatographic separation of the three analytes. The results also showed that methanol and H_2O containing 0.2% formic acid as the mobile phase system provided improved peak shapes, shortened elution time, and coincided with higher MS responses for all three analytes. As can be seen in Figure 5-2, all three analytes were well separated in 7 minutes with good peak shapes. Dicamba had the greatest signal response than 5-OH dicamba and DCSA, indicating the structures of analytes play an important role in their detection sensitivity with the use of ion-pairing reagent.

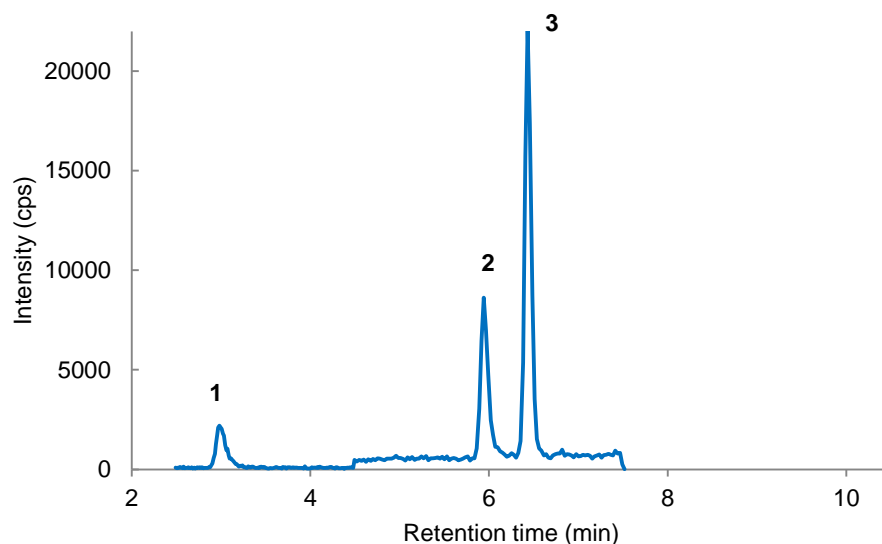


Figure 5-2 Extracted ion chromatograms (EIC) for separation of the three analytes in a standard mixture. The standard solution was injected into the HPLC-MS/MS system using the developed method. The injection volume of the method was 25 μ L. The chromatographic and MS/MS conditions are shown in section 5.2.4. Compound identification: 1, 5-OH dicamba; 2, DCSA; 3, dicamba.

5.3.3 Method Validation

5.3.3.1 Selectivity

Corn stover and soybean forage were investigated as the most complex matrices in this study, and their EICs were used as representatives to exhibit the selectivity of the current method. The chromatograms obtained from corn stover and soybean forage blank, corn stover and soybean forage blank fortified with 10 μ g/kg of the three analytes, along with their IS chromatograms are shown in Figure 5-3. Due to the efficient sample preparation and separation, as well as the high selectivity of MRM, there was no endogenous interference and no cross-interference observed at the retention windows of these analytes in the chromatograms.

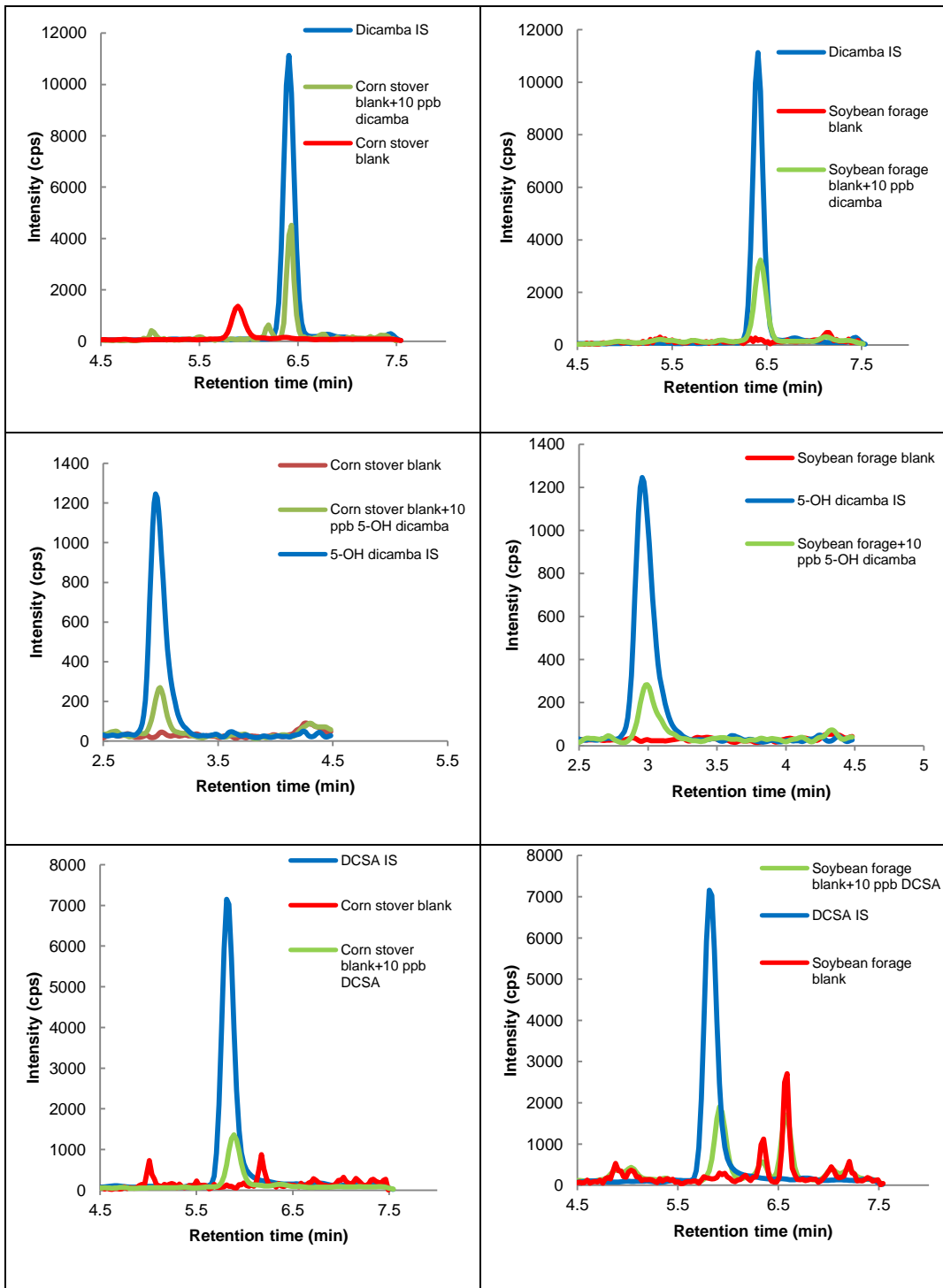


Figure 5-3 Extracted ion chromatograms (EIC) of extracted corn stover blank (left three chromatograms) and soybean forage blank (right three chromatograms). The EICs of the extracted matrix blank, the extracted matrix blank fortified with 10 ppb of the analyte, and the EIC of its associated internal standard were shown in each individual graph. The top two graphs show the selectivity of dicamba in the two extracted matrix blank. The middle two graphs were for 5-OH dicamba, and the graphs for DCSA were shown in the bottom.

The chromatographic and MS/MS conditions were the same as Figure 5-2, and were described in section 5.2.4.

5.3.3.2 Linearity and Sensitivity

All calibration curves exhibited good linearity in the range from 3 to 500 µg/kg with correlation coefficient (r) higher than 0.999. The LOD and LOQ values for dicamba were 0.3 and 1.0 µg/kg, respectively; 1.0 and 3.0 µg/kg, respectively for 5-OH dicamba; 0.6 and 2 µg/kg, respectively for DCSA in these matrices. And they were 2 to 10 folds more sensitive as compared to the previously optimized negative ESI detection method.¹⁹⁵

5.3.3.3 Accuracy and Precision

The results of the accuracy and precision of the three analytes fortified at three different concentration levels are summarized in Table 5-3. The lowest fortified concentration was set at 10 µg/kg as the limit of method validation level (LLMV), not the method LOQs. This is due to the fact that the MRL of an individual dicamba residue regulated in United States is down to 10 µg/kg.¹⁷⁹ The accuracy ranged between 85% and 118%, while the precision ranged from 1% to 10%. All accuracy and precision values were acceptable for quantitative analysis.¹⁹³

Table 5-3 Accuracy and precision values for all analytes

Analyte	5-OH Dicamba		DCSA		Dicamba	
	Mean		Mean		Mean	
Fortified sample matrix ¹	Accuracy	RSD(%)	Accuracy	RSD(%)	Accuracy	RSD(%)
	(%)		(%)		(%)	
Corn grain 10 µg/kg	101	10	101	3	100	3
Corn grain 100 µg/kg	95	2	98	3	101	1
Corn grain 400 µg/kg	95	5	97	2	103	1
Corn stover 10 µg/kg	103	2	106	5	113	7
Corn stover 100 µg/kg	98	5	92	4	100	2
Corn stover 400 µg/kg	99	5	97	1	102	2
Soybean seed 10 µg/kg	88	6	99	2	89	7
Soybean seed 100 µg/kg	85	4	94	3	97	3
Soybean seed 400 µg/kg	85	5	91	4	99	3
Soybean forage 10 µg/kg	86	7	118	1	104	2
Soybean forage 100 µg/kg	95	2	90	4	100	2
Soybean forage 400 µg/kg	100	2	89	4	99	1
Cotton seed 10 µg/kg	102	1	110	3	100	1
Cotton seed 100 µg/kg	97	3	93	3	104	3
Cotton seed 400 µg/kg	97	3	90	3	102	1
Orange 10 µg/kg	102	10	118	7	100	4
Orange 100 µg/kg	96	2	92	1	100	3
Orange 400 µg/kg	97	7	92	2	99	2

¹n=6, six replicates at each fortification level

5.3.3.4 Ionization Effects Evaluation

Ionization effects were evaluated using the two most difficult RAC matrices, corn stover and soybean forage as representatives. In this experiment, a 10 µg/kg mixed standard solution was continuously infused at the post-connector position of the HPLC-PIESI-MS/MS system (see Figure 5-1, dotted lines). The extracted corn stover blank (without IS) was injected into the system and analyzed by the developed HPLC-ESI-MS/MS method. The diluent (0.2% formic acid in 10:90 methanol/H₂O) was also injected for comparison. Ideally, the continuous post-connector infusion of the standard solution produces leveled and smooth curves without any injections or with injections of solvent blanks. Any positive and/or negative peaks observed are caused by co-eluting components from the injected sample matrix, either enhancing (positive peak) or suppressing (negative peak) the ionization signal. This so-called matrix effects, therefore, can be directly observed in real time by this experiment. Figure 5-4 shows EIC of the extracted corn stover blank and the diluent injections with continuous post-connector infusion of the standard solution. There were no obvious positive and negative peaks observed in the corn stover blank curve, indicating that matrix effects were minimal with the currently developed method. Interestingly, the curve for the corn stover matrix overlapped with the solvent blank curve further indicating that the matrix effects of corn stover do not differ significantly from the solvent. It is also noted that a large signal jump appearing at ca. 4.5 min is observed in both chromatograms of corn stover blank and the solvent blank when the MS data acquisition was switched from period 1 to 2 (see Figure 5-4). The ascent incline observed for both curves was caused by the gradient increase of the organic component of the mobile phase in the gradient profile. Analogous in matrix effect behaviors are observed when performing the same experiment for soybean forage when using the developed HPLC-ESI-MS/MS method (see Figure 5-5). Although more

peaks were found in the curve of soybean forage blank as compared to those of corn stover blank, no obvious matrix interference appeared in the analyte retention windows.

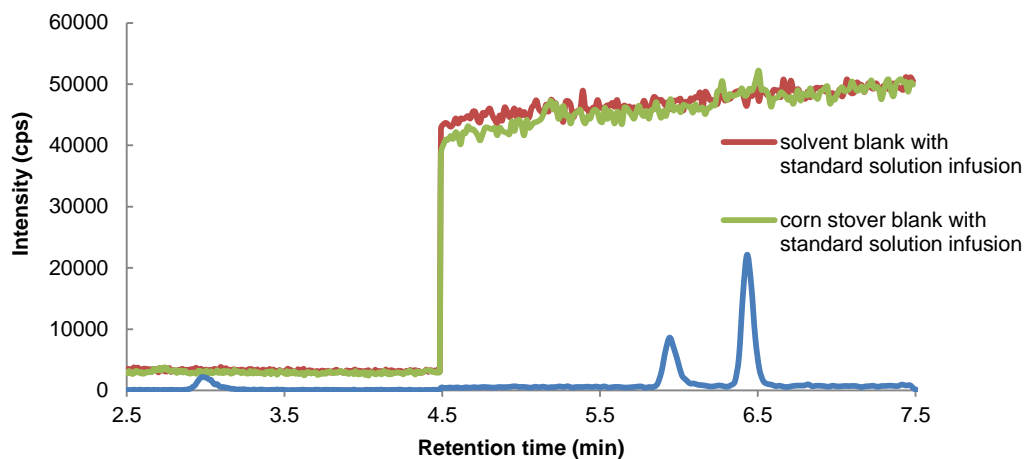


Figure 5-4 Matrix effects evaluation chromatograms of extracted corn stover blank (green colored curve) and the solvent blank (0.2% formic acid in 10:90 methanol/H₂O, red colored curve). For this experiment, 10 ppb of standard solution (without internal standard) was continuously infused into the HPLC-ESI-MS/MS system at post-connector position (see instrumental in Figure 5-1, dotted lines and section 5.2.6). The chromatographic and MS/MS conditions used in this experiment were identical to those described in section 5.2.4. The chromatogram of the mixed standard solution shown here (blue color) was identical to that in Figure 5-2 and was used as reference chromatogram.

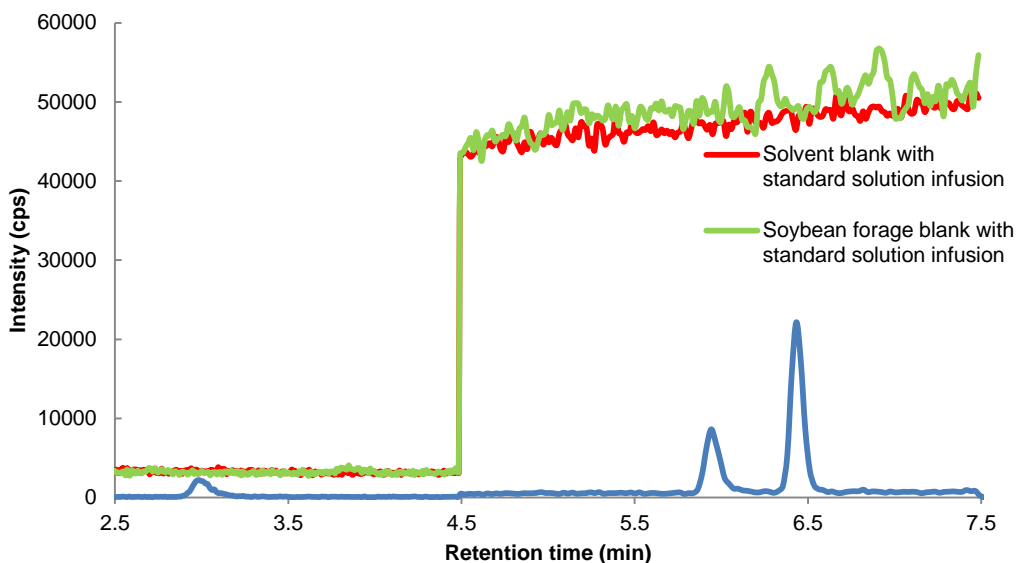


Figure 5-5 Matrix effects evaluation chromatograms of extracted soybean forage blank (green colored curve) and solvent blank (0.2% formic acid in 10:90 methanol/H₂O, red colored curve). For this experiment, 10 ppb of standard solution (without internal standard) was continuously infused into the HPLC-ESI-MS/MS system at post-connector position (see instrumental in section 5.2.6 and Figure 5-1, dotted lines). The chromatographic and MS/MS conditions used in this experiment were identical to those described in section 5.2.4. The chromatogram of the mixed standard solution shown here (blue color) was identical to that in Figure 5-2 and was used as reference chromatogram.

5.4 Conclusions

A HPLC-ESI-MS/MS method with the use of ion-pairing reagents has been developed for trace-level analysis of dicamba residues in raw agricultural commodities (RACs). The negatively charged analytes were monitored and quantitated in positive ESI mode with the use of dicationic ion-pairing reagent, C₅(bpyr)₂-2F. Dicamba and its two major metabolites, 5-OH dicamba and DCSA were separated on a C₈ based stationary

phase with satisfactory separation efficiency and peak shapes. The developed method provided quantitation limits ranging from 1 to 3 µg/kg for these three analytes. Method validation results show that satisfactory accuracy and precision were achieved when the three dicamba residues were fortified into six different types of RACs at three concentration levels. Further evaluation of ionization effects with post-connector infusion of the standard solution demonstrated that minimum matrix effects were present when the HPLC-ESI-MS/MS method was employed. The developed method meets the required residue analysis criteria from many regulatory agencies, and could be broadly applicable to dicamba residue analysis in crops as well as other matrices.

Chapter 6

Reduced Matrix Effects for Anionic Compounds with Paired Ion Electrospray Ionization

Mass Spectrometry

Abstract

It is well-known that matrix effects in high performance liquid chromatography coupled to electrospray ionization mass spectrometry (HPLC-ESI-MS) can seriously compromise quantitative analysis and affect method reproducibility. Paired ion electrospray ionization (PIESI) mass spectrometry is an approach for analyzing ultra-low levels of anions in the positive ion mode. This approach uses a structurally optimized ion-pairing reagent to post-column associate with the anionic analyte, subsequently forming positively charged complexes. These newly formed complex ions are often more surface-active as compared to either the native anion or the ion-pairing reagent. No studies have examined whether or not the PIESI approach mitigates matrix effects. Consequently, a controlled study was done using five analytes in highly controlled and reproducible synthetic groundwater and urine matrices. In addition, two different mass analyzers (linear ion trap and triple quadrupole) were used. Compared to the negative ion mode, the PIESI-MS approach was less susceptible to matrix effects when performed on two different MS platforms. Using PIESI-MS, less dilution of the sample is needed to eliminate ionization suppression which, in turn, permits lower limits of detection and quantitation.

6.1 Introduction

High performance liquid chromatography coupled with electrospray ionization mass spectrometry (ESI-MS) has become one of the most powerful qualitative and quantitative analytical tools. It is characterized by precision, robustness, high sensitivity

and selectivity, allowing for the analyses of trace amounts of target compounds in complex mixtures.^{196,197} Despite these advantages, one important limitation associated with this technique is its susceptibility to matrix effects.¹⁹⁸ A matrix effect is defined as the effect of extraneous co-eluting components on the ionization efficiency of the target analyte.^{199,200} The presence of such matrix components may cause either ionization suppression, or in some cases, ionization enhancement in ESI, leading to quantification errors. Matrix effects also can compromise the limit of detection (LOD), limit of quantification (LOQ), linearity, precision, accuracy and reproducibility of LC-ESI-MS methods.²⁰¹⁻²⁰³ Indeed, matrix effects have been called the “Achilles heel” of quantitative HPLC-ESI-MS.²⁰⁴ Currently, the US Food and Drug Administration’s (FDA) guideline documents require the evaluation of matrix effects during the development and validation of HPLC-MS methods, to ensure no loss of the accuracy, selectivity and sensitivity.^{198,205,206} The mechanisms of matrix effects have not been fully understood since their initial description by Kebarle and Tang in 1993.⁵⁵ Matrix effects emanate from many sources such as trifluoroacetic acid additives,²⁰⁷ endogenous and exogenous compounds, substances introduced from sample preparation steps,²⁰³ and the presence of other co-eluting analytes. Also, factors such as high concentration, polarity, mass and basicity of co-eluting compounds further exacerbate/enhance matrix effects.²⁰⁸

The origin of matrix effects is thought to be related to the mechanism of ESI. During the ESI droplet formation process, co-eluting matrix components may outcompete target ions for the limited space or charge available at the surface of the droplets, thus, inhibiting ejection of the analyte ions trapped inside the droplets.^{63,91,208} The surface activity is a major characteristic that affects the capability of an ion to reach the surface of a droplet.^{38,198,209} Therefore, if a matrix contains undetected components with potentially high surface activities, ionization suppression is common.²¹⁰ Another factor that

contributes to matrix effects is the solvent evaporation subsequent to droplet formation. The presence of nonvolatile compounds and/or high concentrations of interfering compounds may alter the viscosity and surface tension of the ESI droplet. Consequently, it is more difficult for the solvent to evaporate and this inhibits target ion transfer to the gas phase.^{199,207,211,212} Additionally, co-precipitation can occur when nonvolatile impurities are present in the sample matrix, resulting in signal loss of the detected ions.⁶⁴ Neutralization of an acidic analyte and any relatively basic interfering substances can occur in the gas phase, therefore reducing the signal of such target analytes.⁶⁴ Finally, factors that affect the stability of the generated ions in the gas phase also lead to matrix effects.²¹¹

To obtain a robust LC-ESI-MS method, there is a need to reduce or at least quantitatively compensate for the effects of matrix interferences. Various strategies have been applied to these ends. Conventional approaches such as diluting samples, improving chromatographic selectivity, and utilizing optimal sample preparation procedures are routinely performed. Unfortunately, sensitivity and/or analysis time are usually compromised.^{213,214} Some of the newer generation analytical systems can somewhat compensate for these drawbacks.^{213,215} Sometimes, commercially available materials such as hybrid zirconia can be utilized for more selective sample preparations²¹⁶ or chromatographic separations. But they are useful only in a few specific cases. In situations where matrix interfering components are difficult to remove, compensation approaches are often used to correct for the attenuated signal response resulting from matrix effects. Standard addition, matrix-matched calibration, internal standards, and a more recently developed correction technique, postcolumn-infused internal standard²¹⁷ can be used to compensate for matrix effects. With such approaches, quantitative accuracy is improved at the expense of sensitivity. Paired ion electrospray

ionization (PIESI) was developed for the sensitive analysis of anions and some zwitterions in the positive ESI mode.^{2,12,26,28,29,31,33-37,45-47,81,118,119} The PIESI mechanism has been studied and has been shown to involve selective association of anions and some zwitterions to an optimal multiply charged ion-pairing agent, forming a paired ion of positive charge and enhanced surface activity.^{37,119} Anionic analyte LODs are improved one to four orders of magnitude. Other cationic reagents can produce other effects.^{218,219} When comparing PIESI and conventional approaches for analysis of actual environmental and/or biological samples, there often appeared to be subjective differences in matrix effects. However to our knowledge, there have been no reports that have systematically evaluated the effect of PIESI on matrix effects using controlled conditions that can be easily reproduced by others. The focus of this study is to evaluate the response of test compounds to specific matrices. Two of the most currently encountered matrices are groundwater and human urine. Five analytes were selected for this study based on the fact that they were previously reported to suffer from matrix effects.^{43,220-223} Analogous parallel studies are done with two different mass spectrometers, a Thermo ESI-linear ion trap (LIT) and a Shimadzu ESI-triple quadrupole (QqQ). These two MS platforms have different ion source configurations and thus can alter the intensities of matrix effects. No sample pretreatment was done except for dilution.

6.2 Experimental

6.2.1 Reagents and Standards

HPLC-MS grade solvents, methanol and water, were supplied by Honeywell Burdick and Jackson (Morristown, NJ, USA). Ultra-pure water (Milli-Q UV-Plus, Millipore Corp., Bedford, MA, USA) was used for preparation of the artificial matrix solutions. Sodium perchlorate (98% purity), perfluorooctanesulfonate potassium salt (PFOS, ≥98%

purity), monochloroacetic acid (MCA, $\geq 98\%$ purity), clofibric acid (97% purity) and 2,4-D (99.8 % purity) were purchased from Sigma-Aldrich (St. Louis, MO, USA). The structures of these five test compounds were shown in Table 6-1. Components in artificial matrices described below were all obtained from Sigma-Aldrich. The dicationic ion-pairing reagents were synthesized in their bromide form as described previously²⁹ and were subsequently ion-exchanged to their fluoride form prior to analysis to maximize anion/ion-pairing reagent complex formation.⁴⁴ Their structures, abbreviations and exact masses were listed in Table 6-2. These reagents also are available from Sigma-Aldrich (St. Louis, MO, USA). Analyte standard solutions were prepared from a stock solution at 1000 ng/mL monthly and were stored at 4 °C in the dark.

Table 6-1 Structures, abbreviations, names and exact masses of the test compounds

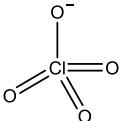
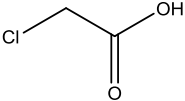
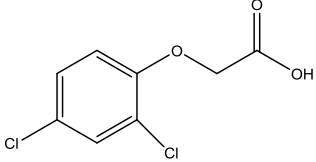
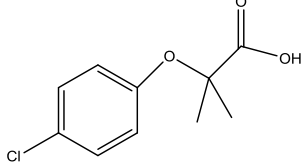
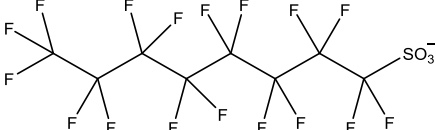
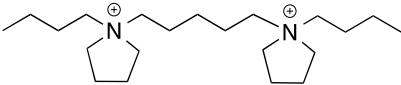
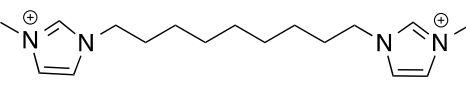
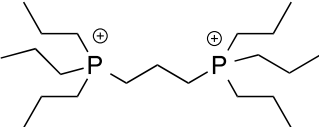
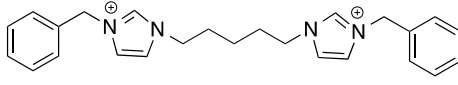
Chemical Name	Abbreviation	Structure	Exact mass
Perchlorate	Perchlorate		99.0
Monochloroacetic acid	MCA		94.0
2,4-Dichlorophenoxyacetic acid	2,4-D		220.0
2-(4-chlorophenoxy)-2-methylpropanoic acid	Clofibric acid		214.0
Perfluorooctanesulfonic acid	PFOS		498.9

Table 6-2 Structures, abbreviations, and exact masses of the ion-pairing reagents used

Dicationic ion-pairing reagent	Abbreviation	Structure	Exact mass
1, 5-pentanediy-bis(1-butylpyrrolidinium)	C ₅ (bpyr) ₂		324.4
1, 9-Nonanediy-bis(3-methylimidazolium)	C ₉ (mim) ₂		290.3
1,3-Propanediy-bis(triethylphosphonium)	C ₃ (tripe) ₂		362.3
1, 5-Pentanediy-bis(3-benzylimidazolium)	C ₅ (benzim) ₂		386.3

6.2.2 Synthetic Matrix Preparation

For this project, standard and reproducible matrices were needed. Actual groundwater and urine are neither.²²⁴ Hence the decision was made to use known synthetic matrices that could be exactly reproduced in any laboratory. The PIESI-MS performance was evaluated in two matrices, groundwater and a more complicated urine medium. The recipe for artificial groundwater (AGW) is based on the Edwards Aquifer groundwater located in San Antonio, Texas.²²⁵ This AGW was made up from laboratory-grade reagents (277 mg L⁻¹ calcium carbonate, 20 mL L⁻¹ of 2% nitric acid, 35 mg L⁻¹ sodium sulfate and 90 mg L⁻¹ magnesium chloride heptahydrate). The pH of the solution was adjusted with 1.2 mL of 1 M potassium hydroxide to 7 (the average pH of the Edwards aquifer groundwater). The artificial urine (AUR) was prepared based on a

procedure outlined in the literature:²²⁴ 10 g of urea, 5.2 g of sodium chloride, 3.2 g of sodium sulfate decahydrate, 2.1 g of sodium bicarbonate, 1.3 g of ammonium chloride, 1.2 g of dipotassium hydrogen phosphate, 0.95 g of potassium dihydrogen phosphate, 0.8 g of creatinine, 0.49 g of magnesium sulfate heptahydrate, 0.4 g of citric acid, 0.37 g of calcium chloride dihydrate, 0.1 g of lactic acid, 0.07 g of uric acid, 0.0012 g of iron II sulfate heptahydrate were mixed in 1 L of ultra-pure water. The pH of the AUR solution was 6.5. The artificial matrix solutions were stored at 4 °C in 1 L amber glass bottles.

6.2.3 Sample Preparation

To closely mimic groundwater and urine matrix effects, samples were prepared in diluted AGW and AUR solutions, with the dilution factors d of 2, 10 and 100, calculated as:

$$d = V_f/V_i$$

Where V_f is the final volume after dilution and V_i is the volume of the initial artificial matrix solution taken for dilution. Although matrix effects at 100-fold dilutions of AGW or AUR may be minimal, their effects on signal response of the analytes help reflect the trends of matrix effects with changes in the matrix concentrations.

The AGW and AUR samples were prepared by the standard addition method,²²⁶ with the concentrations at 0, 10, 20, 30 and 40 ng mL⁻¹, respectively in the 100x diluted artificial matrices (AGW x100 or AUR x100), 0, 50, 100, 150 and 200 ng mL⁻¹, respectively in the 10x diluted artificial matrices (AGW x10 or AUR x10) and 0, 100, 200, 300 and 400 ng mL⁻¹ respectively in the 2x diluted artificial matrices (AGW x2 or AUR x2). All samples were stored at 4 °C in the dark prior to analyses and were analyzed within 30 days, according to the handling and storage recommendations provided by other reports.^{224,227}

6.2.4 PIESI-MS Analysis

The evaluation of the performance of PIESI was carried out on a Finnigan, Thermo Scientific, LXQ linear ion trap mass spectrometer (Finnigan, Thermo Scientific, San Jose, CA, USA) equipped with an off-axis (45 degree) Ion Max ESI source, as well as on a Shimadzu LCMS-8040 triple quadrupole mass spectrometer (Shimadzu, Kyoto, Japan) equipped with an orthogonal ESI source. The instrumental setups for both instruments and optimization of ion-pairing reagents were the same as outlined previously.^{28,31,45,118} Briefly, an ion-pairing reagent aqueous solution was directed by a secondary LC pump (Shimadzu LC-6A, Shimadzu, Columbia, MD, USA) at 100 $\mu\text{L min}^{-1}$, and was then mixed (via a low dead-volume Y-type mixing device) with a 300 $\mu\text{L min}^{-1}$ solvent stream (67/33, v/v, methanol/water) from a HPLC pump. The total concentration of the ion-pairing reagent after mixing was 10 μM , and the final flow contained 50/50 (v/v) of methanol and water with a flow rate of 400 $\mu\text{L min}^{-1}$. All samples were directly injected into the system via a 5- μL sample loop, no columns were used in all these studies. Both selected reaction monitoring (SRM) and selective ion monitoring (SIM) mode were used for the detection of target analytes. In SIM mode, the mass-to-charge ratio (m/z) of the analyte/ion-pairing reagent complex was monitored, while the most intensive ion transition was selected and monitored in the SRM mode, using the corresponding complex as the precursor ion.

Quantitative results obtained in the optimized negative ion mode were used for comparison. To make equal flow conditions, a carrier flow consisting of 50/50 methanol/water at a total flow rate of 400 $\mu\text{L min}^{-1}$ was introduced into the MS directly without ion-pairing reagent.

6.2.5 LIT-MS Conditions

The system consisted of a LXQ linear ion trap system from Thermo Finnigan, a Surveyor HPLC system and a data acquisition/processing software, Xcalibra 2.0. The mass spectrometer was tuned for each compound, optimizing the ionization source parameters, voltages on the lenses and/or collision induced dissociation (CID) energies (SRM mode) in each monitoring mode while continuously infusing a mixture solution containing 1:2 molar ratio of a standard (1 μM) and an ion-pairing reagent (2 μM) via a syringe pump at a flow rate of 20 $\mu\text{L min}^{-1}$. Other operation conditions include as follows: ionization voltage, 3 kV; source temperature, 350 $^{\circ}\text{C}$; sheath gas, 37 arbitrary units (AU); auxiliary gas, 6 AU.

6.2.6 QqQ-MS Conditions

The Shimadzu HPLC system was hyphenated to a triple quadrupole mass spectrometer LCMS-8040 (Shimadzu, Kyoto, Japan) through an orthogonal ESI source. The analytes were monitored in three modes, PIESI-SRM, PIESI-Q3SIM and PIESI-Q1SIM, respectively. Operating conditions of the source were performed as follows: ionization voltage, 3.5 kV; temperature of desolvation line, 250 $^{\circ}\text{C}$; temperature of heating block, 400 $^{\circ}\text{C}$; nebulizing gas, 3 L min^{-1} (N_2); drying gas, 15 L min^{-1} (N_2) respectively. The voltages at Q1 prebias, collision energies or Q3 pre bias were optimized in the same way as that in LIT-MS.

6.2.7 Optimization of Ion-Pairing Reagent Concentration

For AGW sample analysis, a previously optimized concentration of an ion-pairing reagent solution at 10 μM was used.^{29,34,44} However, due to high concentrations of salts present in AUR matrix (100 μM level), the concentration of the ion-pairing reagents used for AUR sample analysis was optimized prior to use. The effect of the concentration of the optimized ion-pairing reagent on the performance of PIESI-MS was investigated at

two different concentrations (10 μM and 50 μM respectively after mixing in the flow stream). Perchlorate and its optimized ion-pairing reagent, $\text{C}_5(\text{benzim})_2$ were used as test model. Perchlorate was spiked into three different diluted AUR matrices (dilution factors of 100, 10 and 2). The total concentrations of these perchlorate samples were all the same at 100 ng mL^{-1} . These samples were detected in both PIESI-SRM and PIESI-SIM modes and were analyzed using LIT-MS. The matrix effects were assessed by comparing the peak areas of perchlorate in neat solvent (50/50, v/v, methanol and water) and in the three different AUR matrices. The concentration of the ion-pairing reagent that minimized matrix effects and ionization suppression more significantly was used in both PIESI-SRM and PIESI-SIM detection modes for AUR sample analysis.

The optimal concentration of ion-pairing reagent was determined as indicated in Figure 6-1. Although the ion-pairing reagent at lower concentration provided higher signal responses in both PIESI-SRM and PIESI-SIM detection modes, the signal responses of these four samples (100 ng mL^{-1} perchlorate spiked in the solvent (50/50, v/v, methanol and water) and in the three AUR matrices with dilution factors of 2, 10, and 100) had a higher degree of variation as compared to the results with the use of 50 μM ion-pairing reagent. This suggests that the concentration of ion-pairing reagent at 50 μM was less affected by the AUR matrix as compared to 10 μM . Therefore, this concentration of ion-pairing reagents was used for the urine sample analysis.

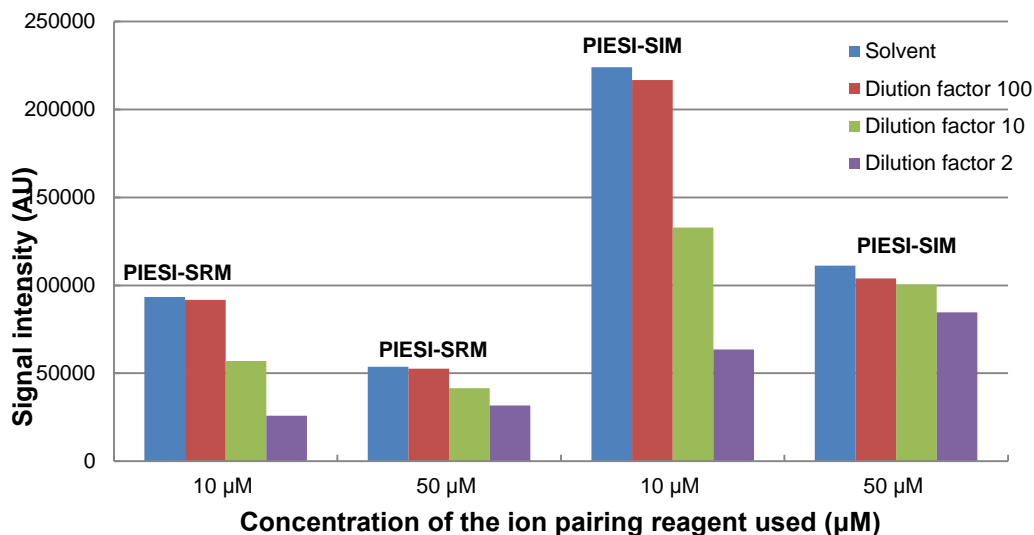


Figure 6-1 Comparison of the effect of concentration of ion-pairing reagent on matrix effects as indicated by signal intensities. Perchlorate standard and perchlorate spiked in diluted artificial urine matrices (total concentrations of perchlorate in solvent (50/50, v/v, methanol and water) and in the three different diluted artificial urine matrices were all the same at 100 ng mL⁻¹) were determined in PIESI-SIM and PIESI-SRM modes using the linear ion trap MS analyzer (see section 6.2.7).

6.2.8 Sample Analysis and Assessment of Matrix Effect

In order to control carry-over effects, the order of the injection was as follows: standards in solvent were the first, followed by AGW x100, AGW x10 and AGW x2 samples. To ensure accuracy and reproducibility of the quantitative results, samples and blanks were run consecutively in the instrument, and the sample cones of both ESI sources were cleaned daily with methanol and water according to the manufacturer's instructions.

Peak area versus sample concentration was utilized for the construction of calibration curves, using weighted ($1/x^2$) linear least-squares regression algorithm. If the

square of the correlation coefficient (R^2) values of calibration curves were less than 0.990, the native samples were respiked and reanalyzed.

The extent of matrix effects (ME%) was studied by comparing the slopes of calibration curves in neat solvent (50/50, v/v, methanol and water in this study) and in the three diluted matrices.^{213,228} They were calculated as follows:

$$ME\% = \frac{\text{Slope of the analyte calibration curve in matrix}}{\text{Slope of the analyte calibration curve in neat solvent}} \times 100\%$$

Ionization suppression would occur if the percentage of the ratio between these slopes were in the range of 0 to <100%. If the ME% was higher than 100%, it would be indicative of ionization enhancement. In the two matrices studied, ionization suppression was observed for all five analytes (see Table 6-1). ME% higher than 90% would be assumed to have little or no matrix effects, because this variation would be close to the repeatability values.

6.3 Results and Discussion

6.3.1 Matrix Effects with PIESI

The nature of the ion-pairing reagent plays an important role on its performance.^{29,31} Thus, the ion-pairing reagents (Table 6-2) selected for each analyte were based on sensitivity, and were evaluated for each analyte in this study as described previously.²⁸ Consequently, $C_5(\text{bpyr})_2$ was used for the analyses of PFOS and MCA, $C_3(\text{triprp})_2$ for clofibric acid and 2,4-D, and $C_5(\text{benzim})_2$ was used for perchlorate. The optimized ion-pairing reagent used with the LIT-MS was also employed for the quantitative analysis of that analyte with the QqQ-MS. The ion/transition that was selectively monitored in each detection mode is given in Table 6-3 (for LIT-MS) and Table 6-4 (for QqQ-MS). Generally, the two instruments produced similar fragmentation patterns in the SRM mode, except for MCA. The LIT-MS was characterized by the

fragment ion of the MCA/C₅(bpyr)₂ complex ion at *m/z* 290.2 corresponding to the *m/z* of the dication moiety C₁₃H₂₆N⁺ and a protonated MCA molecule, but the most sensitive fragment ion was *m/z* 232.1 ([C₁₃H₂₆N⁺ +HCl]) with the QqQ-MS.

The results obtained in the negative ion mode were used for comparison. In this mode, SRM detection was preferentially used if applicable. In contrast to LIT-MS, QqQ-MS generated more quantifiable fragments in the negative-SRM mode as shown in Tables 6-3 and 6-4. The positive ion mode (without the use of PIESI) was not useful for trace level analyses of these anionic compounds because of its low sensitivity (all LODs of the five test compounds were determined to be higher than 500 pg), so it was not used for comparison to the results obtained in the PIESI mode.

6.3.2 Groundwater Matrix Effects Using LIT-MS

Table 6-3 summarizes the calibration slopes and matrix effects as ME% values (see section 6.2.8) for the five test analytes at different concentrations of the AGW matrices using the LIT-MS. Comparative results from the PIESI mode and from the negative ion mode can be seen. Overall, the negative ion mode was not satisfactory. Except for PFOS, the negative ion mode did not provide high sensitivities as indicated from the slopes of the calibration curves. The relatively higher sensitivity of PFOS obtained in the negative ion mode is known to be due to its high surface activity.³⁷ All samples were subject to substantial ionization suppression under the negative ion mode conditions, even for samples that were diluted 100 fold (Table 6-3).

Compared to the negative ion mode analyses, PIESI-MS was less susceptible to ionization suppression from the groundwater matrix as indicated by improved detection sensitivities. From the slopes of the calibration curves shown in Table 6-3, the PIESI-SIM mode provided higher detection sensitivities than the PIESI-SRM mode (with the exception of 2,4-D). Furthermore, all samples suffered less from matrix effects (higher

ME% values) as compared to results obtained in the negative ion mode. As indicated in Table 6-3, the ME%s in 50% diluted AGW were increased by 1.6 to 6.5 times with the use of PIESI-MS as compared to results in the negative ion mode. In 90% diluted AGW, the ME%s for these five compounds increased by 1.6 to 3.6 times, and minimal matrix effects were present in the 99% diluted AGW. The ionization suppression behavior with PIESI-MS differed for the five compounds. Consider, for example, clofibric acid and 2,4-D, which have similar structures, however, these two compounds were subjective to different degrees of ionization suppression in the same sample matrix (2,4-D suffered from a higher degree of ionization suppression than clofibric acid in AGW). This suggests the performance of PIESI-MS on matrix effects is also compound dependent. Interestingly, severe ionization suppression was present in the 90% diluted AGW samples when perchlorate was analyzed in the negative ion mode (ME%=28%, Table 6-3). However, the matrix effects were eliminated in the PIESI-SRM mode (ME%=100%). Therefore, direct injection analysis can be performed for perchlorate analysis in such levels of groundwater matrix. In some cases where the salt concentrations in groundwater are high, matrix effects can be completely minimized using PIESI-MS combined with minimal dilution.

Table 6-3 The ME% values and slopes of the calibration curves for the analyzed standards in solvent and in diluted artificial groundwater obtained with linear ion trap MS analyzer^a

Analyte	Mode ^c	Ion/transition monitored (m/z) ^j	Dilution factor ^b							
			2		10		100		Solvent ^e	
			slope	ME (%) ^d	slope	ME (%) ^d	slope	ME (%) ^d	slope	ME (%) ^d
Perchlorate	Negative-SIM ^f	99.2	7.7	11	19	28	42	63	68	100
	PIESI-SRM ^g	485.3→295.2	207	71	280	100	280	100	289	100
	PIESI-SIM ^h	485.3	466	71	561	83	642	100	647	100
PFOS	Negative-SIM ^f	498.9	362	18	912	43	1612	77	2071	100
	PIESI-SRM ^g	823.3→696.2	98	50	174	91	191	100	196	100
	PIESI-SIM ^h	823.3	634	53	1001	83	1078	91	1228	100
MCA	Negative-SIM ^f	92.8	2.7	10	5.9	22	13	48	27	100
	PIESI-SRM ^g	417.3→290.2	94	37	121	48	247	100	257	100
	PIESI-SIM ^h	417.3	223	33	363	53	668	100	673	100
Clofibrac acid	Negative-SRM ^f	213.6→127	9.6	14	18	24	53	71	74	100
	PIESI-SRM ^g	575.1→187.2	154	50	252	83	284	100	301	100
	PIESI-SIM ^h	575.1	226	44	470	70	841	83	962	100
2,4-D	Negative-SRM ^f	218.8→160.8	6.4	11	15	26	36	63	58	100
	PIESI-SRM ^g	581.0→187.2	116	38	130	43	282	91	304	100
	PIESI-SIM ^h	581.0	79	29	116	42	257	91	279	100

^aThe external calibration curve for each standard in solvent (50/50, v/v, methanol and water) was used for comparison; the calibration curves of analytes in diluted artificial groundwater was obtained by standard addition method.

^bThe final volume after dilution of the sample divide by the volume of the initial artificial ground water matrix; the artificial groundwater was diluted 2, 10 and 100 times, respectively in this study.

^cEach analyte standard was detected and quantified in each detection modes with the use of linear ion trap MS analyzer. The positive ion mode did not provide good sensitivity for these analyzed standards in this study (LODs > 500 pg)

^dMatrix effect: the slope of calibration curve for the analyte in diluted artificial groundwater matrix versus that in solvent (50/50, v/v, methanol and water).

^e50/50 methanol and water (v/v)

^fNegative-selected ion monitoring (SIM) mode

^gPaired Ion Electrospray Ionization (PIESI)-selected reaction monitoring (SRM) mode; the final concentrations of each optimized ion-pairing reagent solutions after mixing were set at 10 µM in PIESI mode.

^hPaired ion electrospray ionization-selected ion monitoring mode

ⁱNegative-selected reaction monitoring mode

^jIons were monitored in SIM mode, and ion transitions were monitored in SRM mode. The ion that was monitored in PIESI-SIM mode was used as the precursor ion in the PIESI-SRM mode.

Table 6-4 The ME% values and slopes of the calibration curves for the analyzed standards in solvent and in diluted artificial groundwater obtained with triple quadrupole MS analyzer^a

Analyte	Mode ^c	Ion/transition monitored (m/z) ^j	Dilution factor ^b								
			2		10		100		Solvent ^e		
			slope	ME (%) ^d	slope	ME (%) ^d	slope	ME (%) ^d	slope	ME (%) ^d	
Perchlorate	Negative-SRM ^f	99.2→83.0	1668	13	5633	45	7742	63	1257	1	100
	PIESI-SRM ^g	485.3→295.2	2872	26	7018	67	1002	100	1081	15	100
	PIESI-Q3SIM ^h	485.3	9762	21	2871	63	4575	100	4597	43	100
	PIESI-Q1SIM ⁱ	485.3	1740	21	4223	53	7385	91	8181	32	100
PFOS	Negative-SRM ^f	498.8→79.9	178	8	668	30	1681	77	2204		100
	PIESI-SRM ^g	823.3→696.2	205	19	445	40	1090	100	1112		100
	PIESI-Q3SIM ^h	823.3	1790	14	4101	32	1209	100	1271		100
	PIESI-Q1SIM ⁱ	823.3	1921	13	4100	28	1409	100	1476		100
MCA	Negative-SRM ^f	92.8→35.0	53	6	104	12	233	26	894		100
	PIESI-SRM ^g	417.3→232.1	1362	12	3763	32	7760	67	1163	3	100
	PIESI-Q3SIM ^h	417.3	6336	18	1364	38	3397	100	3548	0	100
	PIESI-Q1SIM ⁱ	417.3	7909	14	1725	30	4745	83	5694	2	100
Clofibric acid	Negative-SRM ^f	213.6→127	363	4	758	9	1987	24	8340		100
	PIESI-SRM ^g	575.1→187.2	1024	8	1960	15	4530	34	1313	0	100
	PIESI-Q3SIM ^h	575.1	8540	13	2044	30	3968	59	6747	22	100
	PIESI-Q1SIM ⁱ	575.1	1060	11	2555	26	5246	53	9968	11	100
2,4-D	Negative-SRM ^f	218.8→160.8	367	7	679	12	1571	29	5498		100
	PIESI-SRM ^g	581.0→187.2	8370	15	1717	31	3052	56	5494	4	100
	PIESI-Q3SIM ^h	581.0	2022	17	3978	33	8525	71	1193	0	100
	PIESI-Q1SIM ⁱ	581.0	2439	12	4166	21	1052	53	1999	98	100

^aThe external calibration curve for each standard in solvent (50/50, v/v, methanol and water) was used for comparison; the calibration curves of analytes in diluted artificial groundwater was obtained by the standard addition method.

^bThe final volume after dilution of the sample divide by the volume of the initial artificial ground water matrix; the artificial groundwater was diluted 2, 10 and 100 times, respectively in this study.

^cEach analyte standard was detected and quantified in each detection mode with the use of triple quadrupole MS analyzer, except for the positive ion mode. The positive ion mode did not provide good sensitivity for these analyzed standards in this study (LODs > 500 pg)

^dMatrix effect: the slope of calibration curve for the analyte in diluted artificial groundwater matrix versus that in solvent (50/50, v/v, methanol and water); ^e50/50, v/v, methanol and water; ^fNegative-selected reaction monitoring mode

^gPaired Ion Electrospray Ionization (PIESI)-selected reaction monitoring (SRM) mode; the total concentrations of each optimized ion-pairing reagent solution after mixing were set at 10 µM in PIESI-MS mode.

^hPaired ion electrospray ionization-the first quadrupole selected ion monitoring (SIM) mode

ⁱPaired ion electrospray ionization-the third quadrupole selected ion monitoring mode

^jIons were monitored in Q3- and Q1-SIM mode, and ion transitions were monitored in SRM mode. The ion that was monitored in PIESI-SIM mode was used as precursor ion in the PIESI-SRM mode.

Figure 6-2 shows the PIESI-SRM and the negative ion mode calibration slopes of perchlorate in solvent (50/50, v/v, methanol and water) and in the 50% diluted AGW. The calibration slopes obtained in PIESI-SRM mode were higher than those obtained in negative-SIM mode, indicating higher sensitivity of the PIESI-SRM. Moreover, the calibration curves of standards and of the spiked perchlorate in 50% diluted AGW were closer to one another as compared to those obtained in the negative-SIM mode, showing that PIESI-MS helped to mitigate matrix effects.

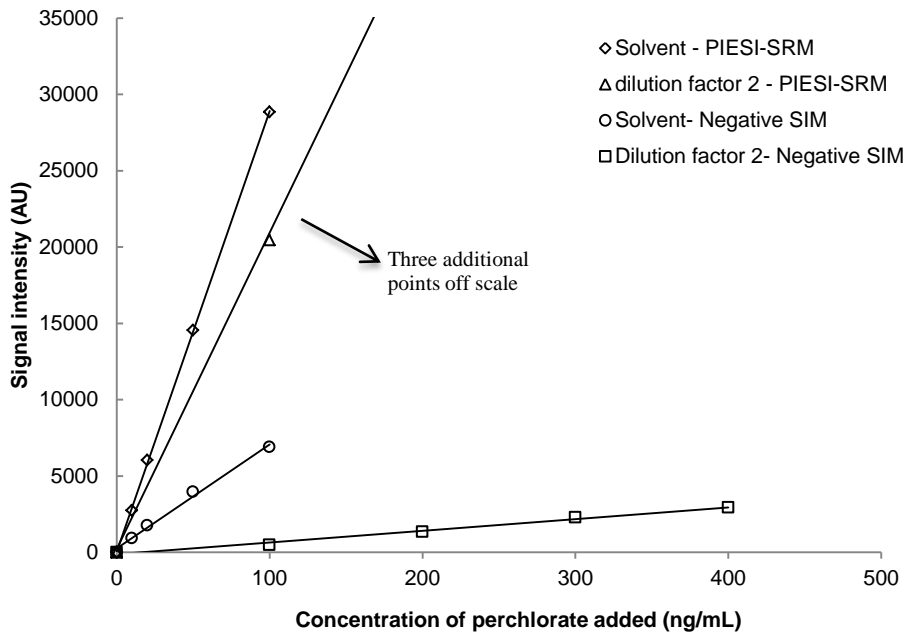


Figure 6-2 Calibration curves of perchlorate in solvent (50/50, v/v, methanol and water) and in the 50% diluted artificial groundwater matrix determined in negative-SIM and PIESI-SRM modes using the linear ion trap MS analyzer

6.3.3 Groundwater Matrix Effects Using QqQ-MS

Table 6-4 summarizes the analogous data for detection and ionization suppression in groundwater when using a QqQ-MS. Data can be compared for the same

five anionic analytes in the PIESI and negative ion modes. As can be seen, the slopes of the PIESI calibration curves were one to two orders of magnitude greater than those obtained in the negative ion mode. In all cases, ionization suppression was less with PIESI-MS (i.e., from 2 to 3.2 x greater ME% at the high AGW level). Note that ME% are quite similar in all cases between the PIESI-SIM and PIESI-SRM mode (Table 6-4). Thus, it appears that matrix effects occur mainly in the initial ionization step.

6.3.4 Urine Matrix Effects Using LIT-MS

Urine specimens are one of the most frequently encountered biological samples.²¹⁷ Five test compounds were spiked individually into three different AUR matrices with dilution factors of 2, 10 and 100. The spiked concentrations of these analytes are specified in section 6.2.3. A 5x greater concentration of the ion-pairing reagent (50 μ M vs. 10 μ M) was used for the AUR matrices to minimize ionization suppression (compared to the AGW matrix). This is thought to be needed due to the much higher ionic strength of urine (see section 6.2.2).^{63,91,229} However, as is known from previous studies, the use of even higher ion-pairing reagent concentrations may be detrimental and act as an additional matrix component and cause increased signal suppression.¹¹⁹

The calibration slopes and ME% values for these AUR samples, obtained with LIT-MS, are summarized in Table 6-5. Overall, the calibration slopes for these analytes (except PFOS) spiked at different concentration levels of AUR were up to 83 times higher using the PIESI-MS method as compared to the slopes determined in the negative ion mode. The results for PFOS, which is a surfactant, were contrary to those of all other test analytes. Indeed it is known that the surface activity of such compounds is enhanced in high ionic strength solutions such as urine and sea water.²³⁰ The improved detection capability of PIESI-MS is illustrated in Figure 6-3. Perchlorate was spiked in the 50%

diluted AUR matrix at four different concentrations (total concentration after spiking were 100, 200, 300 and 400 ng mL⁻¹). These samples were detected in both PIESI-SRM and negative-SIM modes using the LIT-MS. As observed from the overlaid perchlorate peaks via direct injection analysis (Figure 6-3), the signal response (peak area) at each concentration determined in the PIESI-SRM detection mode was approximately 20 times higher as compared to the signal response of the analyte at the same concentration acquired in the negative SIM detection mode.

Except for PFOS (*vide supra*), ion suppression was less for all analytes and at all levels of the AUR matrices with PIESI-MS as compared to the negative ion mode (Table 6-5). The ME% values of the four non-surface-active compounds increased by 2.0 to 6.2 times in the 50% diluted AU matrix using PIESI-MS, as compared to the results obtained in the negative ion mode. The most dramatic result was observed in the case of 2,4-D. It exhibited severe ionization suppression (ME%=8%) in the 50% diluted AUR when analyzed in the negative ion mode (Table 6-5), while the ME% was increased to 50% with the PIESI-MS approach. At medium and low AUR levels, the matrix effects were reduced up to 4.5 and 3.0 times, respectively. Using the PIESI-MS approach, simple dilution eliminated most of the matrix effects for these analytes.

The calibration curves of 2,4-D standard solutions and of spiked 2,4-D in the 90% diluted AUR, obtained in the negative-SRM and PIESI-SRM modes are shown in Figure 6-3. Similar trends were observed as those for perchlorate in the 50% diluted AGW described in Figure 6-1 and in section 6.3.2.

Table 6-5 The ME% values and calibration slopes for the analyte standards in solvent and in artificial urine with different dilution factors obtained with the linear ion trap MS analyzer^a

alyte	Mode ^c	Dilution factor ^b							
		2		10		100		solvent ^e	
		slope	ME (%) ^d	slope	ME (%) ^d	slope	ME (%) ^d	slope	ME (%) ^d
Perchlorate	Negative-SIM ^f	10	15	23	33	54	77	68	100
	PIESI-SRM ^g	316	59	413	77	526	100	536	100
	PIESI-SIM ^h	833	71	1004	100	1038	100	1115	100
PFOS	Negative-SIM ^f	1090	53	1593	77	1718	83	2071	100
	PIESI-SRM ^g	7.8	22	12	34	21	59	35	100
	PIESI-SIM ^h	61	36	81	48	100	59	170	100
MCA	Negative-SIM ^f	4.1	15	6.6	24	14	50	27	100
	PIESI-SRM ^g	15	30	19	38	24	50	49	100
	PIESI-SIM ^h	39	26	61	40	86	56	153	100
Clofibric acid	Negative-SRM ⁱ	13	17	15	20	25	33	74	100
	PIESI-SRM ^g	27	26	39	37	97	91	104	100
	PIESI-SIM ^h	133	34	252	45	397	100	387	100
2,4-D	Negative-SRM ⁱ	4.8	8	8.2	14	25	43	58	100
	PIESI-SRM ^g	53	50	66	63	93	91	104	100
	PIESI-SIM ^h	91	45	106	53	181	91	198	100

^aThe external calibration curve for each standard in solvent (50/50, v/v, methanol and water) was used for comparison; the calibration curves of analytes in diluted artificial groundwater were obtained by the standard addition method.

^bThe final volume after dilution of the sample divide by the volume of the initial artificial urine matrix; the artificial groundwater was diluted into 2, 10 and 100 times, respectively in this study.

^cEach analyte standard was detected and quantified in each detection modes with the use of linear ion trap MS analyzer, expect for the positive ion mode. The positive ion mode did not provide good sensitivity for these analyzed standards in this study (LODs > 500 pg); the ion and ion transitions monitored were the same as those in Table 3 for each analyte.

^dMatrix effect: the slope of calibration curve for the analyte in diluted artificial groundwater matrix versus that in neat solvent (50/50, v/v, methanol and water)

^e50/50, v/v, methanol and water

^fNegative-selected ion monitoring (SIM) mode

^gPaired Ion Electrospray Ionization (PIESI)-selected reaction monitoring (SRM) mode; the total concentrations of each optimized ion-pairing reagent solution after mixing were set at 50 μ M in PIESI-MS mode.

^hPaired ion electrospray ionization-selected ion monitoring mode

ⁱNegative-selected reaction monitoring mode

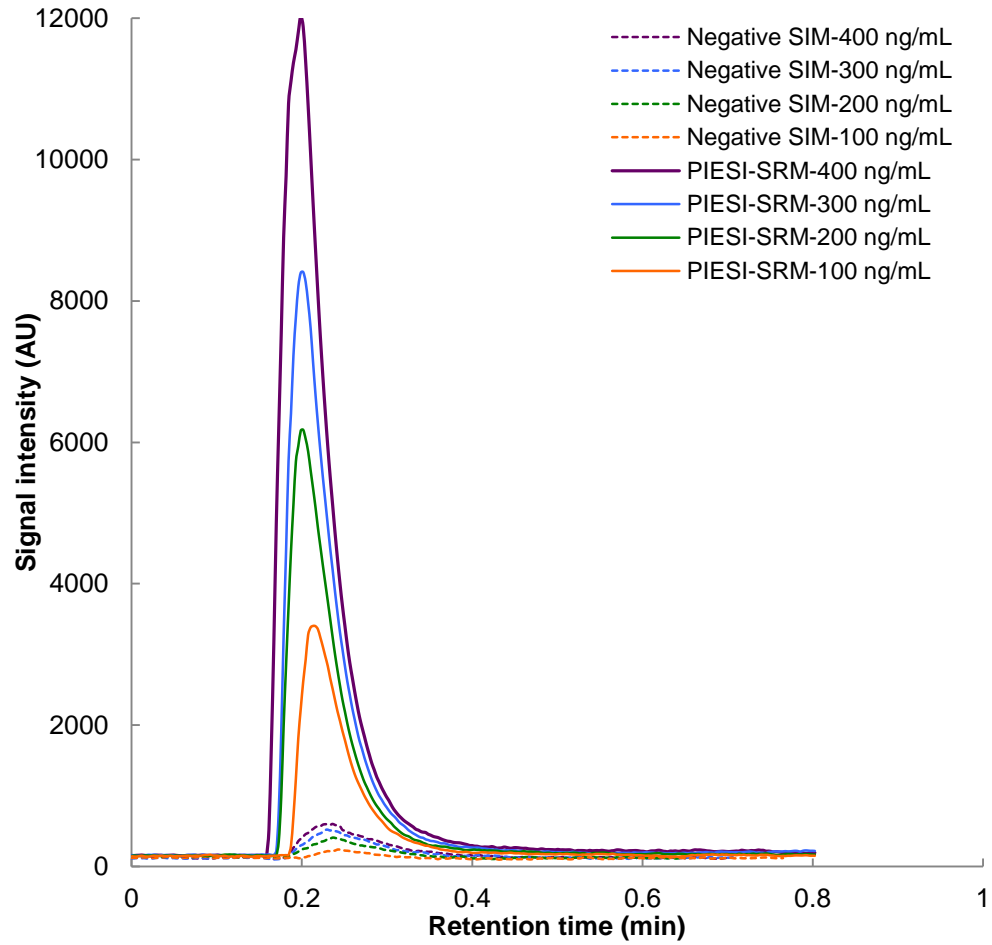


Figure 6-3 Overlaid peaks of the standard addition plots of perchlorate in the 50% diluted artificial urine. Analyses were done in both PIESI-SRM and negative-SIM modes using linear ion trap MS analyzer. Samples at the same concentration were labeled with the same color.

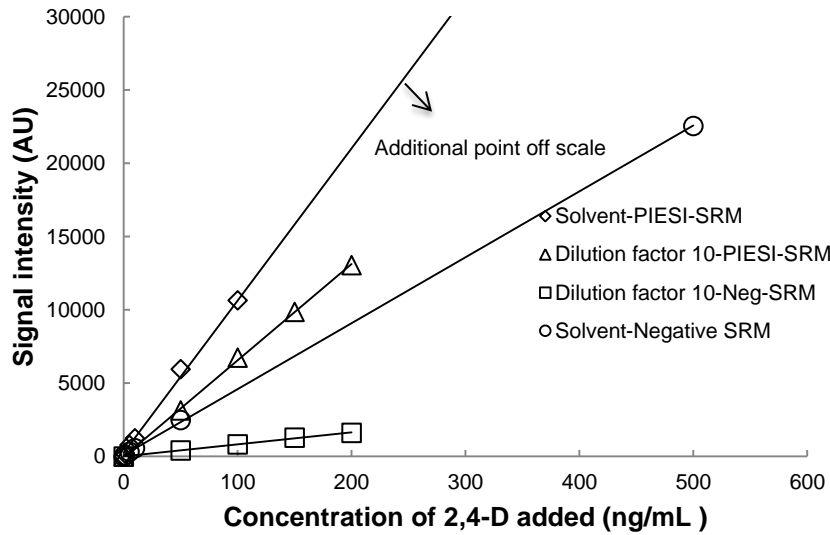


Figure 6-4 Calibration curves of 2,4-D in solvent (50/50, v/v, methanol and water) and in the 90% diluted artificial urine determined in the negative-SRM and PIESI-SRM modes using the linear ion trap MS analyzer

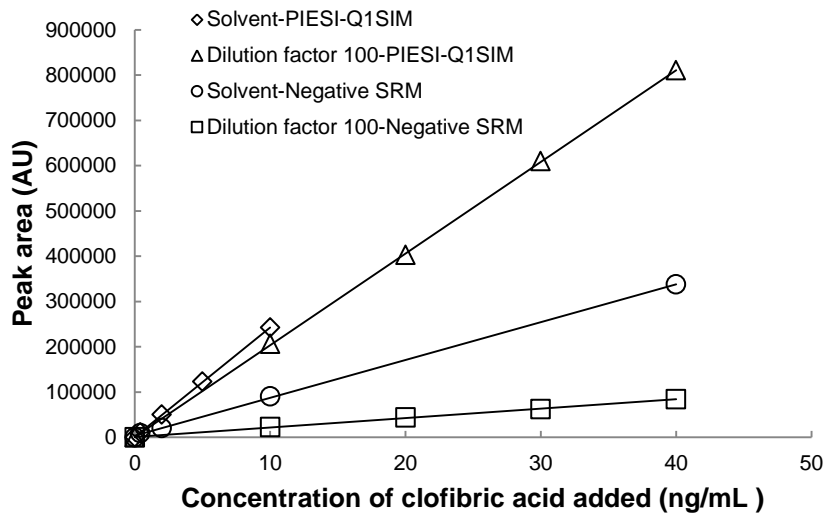


Figure 6-5 Calibration curves of clofibric acid in solvent (50/50, v/v, methanol and water) and in the 99% diluted artificial urine, as determined in the PIESI-SRM and negative-SRM modes using the triple quadrupole MS analyzer

6.3.5 Urine Matrix Effects Using QqQ-MS

As shown in Table 6-6, the sensitivities for the detection of these analytes (except for PFOS, *vide supra*) in all urine samples were improved by up to two orders of magnitude by comparing the slopes obtained in PIESI and the negative ion modes. A definitive example is the case of MCA in the 50% diluted AUR. The calibration slope of MCA was 300 times higher in the PIESI-Q1SIM mode than the negative ion mode.

The PIESI-MS method also had reduced matrix effects for these analytes in AUR matrices (see Table 6-6). In the 50% diluted AUR, the matrix effects were by 1.2 to 6.0 times less with the use of PIESI-MS. For example, clofibric acid suffered from severe matrix effects (ME%= 3% in 50% diluted AUR), while the matrix effects were reduced by six fold (ME%=18% in 50% diluted AUR) in the PIESI-Q1SIM mode. In many cases, matrix effects were nearly eliminated in AUR with dilution factors up to 100.

The calibration slopes of clofibric acid in the 99% diluted AUR obtained in both PIESI-Q1SIM and negative-SIM modes are shown in Figure 6-4. As indicated in this figure, PIESI-Q1SIM mode showed higher detection sensitivity for clofibric acid in this urine matrix than the negative-SRM mode (higher slopes obtained in PIESI-Q1SIM mode). Moreover, the calibration curve of the spiked clofibric acid samples nearly coincides with that of the standard solution, suggesting that matrix effects were minimal in this AUR matrix when PIESI-Q1SIM was utilized.

Table 6-6 The ME% values and calibration slopes for the analyzed standards in solvent and in diluted artificial urine matrixes obtained with the triple quadrupole MS analyzer

Analyte	Mode ^c	Dilution factor ^b							
		2		10		100		solvent ^e	
		slope	ME (%) ^d	slope	ME (%) ^d	slope	ME (%) ^d	slope	ME (%) ^d
Perchlorate	Negative-SRM ^f	2118	17	3608	29	8512	67	12571	100
	PIESI-SRM ^g	4081	29	11463	83	13804	100	13824	100
	PIESI-Q3SIM ^h	17114	34	41124	83	43264	91	48926	100
	PIESI-Q1SIM ⁱ	20881	38	43866	83	49259	91	53760	100
PFOS	Negative-SRM ^f	600	27	986	45	1603	71	2204	100
	PIESI-SRM ^g	28	28	52	53	93	91	100	100
	PIESI-Q3SIM ^h	1600	32	3258	67	5722	100	4985	100
	PIESI-Q1SIM ⁱ	1808	31	3129	56	4388	77	5717	100
MCA	Negative-SRM ^f	53	6	72	8	233	26	894	100
	PIESI-SRM ^g	1202	29	1530	38	2163	53	4042	100
	PIESI-Q3SIM ^h	5119	18	7845	28	10395	36	28609	100
	PIESI-Q1SIM ⁱ	15706	25	18692	33	20061	42	31313	100
Clofibric acid	Negative-SRM ^f	236	3	575	7	2082	25	8340	100
	PIESI-SRM ^g	1698	11	5208	32	7180	45	16065	100
	PIESI-Q3SIM ^h	3037	14	5241	24	14993	71	21344	100
	PIESI-Q1SIM ⁱ	4239	18	9440	38	20237	83	24151	100
2,4-D	Negative-SRM ^f	358	7	614	11	2263	42	5498	100
	PIESI-SRM ^g	1341	11	2221	25	10981	71	12368	100
	PIESI-Q3SIM ^h	2648	15	6391	36	14308	83	17784	100
	PIESI-Q1SIM ⁱ	2399	10	7132	31	18125	77	22954	100

^aThe external calibration curve for each standard in solvent (50/50, v/v, methanol and water) was used for comparison; the calibration curves of analytes in diluted artificial urine were obtained by the standard addition method.

^bThe final volume after dilution of the sample divide by the volume of the initial artificial urine matrix; the artificial urine was diluted 2, 10 and 100 times, respectively in this study.

^cEach analyte standard was detected and quantified in each detection modes with the use of triple quadrupole MS analyzer, except for the positive ion mode. The positive ion mode did not provide good sensitivity for these analyzed standards in this study (LODs > 500 pg); the ion and ion transitions monitored were the same as those in Table 4 for each analyte.

^dMatrix effect: the slope of calibration curve for the analytes in diluted artificial groundwater matrix versus that in neat solvent (50/50, v/v, methanol and water)

^e50/50, v/v, methanol and water

^fNegative-selected reaction monitoring (SRM) mode

^gPaired Ion Electrospray Ionization (PIESI)-selected reaction monitoring (SRM) mode; the total concentrations of each optimized ion-pairing reagent solutions after mixing were set at 50 µM in PIESI-MS mode.

^hPaired ion electrospray ionization-the first quadrupole selected ion monitoring mode

ⁱPaired ion electrospray ionization-the third quadrupole selected ion monitoring mode

6.4 Conclusions

The PIESI-MS approach was demonstrated as an effective way for the reduction of matrix effects for five test chemicals often without compromising their detection sensitivities. This can be attributed to a combination of reasons including: (a) the formation of a stable analyte/ion-pairing reagent complex, (b) the enhanced surface activity of the analyte/ion-pairing reagent complex, (c) beneficial competition of ion-pairing reagent vs. proton and other small metal cations for anionic sites and (d) more efficient ionization of the analyte/ion-pairing reagent complex. PIESI-MS provided higher detection sensitivity than negative ion mode by comparing the calibration slopes. For two frequently encounter matrices, groundwater and urine, PIESI-MS showed reduced ionization suppression in both cases as compared to those obtained in the negative ion mode without using ion-pairing reagents. The study was performed in selective ion monitoring (SIM) and selective reaction monitoring (SRM) modes using two different MS platforms, a linear ion trap as well as a triple quadrupole. PIESI-MS provided enhanced detection sensitivity and reduced matrix effects for the tested analytes in different types of matrices on both MS spectrometers. It was also found that a higher concentration of the optimized ion-pairing reagent can be used for a high ionic strength sample, resulting in fewer matrix effects for the test analytes. In many cases, minimal matrix effects were observed in low groundwater and urine levels with the use of the PIESI-MS approach. For many samples in complex matrices, direct injection analysis with minimal dilution eliminated most of the matrix effects for these analytes. In contrast, simple dilution without the use of PIESI did not completely eliminate suppression in the negative ion mode, and would require more sample preparation time, lead to more opportunities for errors and worse LODs. Overall, this PIESI-MS strategy should be applicable to other groups of anionic compounds and different types of matrices.

Chapter 7

General Summary

7.1 Part one (Chapter 2)

This section of the dissertation describes the design and synthesis of two novel dicationic ion-pairing reagents with unsymmetrical structures and their utilization for anion detection in the PIESI-MS mode. As compared to the corresponding symmetrical ion-pairing reagents (which are not surface-active species), the symmetrical ion-pairing reagents provided improved detection limits for anions by 1.5 to 12 times in the SIM mode. The SRM mode further improved the detection sensitivities for the anions by 1.2 to 9 times using PIESI. It was also found that the effective concentration range of these surface-active ion-pairing reagents was 1 - 10 μM . Further increases in the concentration of these unsymmetrical ion-pairing reagents resulted in a decrease in the LODs of all anions. This limitation of sensitivity at high dication concentrations was attributed to the enrichment of micellar surface-active ion-pairing reagents in the interior of the aerosol droplet, which compete for the anions on the droplet surface leading to a surface dilution of the anion/ion-pairing reagent complex. The mechanism of PIESI in sensitive detection was further explored based on the equilibrium partitioning model. It was proposed that the use of unsymmetrical dicationic ion-pairing reagents results in the formation of highly surface-active anion/ion-pairing reagent complex and thus an enhanced partitioning of the anion to the droplet surface according to the results of the surface tension titrations and ESI response studies. This study confirms that surface activity plays a key role in the sensitive detection of anions using PIESI. The results of this study also provide a basis for future ion-pairing reagent design and applications.

7.2 Part Two (Chapters 3 to 6)

Novel applications of the PIESI approach in ultra-sensitive detection and/or determination of biologically, environmentally and clinically challenging anionic compounds were demonstrated in Chapters 3-6. Biological intermediates, anionic sugars; abused drug metabolites; and acidic pesticides (dicamba residues) were sensitively detected and/or analyzed utilizing the PIESI technique. In some cases, detection limits down to sub-pg levels were obtained for these analytes with the use of optimal symmetrical or unsymmetrical ion-pairing reagents. As compared to the detection limits obtained from HPLC-MS methods based on negative ESI detection and other reported methodologies, the currently developed HPLC-MS methods based on PIESI provided LODs one to three orders of magnitude lower. Chapter 3 described the ultra-sensitive detection of anionic sugars using PIESI-MS. The traditional analytical methods for anionic sugars faced challenges in terms of detection sensitivity and selectivity. The PIESI approach was able to improve the detection limits for these anionic sugars by 2 to 167 fold as compared to those obtained in negative mode ESI. LODs obtained with the optimal ion-pairing reagents ranged from 15 to 200 pg, which were one to three orders of magnitude more sensitive when compared to other reported HPLC-MS methods (mostly detected in negative ESI). To improve the selectivity of anionic sugars particularly the isomeric sugar phosphates, a chromatographic separation based on the mixed-mode vancomycin stationary phase was developed. Chapter 4 outlined the novel application of PIESI for the ultra-sensitive detection of abused drugs by detecting their glucuronate or sulfate conjugates. The method developed based on PIESI was shown to be sensitive and efficient for the analysis of abused drugs including performance-enhancing drugs and alcohols. LODs in the sub-pg range were obtained for the drug conjugates. It was found that the two unsymmetrical ion-pairing reagents (that were mentioned in Chapter 2)

provided further sensitivity enhancement and complimentary performance in detecting these drug metabolites. A HPLC-PIESI-MS/MS method was successfully developed for the simultaneous analysis of these drug metabolites with excellent recovery and minimal matrix effects. Chapter 5 described the novel application of PIESI for the sensitive analysis of dicamba residues in raw agricultural commodities. A sensitive and selective HPLC-PIESI-MS/MS method was developed with the use of a commercially available ion-pairing reagent, $C_5(bpyr)_2$. The developed method was validated according to SANCO guidelines and demonstrated excellent sensitivity, linearity, precision and accuracy. The results of ionization effect studies showed that minimal matrix effects were present in these crop matrices with the developed HPLC-PIESI-MS/MS method. The developed method also meets the required residue analysis criteria from many regulatory agencies, and could be broadly applicable to dicamba residue analysis in crops as well as other matrices. Chapter 6 demonstrated another advantage of PIESI in the analysis of anionic compounds. The PIESI technique often mitigated matrix effects that were observed when analyzing samples with negative ESI. The performance of PIESI on reduction of matrix effects was carried out using two reproducible synthetic matrices, urine and groundwater, and was evaluated on two MS platforms, a Thermo LXQ linear ion trap and a Shimadzu triple quadrupole mass spectrometer. For the two frequently encountered matrices, PIESI showed reduced matrix effects for anions on both MS platforms. Moreover, the detection sensitivities for these anions were not compromised as indicated by comparing their calibration slopes. It was interesting that the diminution of matrix effects behaviors were quite similar between the PIESI-SIM and PIESI-SRM modes, indicating that matrix effects mainly occur in the initial ionization step. Optimization of ion-pairing reagent concentration showed that higher concentrations of the ion-pairing reagent resulted in fewer matrix effects in a higher ionic strength sample such as urine. Therefore, it is

important to optimize both the ion-pairing reagent for the analyte and the concentration of the optimized ion-pairing reagent. Overall, minimal matrix effects were observed in partially diluted groundwater and urine samples with the use of PIESI. For many samples in complex matrices, direct injection analysis with minimal dilution eliminated most of the matrix effects. However, simple dilution without the use of PIESI did not completely eliminate suppression in the negative ion mode, and thus would require more sample preparation time, which could lead to more opportunities for error and worse LODs.

In summary, the mechanism of the enhanced sensitivity in PIESI was further studied using two rational designed surface-active ion-pairing reagents. It was shown that the high sensitivity of PIESI was related to the enhanced surface-activity of the analyte/ion-pairing reagent complex ions (based on the equilibrium partitioning model), resulting in higher ionization efficiency of the analyte in the ESI droplet. The PIESI approach has been successfully used for sensitive analysis of various types of anionic compounds including anionic sugars, metabolites of abused drug and dicamba pesticides. It was also found that the PIESI approach was less susceptible to matrix effects for anionic compounds than negative mode ESI. The current studies should provide a basis for future HPLC-MS method development for real complex sample analyses based on PIESI with enhanced detection sensitivity and selectivity.

Appendix A

Publication Information and Contributing Authors

Chapter 2: A manuscript published in *Analytical Chemistry*. Chengdong Xu, Hongyue Guo, Zachary S. Breitbach and Daniel W. Armstrong, 2014, 86, 2665-2672. DOI: 10.1021/ac404005v. Copyright ©2014 with permission from American Chemistry Society.

Chapter 3: A manuscript in preparation. Hongyue Guo and Daniel W. Armstrong.

Chapter 4: A manuscript published in *International Journal of Mass Spectrometry*. Hongyue Guo, Maressa D. Dolzan, Daniel A. Spudeit, Chengdong Xu, Zachary S. Breitbach, Uma Sreenivasan and Daniel W. Armstrong, 2015, 389, 14-25. DOI: 10.1016/j.ijms.2015.08.005. Copyright ©2015 with permission from Elsevier.

Chapter 5: A manuscript published in *Talanta*. Hongyue Guo, Leah S Riter, Chad E Wujcik and Daniel W Armstrong, 2015, 149, 103-109. DOI: 10.1016/j.talanta.2015.11.043. Copyright ©2015 with permission from Elsevier.

Chapter 6: A manuscript published in *Analytica Chimica Acta*. Hongyue Guo, Zachary S. Breitbach and Daniel W. Armstrong, 2016, 912, 74-84. DOI: 10.1016/j.aca.2016.01.038. Copyright ©2016 with permission from Elsevier.

Appendix B
Copyright and Permissions

Title: Mechanism and Sensitivity of Anion Detection Using Rationally Designed Unsymmetrical Dications in Paired Ion Electrospray Ionization Mass Spectrometry
Author: Chengdong Xu, Hongyue Guo, Zachary S. Breitbach, et al
Publication: Analytical Chemistry
Publisher: American Chemical Society
Date: Mar 1, 2014

Copyright © 2014, American Chemical Society

PERMISSION/LICENSE IS GRANTED FOR YOUR ORDER AT NO CHARGE

This type of permission/license, instead of the standard Terms & Conditions, is sent to you because no fee is being charged for your order. Please note the following:

- Permission is granted for your request in both print and electronic formats, and translations.
- If figures and/or tables were requested, they may be adapted or used in part.
- Please print this page for your records and send a copy of it to your publisher/graduate school.
- Appropriate credit for the requested material should be given as follows: "Reprinted (adapted) with permission from (COMPLETE REFERENCE CITATION). Copyright (YEAR) American Chemical Society." Insert appropriate information in place of the capitalized words.
- One-time permission is granted only for the use specified in your request. No additional uses are granted (such as derivative works or other editions). For any other uses, please submit a new request.

**ELSEVIER LICENSE
TERMS AND CONDITIONS**

Mar 03, 2016

This is a License Agreement between Hongyue Guo ("You") and Elsevier ("Elsevier") provided by Copyright Clearance Center ("CCC"). The license consists of your order details, the terms and conditions provided by Elsevier, and the payment terms and conditions.

All payments must be made in full to CCC. For payment instructions, please see information listed at the bottom of this form.

Supplier	Elsevier Limited The Boulevard, Langford Lane Kidlington, Oxford, OX5 1GB, UK
Registered Company Number	1982084
Customer name	Hongyue Guo
Customer address	700 Planetarium Place ARLINGTON, TX 76019
License number	3821120361368
License date	Mar 02, 2016
Licensed content publisher	Elsevier
Licensed content publication	International Journal of Mass Spectrometry
Licensed content title	Sensitive detection of anionic metabolites of drugs by positive ion mode HPLC-PIESI-MS
Licensed content author	Hongyue Guo, Maressa D. Dolzan, Daniel A. Spudeit, Chengdong Xu, Zachary S. Breitbach, Uma Sreenivasan, Daniel W. Armstrong
Licensed content date	15 October 2015
Licensed content volume number	389
Licensed content issue number	n/a
Number of pages	12
Start Page	14
End Page	25

Portion	full article
Format	both print and electronic
Are you the author of this Elsevier article?	Yes
Will you be translating?	No
Title of your thesis/dissertation	MECHANISM AND USE OF PAIRED ION ELECTROSPRAY IONIZATION (PIESI) IN HIGH-PERFORMANCE LIQUID CHROMATOGRAPHY-MASS SPECTROMETRY (HPLC-MS) FOR SENSITIVE ANALYSIS OF ANIONIC COMPOUNDS
Expected completion date	May 2016
Estimated size (number of pages)	150
Elsevier VAT number	GB 494 6272 12
Permissions price	0.00 USD
VAT/Local Sales Tax	0.00 USD / 0.00 GBP
Total	0.00 USD

ELSEVIER LICENSE TERMS AND CONDITIONS

Mar 03, 2016

This is a License Agreement between Hongyue Guo ("You") and Elsevier ("Elsevier") provided by Copyright Clearance Center ("CCC"). The license consists of your order details, the terms and conditions provided by Elsevier, and the payment terms and conditions.

All payments must be made in full to CCC. For payment instructions, please see information listed at the bottom of this form.

Supplier	Elsevier Limited The Boulevard, Langford Lane Kidlington, Oxford, OX5 1GB, UK
Registered Company Number	1982084
Customer name	Hongyue Guo
Customer address	700 Planetarium Place ARLINGTON, TX 76019
License number	3821120562387
License date	Mar 02, 2016
Licensed content publisher	Elsevier
Licensed content publication	Talanta
Licensed content title	Quantitative analysis of dicamba residues in raw agricultural commodities with the use of ion-pairing reagents in LC-ESI-MS/MS
Licensed content author	Hongyue Guo, Leah S Riter, Chad E Wujcik, Daniel W Armstrong
Licensed content date	1 March 2016
Licensed content volume number	149
Licensed content issue number	n/a
Number of pages	7
Start Page	103
End Page	109
Type of Use	reuse in a thesis/dissertation
Intended publisher of new work	other

Portion	full article
Format	both print and electronic
Are you the author of this Elsevier article?	Yes
Will you be translating?	No
Title of your thesis/dissertation	MECHANISM AND USE OF PAIRED ION ELECTROSPRAY IONIZATION (PIESI) IN HIGH-PERFORMANCE LIQUID CHROMATOGRAPHY-MASS SPECTROMETRY (HPLC-MS) FOR SENSITIVE ANALYSIS OF ANIONIC COMPOUNDS
Expected completion date	May 2016
Estimated size (number of pages)	150
Elsevier VAT number	GB 494 6272 12
Permissions price	0.00 USD
VAT/Local Sales Tax	0.00 USD / 0.00 GBP
Total	0.00 USD

ELSEVIER LICENSE TERMS AND CONDITIONS

Mar 03, 2016

This is a License Agreement between Hongyue Guo ("You") and Elsevier ("Elsevier") provided by Copyright Clearance Center ("CCC"). The license consists of your order details, the terms and conditions provided by Elsevier, and the payment terms and conditions.

All payments must be made in full to CCC. For payment instructions, please see information listed at the bottom of this form.

Supplier	Elsevier Limited The Boulevard, Langford Lane Kidlington, Oxford, OX5 1GB, UK
Registered Company Number	1982084
Customer name	Hongyue Guo
Customer address	700 Planetarium Place ARLINGTON, TX 76019
License number	3821120699857
License date	Mar 02, 2016
Licensed content publisher	Elsevier
Licensed content publication	Analytica Chimica Acta
Licensed content title	Reduced matrix effects for anionic compounds with paired ion electrospray ionization mass spectrometry
Licensed content author	Hongyue Guo, Zachary S. Breitbach, Daniel W. Armstrong
Licensed content date	17 March 2016
Licensed content volume number	912
Licensed content issue number	n/a
Number of pages	11
Start Page	74
End Page	84
Type of Use	reuse in a thesis/dissertation
Intended publisher of new work	other
Portion	full article

Format	both print and electronic
Are you the author of this Elsevier article?	Yes
Will you be translating?	No
Title of your thesis/dissertation	MECHANISM AND USE OF PAIRED ION ELECTROSPRAY IONIZATION (PIESI) IN HIGH-PERFORMANCE LIQUID CHROMATOGRAPHY-MASS SPECTROMETRY (HPLC-MS) FOR SENSITIVE ANALYSIS OF ANIONIC COMPOUNDS
Expected completion date	May 2016
Estimated size (number of pages)	150
Elsevier VAT number	GB 494 6272 12
Permissions price	0.00 USD
VAT/Local Sales Tax	0.00 USD / 0.00 GBP
Total	0.00 USD

References

- (1) Boltz, D. F.; Lambert, J. L. *C R C Critical Reviews in Analytical Chemistry* **1973**, *3*, 147-199.
- (2) Martinelango, P. K.; Anderson, J. L.; Dasgupta, P. K.; Armstrong, D. W.; Al-Horr, R. S.; Slingsby, R. W. *Anal. Chem.* **2005**, *77*, 4829-4835.
- (3) Patsias, J.; Papadopoulou, A.; Papadopoulou-Mourkidou, E. *J. Chromatogr. A* **2001**, *932*, 83-90.
- (4) Luo, B.; Groenke, K.; Takors, R.; Wandrey, C.; Oldiges, M. *J. Chromatogr. A* **2007**, *1147*, 153-164.
- (5) Yang, W.-C.; Sedlak, M.; Regnier, F. E.; Mosier, N.; Ho, N.; Adamec, J. *Anal. Chem.* **2008**, *80*, 9508-9516.
- (6) You, Y.; Uboh, C. E.; Soma, L. R.; Guan, F.; Li, X.; Rudy, J. A.; Chen, J. *Rapid Commun. Mass Spectrom.* **2007**, *21*, 3785-3794.
- (7) Badoud, F.; Grata, E.; Boccard, J.; Guillarme, D.; Veuthey, J.-L.; Rudaz, S.; Saugy, M. *Analytical and Bioanalytical Chemistry* **2011**, *400*, 503-516.
- (8) Fung, Y. S.; Lau, K. M. *ELECTROPHORESIS* **2003**, *24*, 3224-3232.
- (9) Zhu, Y.; Guo, Y.; Ye, M.; James, F. S. *J. Chromatogr. A* **2005**, *1085*, 143-146.
- (10) Grob, M.; Steiner, F. *ELECTROPHORESIS* **2002**, *23*, 1921-1927.
- (11) Im, S. H.; Jeong, Y. H.; Ryoo, J. J. *Anal. Chim. Acta* **2008**, *619*, 129-136.
- (12) Santos, I. C.; Guo, H.; Mesquita, R. B. R.; Rangel, A. O. S. S.; Armstrong, D. W.; Schug, K. A. *Talanta* **2015**, *143*, 320-327.
- (13) López-Ruiz, B. *J. Chromatogr. A* **2000**, *881*, 607-627.
- (14) Cochrane, R. A.; Hillman, D. E. *J. Chromatogr. A* **1982**, *241*, 392-394.
- (15) Haddad, P. R. *Anal. Bioanal. Chem.* **2004**, *379*, 341-343.
- (16) Kuban, P.; Dasgupta, P. K. *J. Sep. Sci.* **2004**, *27*, 1441-1457.
- (17) Miró, M.; Frenzel, W. *Microchimica Acta* **2004**, *148*, 1-20.
- (18) Hansen, E. H.; Wang, J. *Anal. Lett.* **2004**, *37*, 345-359.
- (19) Atienza, J.; Herrero, M. A.; Maquieira, A.; Puchades, R. *Crit. Rev. Anal. Chem.* **1991**, *22*, 331-344.
- (20) Fernandes, C.; Leite, R. S.; Lanças, F. M. *J. Chromatogr. Sci.* **2007**, *45*, 236-241.
- (21) Wamelink, M. M. C.; Struys, E. A.; Huck, J. H. J.; Roos, B.; van der Knaap, M. S.; Jakobs, C.; Verhoeven, N. M. *J. Chromatogr. B* **2005**, *823*, 18-25.
- (22) Soga, T.; Imaizumi, M. *ELECTROPHORESIS* **2001**, *22*, 3418-3425.
- (23) Soga, T.; Ohashi, Y.; Ueno, Y.; Naraoka, H.; Tomita, M.; Nishioka, T. *J. Proteome Res.* **2003**, *2*, 488-494.
- (24) Soga, T.; Ueno, Y.; Naraoka, H.; Ohashi, Y.; Tomita, M.; Nishioka, T. *Anal. Chem.* **2002**, *74*, 2233-2239.
- (25) Dwivedi, P.; Matz, L. M.; Atkinson, D. A.; Hill, J. H. H. *Analyst* **2004**, *129*, 139-144.
- (26) Guo, H.; Riter, L. S.; Wujcik, C. E.; Armstrong, D. W. *Talanta* **2016**, *149*, 103-109.
- (27) Cech, N. B.; Enke, C. G. *Mass Spectrom. Rev.* **2001**, *20*, 362-387.
- (28) Soukup-Hein, R. J.; Remsburg, J. W.; Dasgupta, P. K.; Armstrong, D. W. *Anal. Chem.* **2007**, *79*, 7346-7352.
- (29) Remsburg, J. W.; Soukup-Hein, R. J.; Crank, J. A.; Breitbach, Z. S.; Payagala, T.; Armstrong, D. W. *J. Am. Soc. Mass. Spectrom.* **2008**, *19*, 261-269.
- (30) Straub, R. F.; Voyksner, R. D. *J. Am. Soc. Mass. Spectrom.* **1993**, *4*, 578-587.
- (31) Xu, C.; Armstrong, D. W. *Anal. Chim. Acta* **2013**, *792*, 1-9.
- (32) Henriksen, T.; Juhler, R. K.; Svensmark, B.; Cech, N. B. *J. Am. Soc. Mass. Spectrom.* **2005**, *16*, 446-455.

- (33) Warnke, M. M.; Breitbach, Z. S.; Dodbiba, E.; Wanigasekara, E.; Zhang, X.; Sharma, P.; Armstrong, D. W. *J. Am. Soc. Mass. Spectrom.* **2009**, *20*, 529-538.
- (34) Soukup-Hein, R. J.; Remsburg, J. W.; Breitbach, Z. S.; Sharma, P. S.; Payagala, T.; Wanigasekara, E.; Huang, J.; Armstrong, D. W. *Anal. Chem.* **2008**, *80*, 2612-2616.
- (35) Dodbiba, E.; Breitbach, Z. S.; Wanigasekara, E.; Payagala, T.; Zhang, X.; Armstrong, D. W. *Anal. Bioanal. Chem.* **2010**, *398*, 367-376.
- (36) Dodbiba, E.; Xu, C.; Payagala, T.; Wanigasekara, E.; Moon, M. H.; Armstrong, D. W. *Analyst* **2011**, *136*, 1586-1593.
- (37) Breitbach, Z. S.; Wanigasekara, E.; Dodbiba, E.; Schug, K. A.; Armstrong, D. W. *Anal. Chem.* **2010**, *82*, 9066-9073.
- (38) Kebarle, P.; Verkerk, U. H. *Mass Spectrom. Rev.* **2009**, *28*, 898-917.
- (39) Eksborg, S.; Lagerström, P.-O.; Modin, R.; Schill, G. *J. Chromatogr. A* **1973**, *83*, 99-110.
- (40) Michopoulos, F.; Whalley, N.; Theodoridis, G.; Wilson, I. D.; Dunkley, T. P. J.; Critchlow, S. E. *J. Chromatogr. A* **2014**, *1349*, 60-68.
- (41) Anderson, J. L.; Ding, R.; Ellern, A.; Armstrong, D. W. *J. Am. Chem. Soc.* **2005**, *127*, 593-604.
- (42) Kirk, A. B.; Martinelango, P. K.; Tian, K.; Dutta, A.; Smith, E. E.; Dasgupta, P. K. *Environmental Science & Technology* **2005**, *39*, 2011-2017.
- (43) Martinelango, P. K.; Gümüş, G.; Dasgupta, P. K. *Anal. Chim. Acta* **2006**, *567*, 79-86.
- (44) Martinelango, P. K.; Dasgupta, P. K. *Anal. Chem.* **2007**, *79*, 7198-7200.
- (45) Breitbach, Z. S.; Warnke, M. M.; Wanigasekara, E.; Zhang, X.; Armstrong, D. W. *Anal. Chem.* **2008**, *80*, 8828-8834.
- (46) Zhang, X.; Wanigasekara, E.; Breitbach, Z. S.; Dodbiba, E.; Armstrong, D. W. *Rapid Commun. Mass Spectrom.* **2010**, *24*, 1113-1123.
- (47) Xu, C.; Pinto, E. C.; Armstrong, D. W. *Analyst* **2014**, *139*, 4169-4175.
- (48) Xu, C.; Dodbiba, E.; Padivitage, N. L. T.; Breitbach, Z. S.; Armstrong, D. W. *Rapid Commun. Mass Spectrom.* **2012**, *26*, 2885-2896.
- (49) Dodbiba, E.; Xu, C.; Wanigasekara, E.; Armstrong, D. W. *Rapid Commun. Mass Spectrom.* **2012**, *26*, 1005-1013.
- (50) Taylor, G. *Proceedings of the Royal Society of London A: Mathematical, Physical and Engineering Sciences* **1964**, *280*, 383-397.
- (51) Taflin, D. C.; Ward, T. L.; Davis, E. J. *Langmuir* **1989**, *5*, 376-384.
- (52) Iribarne, J. V.; Thomson, B. A. *The Journal of Chemical Physics* **1976**, *64*, 2287-2294.
- (53) Dole, M.; Mack, L. L.; Hines, R. L.; Mobley, R. C.; Ferguson, L. D.; Alice, M. B. *The Journal of Chemical Physics* **1968**, *49*, 2240-2249.
- (54) Zhou, S.; Cook, K. D. *J. Am. Soc. Mass. Spectrom.* **2001**, *12*, 206-214.
- (55) Kebarle, P.; Tang, L. *Anal. Chem.* **1993**, *65*, 972A-986A.
- (56) Fenn, J. B. *J. Am. Soc. Mass. Spectrom.* **1993**, *4*, 524-535.
- (57) Tang, L.; Kebarle, P. *Anal. Chem.* **1993**, *65*, 3654-3668.
- (58) Iribarne, J. V.; Dziedzic, P. J.; Thomson, B. A. *International Journal of Mass Spectrometry and Ion Physics* **1983**, *50*, 331-347.
- (59) Cech, N. B.; Krone, J. R.; Enke, C. G. *Anal. Chem.* **2001**, *73*, 208-213.
- (60) Tang, K.; Smith, R. D. *J. Am. Soc. Mass. Spectrom.* **2001**, *12*, 343-347.
- (61) Cech, N. B.; Enke, C. G. *Anal. Chem.* **2000**, *72*, 2717-2723.
- (62) Cech, N. B.; Enke, C. G. *Anal. Chem.* **2001**, *73*, 4632-4639.
- (63) Enke, C. G. *Anal. Chem.* **1997**, *69*, 4885-4893.
- (64) Annesley, T. M. *Clin. Chem.* **2003**, *49*, 1041-1044.
- (65) Yamashita, M.; Fenn, J. B. *J. Phys. Chem.* **1984**, *88*, 4451-4459.

- (66) Yamashita, M.; Fenn, J. B. *J. Phys. Chem.* **1984**, *88*, 4671-4675.
- (67) Whitehouse, C. M.; Dreyer, R. N.; Yamashita, M.; Fenn, J. B. *Anal. Chem.* **1985**, *57*, 675-679.
- (68) Fenn, J.; Mann, M.; Meng, C.; Wong, S.; Whitehouse, C. *Science* **1989**, *246*, 64-71.
- (69) Loo, J. A. *Mass Spectrom. Rev.* **1997**, *16*, 1-23.
- (70) Katta, V.; Chait, B. T. *J. Am. Chem. Soc.* **1993**, *115*, 6317-6321.
- (71) McEwen, C. N.; Simonsick, W. J.; Larsen, B. S.; Ute, K.; Hatada, K. *J. Am. Soc. Mass. Spectrom.* **1995**, *6*, 906-911.
- (72) Hop, C. E. C. A.; Bakhtiar, R. *J. Chem. Educ.* **1996**, *73*, A162.
- (73) Beck, J. L.; Colgrave, M. L.; Ralph, S. F.; Sheil, M. M. *Mass Spectrom. Rev.* **2001**, *20*, 61-87.
- (74) Brugger, B.; Erben, G.; Sandhoff, R.; Wieland, F. T.; Lehmann, W. D. *Proceedings of the National Academy of Sciences of the United States of America* **1997**, *94*, 2339-2344.
- (75) Hsu, F. F.; Bohrer, A.; Turk, J. *J. Am. Soc. Mass. Spectrom.* **1998**, *9*, 516-526.
- (76) Lu, W.; Yang, G.; Cole, R. B. *ELECTROPHORESIS* **1995**, *16*, 487-492.
- (77) Schultz, C. L.; Moini, M. *Anal. Chem.* **2003**, *75*, 1508-1513.
- (78) Cole, R. B.; Zhu, J. *Rapid Commun. Mass Spectrom.* **1999**, *13*, 607-611.
- (79) Cole, R. B.; Harrata, A. K. *Rapid Commun. Mass Spectrom.* **1992**, *6*, 536-539.
- (80) Cole, R. B.; Harrata, A. K. *J. Am. Soc. Mass. Spectrom.* **1993**, *4*, 546-556.
- (81) Breitbach, Z. S.; Berthod, A.; Huang, K.; Armstrong, D. W. *Mass Spectrom. Rev.* **2016**, *35*, 201-218.
- (82) Kappes, T.; Schnierle, P.; Hauser, P. C. *Anal. Chim. Acta* **1997**, *350*, 141-147.
- (83) Isildak, I.; Asan, A. *Talanta* **1999**, *48*, 967-978.
- (84) Gjerde, D. T.; Fritz, J. S.; Schmuckler, G. *J. Chromatogr. A* **1979**, *186*, 509-519.
- (85) Kuban, P.; Hauser, P. C. *Anal. Chim. Acta* **2008**, *607*, 15-29.
- (86) Harwood, J. J.; Wen, S. *J. Chromatogr. A* **1997**, *788*, 105-111.
- (87) Tak, V.; Purhoit, A.; Pardasani, D.; Garg, P.; Jain, R.; Dubey, D. K. *Rapid Commun. Mass Spectrom.* **2012**, *26*, 2637-2648.
- (88) Kornahrens, H.; Cook, K. D.; Armstrong, D. W. *Anal. Chem.* **1982**, *54*, 1325-1329.
- (89) Rundlett, K. L.; Armstrong, D. W. *Anal. Chem.* **1996**, *68*, 3493-3497.
- (90) Armstrong, D. W.; Hinzet, W. L.; Bui, K. H.; Singh, H. N. *Anal. Lett.* **1981**, *14*, 1659-1667.
- (91) Sherman, C. L.; Brodbelt, J. S. *Anal. Chem.* **2003**, *75*, 1828-1836.
- (92) Sherman, C. L.; Brodbelt, J. S. *Anal. Chem.* **2005**, *77*, 2512-2523.
- (93) Thomson, B. A.; Iribarne, J. V. *The Journal of Chemical Physics* **1979**, *71*, 4451-4463.
- (94) Menger, F. M.; Littau, C. A. *J. Am. Chem. Soc.* **1993**, *115*, 10083-10090.
- (95) Menger, F. M.; Bian, J.; Sizova, E.; Martinson, D. E.; Seredyuk, V. A. *Org. Lett.* **2004**, *6*, 261-264.
- (96) Fiehn, O.; Kopka, J.; Dormann, P.; Altmann, T.; Trethewey, R. N.; Willmitzer, L. *Nat Biotech* **2000**, *18*, 1157-1161.
- (97) Fiehn, O. *Comparative and Functional Genomics* **2001**, *2*, 155-168.
- (98) Raamsdonk, L. M.; Teusink, B.; Broadhurst, D.; Zhang, N.; Hayes, A.; Walsh, M. C.; Berden, J. A.; Brindle, K. M.; Kell, D. B.; Rowland, J. J.; Westerhoff, H. V.; van Dam, K.; Oliver, S. G. *Nat Biotech* **2001**, *19*, 45-50.
- (99) Buescher, J. M.; Moco, S.; Sauer, U.; Zamboni, N. *Anal. Chem.* **2010**, *82*, 4403-4412.
- (100) Shimizu, K. *Metabolites* **2014**, *4*, 1-35.
- (101) Huck, J. H. J.; Verhoeven, N. M.; Struys, E. A.; Salomons, G. S.; Jakobs, C.; van der Knaap, M. S. *Am. J. Hum. Genet.* **2004**, *74*, 745-751.

- (102) Verhoeven, N. M.; Huck, J. H. J.; Roos, B.; Struys, E. A.; Salomons, G. S.; Douwes, A. C.; van der Knaap, M. S.; Jakobs, C. *Am. J. Hum. Genet.* **2001**, *68*, 1086-1092.
- (103) Hinterwirth, H.; Lämmerhofer, M.; Preinerstorfer, B.; Gargano, A.; Reischl, R.; Bicker, W.; Trapp, O.; Brecker, L.; Lindner, W. *J. Sep. Sci.* **2010**, *33*, 3273-3282.
- (104) Ruijter, G. J. G.; Visser, J. *J. Microbiol. Methods* **1996**, *25*, 295-302.
- (105) Theobald, U.; Mailinger, W.; Baltus, M.; Rizzi, M.; Reuss, M. *Biotechnol. Bioeng.* **1997**, *55*, 305-316.
- (106) Stitt, M.; Fernie, A. R. *Curr. Opin. Biotechnol.* **2003**, *14*, 136-144.
- (107) Fiehn, O.; Kopka, J.; Trethewey, R. N.; Willmitzer, L. *Anal. Chem.* **2000**, *72*, 3573-3580.
- (108) Kanani, H.; Chrysanthopoulos, P. K.; Klapa, M. I. *J. Chromatogr. B* **2008**, *871*, 191-201.
- (109) Sato, S.; Soga, T.; Nishioka, T.; Tomita, M. *The Plant Journal* **2004**, *40*, 151-163.
- (110) Monton, M. R. N.; Soga, T. *J. Chromatogr. A* **2007**, *1168*, 237-246.
- (111) Smits, H. P.; Cohen, A.; Buttler, T.; Nielsen, J.; Olsson, L. *Anal. Biochem.* **1998**, *261*, 36-42.
- (112) Picioreanu, S.; Poels, I.; Frank, J.; van Dam, J. C.; van Dedem, G. W. K.; Nagels, L. *J. Anal. Chem.* **2000**, *72*, 2029-2034.
- (113) Bhattacharya, M.; Fuhrman, L.; Ingram, A.; Nickerson, K. W.; Conway, T. *Anal. Biochem.* **1995**, *232*, 98-106.
- (114) Ritter, J. B.; Genzel, Y.; Reichl, U. *J. Chromatogr. B* **2006**, *843*, 216-226.
- (115) Niessen, W. M. A. *J. Chromatogr. A* **1999**, *856*, 179-197.
- (116) van der Ham, M.; Prinsen, B. H. C. M. T.; Huijmans, J. G. M.; Abeling, N. G. G. M.; Dorland, B.; Berger, R.; de Koning, T. J.; de Sain-van der Velden, M. G. M. *J. Chromatogr. B* **2007**, *848*, 251-257.
- (117) Kebarle, P.; Verkerk, U. H. In *Electrospray and MALDI Mass Spectrometry*; John Wiley & Sons, Inc., 2010, pp 1-48.
- (118) Guo, H.; Dolzan, M. D.; Spudeit, D. A.; Xu, C.; Breitbach, Z. S.; Sreenivasan, U.; Armstrong, D. W. *Int. J. Mass spectrom.* **2015**, *389*, 14-25.
- (119) Xu, C.; Guo, H.; Breitbach, Z. S.; Armstrong, D. W. *Anal. Chem.* **2014**, *86*, 2665-2672.
- (120) Armstrong, D. W.; Tang, Y.; Chen, S.; Zhou, Y.; Bagwill, C.; Chen, J.-R. *Anal. Chem.* **1994**, *66*, 1473-1484.
- (121) Berthod, A.; Chen, X.; Kullman, J. P.; Armstrong, D. W.; Gasparrini, F.; D'Acquaric, I.; Villani, C.; Carotti, A. *Anal. Chem.* **2000**, *72*, 1767-1780.
- (122) Tebani, A.; Schlemmer, D.; Imbard, A.; Rigal, O.; Porquet, D.; Benoist, J.-F. *J. Chromatogr. B* **2011**, *879*, 3694-3699.
- (123) Bajad, S. U.; Lu, W.; Kimball, E. H.; Yuan, J.; Peterson, C.; Rabinowitz, J. D. *J. Chromatogr. A* **2006**, *1125*, 76-88.
- (124) van der Ham, M.; de Koning, T. J.; Lefeber, D.; Fleer, A.; Prinsen, B. H. C. M. T.; de Sain-van der Velden, M. G. M. *J. Chromatogr. B* **2010**, *878*, 1098-1102.
- (125) Kloos, D.; Derks, R. J. E.; Wijtmans, M.; Lingeman, H.; Mayboroda, O. A.; Deelder, A. M.; Niessen, W. M. A.; Giera, M. *J. Chromatogr. A* **2012**, *1232*, 19-26.
- (126) Huck, J. H. J.; Struys, E. A.; Verhoeven, N. M.; Jakobs, C.; van der Knaap, M. S. *Clin. Chem.* **2003**, *49*, 1375-1380.
- (127) Cruz, J. A.; Emery, C.; Wüst, M.; Kramer, D. M.; Lange, B. M. *The Plant Journal* **2008**, *55*, 1047-1060.
- (128) Desai, M. J.; Armstrong, D. W. *J. Chromatogr. A* **2004**, *1035*, 203-210.
- (129) Verstraete, A. G. *Ther. Drug Monit.* **2004**, *26*, 200-205.

- (130) Reiter, A.; Hake, J.; Meissner, C.; Rohwer, J.; Friedrich, H. J.; Oehmichen, M. *Forensic Sci. Int.* **2001**, *119*, 248-253.
- (131) Kim, I.; Oyler, J. M.; Moolchan, E. T.; Cone, E. J.; Huestis, M. A. *Ther. Drug Monit.* **2004**, *26*, 664-672.
- (132) Kim, I.; Barnes, A. J.; Oyler, J. M.; Schepers, R.; Joseph, R. E., Jr.; Cone, E. J.; Lafko, D.; Moolchan, E. T.; Huestis, M. A. *Clin. Chem.* **2002**, *48*, 1486-1496.
- (133) Scheidweiler, K. B.; Spargo, E. A.; Kelly, T. L.; Cone, E. J.; Barnes, A. J.; Huestis, M. A. *Ther. Drug Monit.* **2010**, *32*, 628-637.
- (134) Baumann, M. H.; Zolkowska, D.; Kim, I.; Scheidweiler, K. B.; Rothman, R. B.; Huestis, M. A. *Drug metabolism and disposition: the biological fate of chemicals* **2009**, *37*, 2163-2170.
- (135) Schwaninger, A. E.; Meyer, M. R.; Barnes, A. J.; Kolbrich-Spargo, E. A.; Gorelick, D. A.; Goodwin, R. S.; Huestis, M. A.; Maurer, H. H. *Biochem. Pharmacol.* **2012**, *83*, 131-138.
- (136) Wainer, I. W.; Dekker, 1993, pp 424-pp.
- (137) Tozer, T. N., Rowland M. *Introduction to Pharmacokinetics and Pharmacodynamics: The Quantitative Basis of Drug Therapy*; Lippincott, Williams & Wilkins, : Philadelphia, 2006.
- (138) Mangoni, A. A.; Jackson, S. H. *British journal of clinical pharmacology* **2004**, *57*, 6-14.
- (139) Anderson, G. D. *Journal of women's health* **2005**, *14*, 19-29.
- (140) Iwata, J.; Suga, T. *Clin. Chem.* **1989**, *35*, 794-799.
- (141) Bowers, L. D. *Clin. Chem.* **1997**, *43*, 1299-1304.
- (142) Bowers, L. D.; Sanallah. *Journal of chromatography. B, Biomedical applications* **1996**, *687*, 61-68.
- (143) Borts, D. J.; Bowers, L. D. *J. Mass Spectrom.* **2000**, *35*, 50-61.
- (144) Kuuranne, T.; Vahermo, M.; Leinonen, A.; Kostianen, R. *J. Am. Soc. Mass Spectrom.* **2000**, *11*, 722-730.
- (145) Ismail, A. A.; Walker, P. L.; Cawood, M. L.; Barth, J. H. *Ann. Clin. Biochem.* **2002**, *39*, 366-373.
- (146) Maralikova, B.; Weinmann, W. *Journal of chromatography. B, Analytical technologies in the biomedical and life sciences* **2004**, *811*, 21-30.
- (147) Kushnir, M. M.; Neilson, R.; Roberts, W. L.; Rockwood, A. L. *Clin. Biochem.* **2004**, *37*, 357-362.
- (148) Catlin, D. H.; Sekera, M. H.; Ahrens, B. D.; Starcevic, B.; Chang, Y. C.; Hatton, C. K. *Rapid Commun. Mass Spectrom.* **2004**, *18*, 1245-1049.
- (149) Sekera, M. H.; Ahrens, B. D.; Chang, Y. C.; Starcevic, B.; Georgakopoulos, C.; Catlin, D. H. *Rapid Commun. Mass Spectrom.* **2005**, *19*, 781-784.
- (150) Guo, T.; Taylor, R. L.; Singh, R. J.; Soldin, S. J. *Clin. Chim. Acta* **2006**, *372*, 76-82.
- (151) Kushnir, M. M.; Rockwood, A. L.; Roberts, W. L.; Pattison, E. G.; Owen, W. E.; Bunker, A. M.; Meikle, A. W. *Clin. Chem.* **2006**, *52*, 1559-1567.
- (152) Georgakopoulos, C. G.; Vonaparti, A.; Stamou, M.; Kiouisi, P.; Lyris, E.; Angelis, Y. S.; Tsoupras, G.; Wuest, B.; Nielen, M. W.; Panderi, I.; Koupparis, M. *Rapid Commun. Mass Spectrom.* **2007**, *21*, 2439-2446.
- (153) Kushnir, M. M.; Rockwood, A. L.; Bergquist, J.; Varshavsky, M.; Roberts, W. L.; Yue, B.; Bunker, A. M.; Meikle, A. W. *American journal of clinical pathology* **2008**, *129*, 530-539.
- (154) Pozo, O. J.; Van Eenoo, P.; Van Thuyne, W.; Deventer, K.; Delbeke, F. T. *J. Chromatogr. A* **2008**, *1183*, 108-118.

- (155) Strahm, E.; Kohler, I.; Rudaz, S.; Martel, S.; Carrupt, P. A.; Veuthey, J. L.; Saugy, M.; Saudan, C. *J. Chromatogr. A* **2008**, *1196-1197*, 153-160.
- (156) Pozo, O. J.; Van Eenoo, P.; Deventer, K.; Elbardissy, H.; Grimalt, S.; Sancho, J. V.; Hernandez, F.; Ventura, R.; Delbeke, F. T. *Anal. Chim. Acta* **2011**, *684*, 98-111.
- (157) Badoud, F.; Grata, E.; Boccard, J.; Guillarme, D.; Veuthey, J. L.; Rudaz, S.; Saugy, M. *Anal. Bioanal. Chem.* **2011**, *400*, 503-516.
- (158) Boccard, J.; Badoud, F.; Grata, E.; Ouertani, S.; Hanafi, M.; Mazerolles, G.; Lanteri, P.; Veuthey, J. L.; Saugy, M.; Rudaz, S. *Forensic Sci. Int.* **2011**, *213*, 85-94.
- (159) Guinan, T.; Ronci, M.; Kobus, H.; Voelcker, N. H. *Talanta* **2012**, *99*, 791-798.
- (160) Badoud, F.; Boccard, J.; Schweizer, C.; Pralong, F.; Saugy, M.; Baume, N. *J. Steroid Biochem. Mol. Biol.* **2013**, *138*, 222-235.
- (161) Lacey, J. M.; Minutti, C. Z.; Magera, M. J.; Tauscher, A. L.; Casetta, B.; McCann, M.; Lymp, J.; Hahn, S. H.; Rinaldo, P.; Matern, D. *Clin. Chem.* **2004**, *50*, 621-625.
- (162) Ionita, I. A.; Fast, D. M.; Akhlaghi, F. *Journal of chromatography. B, Analytical technologies in the biomedical and life sciences* **2009**, *877*, 765-772.
- (163) Singh, R. J. *Steroids* **2008**, *73*, 1339-1344.
- (164) Rauh, M.; Groschl, M.; Rascher, W.; Dorr, H. G. *Steroids* **2006**, *71*, 450-458.
- (165) Carvalho, V. M.; Nakamura, O. H.; Vieira, J. G. *Journal of chromatography. B, Analytical technologies in the biomedical and life sciences* **2008**, *872*, 154-161.
- (166) Thomas, A.; Sigmund, G.; Guddat, S.; Schanzer, W.; Thevis, M. *Eur J Mass Spectrom (Chichester, Eng)* **2008**, *14*, 135-143.
- (167) Bijlsma, L.; Sancho, J. V.; Hernandez, F.; Niessen, W. M. *J. Mass Spectrom.* **2011**, *46*, 865-875.
- (168) Murray, G. J.; Danaceau, J. P. *Journal of chromatography. B, Analytical technologies in the biomedical and life sciences* **2009**, *877*, 3857-3864.
- (169) Berset, J. D.; Brenneisen, R.; Mathieu, C. *Chemosphere* **2010**, *81*, 859-866.
- (170) Athanasiadou, I.; Angelis, Y. S.; Lyris, E.; Georgakopoulos, C. *Trac-Trend Anal Chem* **2013**, *42*, 137-156.
- (171) Buiarelli, F.; Coccioli, F.; Merolle, M.; Neri, B.; Terracciano, A. *Anal. Chim. Acta* **2004**, *526*, 113-120.
- (172) Kushnir, M. M.; Rockwood, A. L.; Roberts, W. L.; Yue, B.; Bergquist, J.; Meikle, A. W. *Clin. Biochem.* **2011**, *44*, 77-88.
- (173) Field, J. A.; Field, T. M.; Poiger, T.; Giger, W. *Environ. Sci. Technol.* **1994**, *28*, 497-503.
- (174) Shackleton, C. *J. Steroid Biochem. Mol. Biol.* **2010**, *121*, 481-490.
- (175) Fabregat, A.; Pozo, O. J.; Marcos, J.; Segura, J.; Ventura, R. *Anal. Chem.* **2013**, *85*, 5005-5014.
- (176) Yu, J. T.; Bisceglia, K. J.; Bouwer, E. J.; Roberts, A. L.; Coelhan, M. *Anal. Bioanal. Chem.* **2012**, *403*, 583-591.
- (177) Jia, Q.; Hong, M. F.; Pan, Z. X.; Orndorff, S. *Journal of chromatography. B, Biomedical sciences and applications* **2001**, *750*, 81-91.
- (178) Sjoqvist, F.; Garle, M.; Rane, A. *Lancet* **2008**, *371*, 1872-1882.
- (179) Database, G. M., 2015.
- (180) Koesukwivat, U.; Sanguankaew, K.; Leepipatpiboon, N. *Anal. Chim. Acta* **2008**, *626*, 10-20.
- (181) Agency, E. P.
- (182) Sandmann, E. R.; Loos, M. A.; van Dyk, L. P. *Rev. Environ. Contam. Toxicol.* **1988**, *101*, 1-53.
- (183) Thurman, E. M.; Meyer, M.; Pomes, M.; Perry, C. A.; Schwab, A. P. *Anal. Chem.* **1990**, *62*, 2043-2048.

- (184) Clegg, B. S.; Stephenson, G. R.; Hall, J. C. *J. Agric. Food. Chem.* **2001**, *49*, 2168-2174.
- (185) Lanças, F. M.; Rissato, S. R.; Galhiane, M. S. *Chromatographia* **1999**, *50*, 35-40.
- (186) LUCAS-DELFA; A., M.; PEREZ-ARRIBAS; V., L.; NAVARRO-VILLOSLADA; F.; LEON-GONZALEZ; E., M.; POLO-DIEZ; M., L. *Determination of chlorophenoxy acid and dicamba herbicide residues by capillary reversed-phase liquid chromatography*; Taylor & Francis: Colchester, ROYAUME-UNI, 2000; Vol. 23.
- (187) Voos, G.; Groffman, P. M.; Pfeil, M. *J. Agric. Food Chem.* **1994**, *42*, 2502-2507.
- (188) Díez, C.; Traag, W. A.; Zommer, P.; Marinero, P.; Atienza, J. *J. Chromatogr. A* **2006**, *1131*, 11-23.
- (189) Bogialli, S.; Curini, R.; Di Corcia, A.; Laganà, A.; Stabile, A.; Sturchio, E. *J. Chromatogr. A* **2006**, *1102*, 1-10.
- (190) Shin, E.-H.; Choi, J.-H.; Abd El-Aty, A. M.; Khay, S.; Kim, S.-J.; Im, M. H.; Kwon, C.-H.; Shim, J.-H. *Biomed. Chromatogr.* **2011**, *25*, 124-135.
- (191) Alder, L.; Greulich, K.; Kempe, G.; Vieth, B. *Mass Spectrom. Rev.* **2006**, *25*, 838-865.
- (192) Zoellner, P.; Leitner, A.; Jodlbauer, J.; Mayer, B. X.; Linder, W. *LC-GC Eur.* **2003**, *16*, 354, 356, 358, 360, 362.
- (193) Commission, E., 2010.
- (194) Riter, L. S.; Lynn, K. J.; Wujcik, C. E.; Buchholz, L. M. *J. Agric. Food. Chem.* **2015**, *63*, 4405-4408.
- (195) Riter, L. H., W.; Allan, J.; Hua, F.; South, S.; Howard, D.; Wujcik, C.. In *61st American Society of Mass Spectrometry*; Minneapolis, MN, 2013.
- (196) Dams, R.; Huestis, M. A.; Lambert, W. E.; Murphy, C. M. *J. Am. Soc. Mass Spectrom.* **2003**, *14*, 1290-1294.
- (197) Pascoe, R.; Foley, J. P.; Gusev, A. I. *Anal. Chem.* **2001**, *73*, 6014-6023.
- (198) Matuszewski, B. K.; Constanzer, M. L.; Chavez-Eng, C. M. *Anal. Chem.* **2003**, *75*, 3019-3030.
- (199) Van Eeckhaut, A.; Lanckmans, K.; Sarre, S.; Smolders, I.; Michotte, Y. *J. Chromatogr. B* **2009**, *877*, 2198-2207.
- (200) Remane, D.; Meyer, M. R.; Wissenbach, D. K.; Maurer, H. H. *Rapid Commun. Mass Spectrom.* **2010**, *24*, 3103-3108.
- (201) Benijts, T.; Dams, R.; Lambert, W.; De Leenheer, A. *J. Chromatogr. A* **2004**, *1029*, 153-159.
- (202) Fu, I.; Woolf, E. J.; Matuszewski, B. K. *J. Pharm. Biomed. Anal.* **1998**, *18*, 347-357.
- (203) Mei, H.; Hsieh, Y.; Nardo, C.; Xu, X.; Wang, S.; Ng, K.; Korfmacher, W. A. *Rapid Commun. Mass Spectrom.* **2003**, *17*, 97-103.
- (204) Taylor, P. J. *Clin. Biochem.* **2005**, *38*, 328-334.
- (205) Shah, V. P.; Midha, K. K.; Findlay, J. W.; Hill, H. M.; Hulse, J. D.; McGilveray, I. J.; McKay, G.; Miller, K. J.; Patnaik, R. N.; Powell, M. L.; Tonelli, A.; Viswanathan, C. T.; Yacobi, A. *Pharm. Res.* **2000**, *17*, 1551-1557.
- (206) SERVICES, D. O. H. A. H.; Administration, F. a. D. In *Federal Register Volume 66, Issue 100 (May 23, 2001)*, AND, D. O. H.; SERVICES, H.; Administration, F. a. D., Eds.; Office of the Federal Register, National Archives and Records Administration, 2001, pp 28526-28527.
- (207) Mallet, C. R.; Lu, Z.; Mazzeo, J. R. *Rapid Commun. Mass Spectrom.* **2004**, *18*, 49-58.
- (208) Jessome, L. L.; Volmer, D. A. *LC-GC North America* **2006**, *24*, 498-510.
- (209) Bruins, A. P. *J. Chromatogr. A* **1998**, *794*, 345-357.

- (210) Bruins, C. H. P.; Jeronimus-Stratingh, C. M.; Ensing, K.; van Dongen, W. D.; de Jong, G. J. *J. Chromatogr. A* **1999**, *863*, 115-122.
- (211) Antignac, J.-P.; de Wasch, K.; Monteau, F.; De Brabander, H.; Andre, F.; Le Bizec, B. *Anal. Chim. Acta* **2005**, *529*, 129-136.
- (212) King, R.; Bonfiglio, R.; Fernandez-Metzler, C.; Miller-Stein, C.; Olah, T. *J. Am. Soc. Mass. Spectrom.* **2000**, *11*, 942-950.
- (213) Ferrer, C.; Lozano, A.; Aguera, A.; Giron, A. J.; Fernandez-Alba, A. R. *J. Chromatogr. A* **2011**, *1218*, 7634-7639.
- (214) Siegel, D.; Permentier, H.; Reijngoud, D.-J.; Bischoff, R. *J. Chromatogr. B* **2014**, *966*, 21-33.
- (215) Du, L.; White, R. L. *Rapid Commun. Mass Spectrom.* **2008**, *22*, 3362-3370.
- (216) Pucci, V.; Di Palma, S.; Alfieri, A.; Bonelli, F.; Monteagudo, E. *J. Pharm. Biomed. Anal.* **2009**, *50*, 867-871.
- (217) Liao, H. W.; Chen, G. Y.; Tsai, I. L.; Kuo, C. H. *J. Chromatogr. A* **2014**, *1327*, 97-104.
- (218) Holčapek, M.; Volná, K.; Jandera, P.; Kolářová, L.; Lemr, K.; Exner, M.; Církva, A. *J. Mass Spectrom.* **2004**, *39*, 43-50.
- (219) Gao, Y.; Yang, J.; Cancellia, M. T.; Meng, F.; McLuckey, S. A. *Anal. Chem.* **2013**, *85*, 4713-4720.
- (220) Duan, J.; Li, W.; Sun, P.; Lai, Q.; Mulcahy, D.; Guo, S. *Anal. Lett.* **2013**, *46*, 569-588.
- (221) Heberer, T. *Journal of Hydrology* **2002**, *266*, 175-189.
- (222) Takino, M.; Daishima, S.; Nakahara, T. *Rapid Commun. Mass Spectrom.* **2003**, *17*, 383-390.
- (223) Köck-Schulmeyer, M.; Olmos, M.; López de Alda, M.; Barceló, D. *J. Chromatogr. A* **2013**, *1305*, 176-187.
- (224) Brooks, T.; Keevil, C. W. *Lett. Appl. Microbiol.* **1997**, *24*, 203-206.
- (225) Qafoku, N.; Brown, C. F.; Wang, G.; Sullivan, E. C.; Lawter, A. R.; Harvey, O. R.; Bowden, M., Geochemical Impacts of Leaking CO₂ from Subsurface Storage Reservoirs to Unconfined and Confined Aquifers; PNNL-22420; Other: AA9010200 United States10.2172/1079744Other: AA9010200Thu Dec 05 08:06:45 EST 2013PNNLEnglish2013.
- (226) Harris, D. C. *Quantitative Chemical Analysis, Sixth Edition*; W. H. Freeman, 2003.
- (227) Koester, C. J.; Beller, H. R.; Halden, R. U. *Environmental Science & Technology* **2000**, *34*, 1862-1864.
- (228) Kang, J.; Hick, L. A.; Price, W. E. *Rapid Commun. Mass Spectrom.* **2007**, *21*, 4065-4072.
- (229) Constantopoulos, T.; Jackson, G.; Enke, C. *J. Am. Soc. Mass. Spectrom.* **1999**, *10*, 625-634.
- (230) Armstrong, D. W.; Lafranchise, F.; Young, D. *Anal. Chim. Acta* **1982**, *135*, 165-168.

Biographical Information

Hongyue Guo received his M.S. degree in Pharmaceutical Engineering in 2012 from East China University of Science and Technology in China. His Research area focused on development and synthesis of novel hydrophilic interaction liquid chromatographic (HILIC) stationary phases for separations of Traditional Chinese Medicine in the master degree program. He obtained his Ph.D. in Analytical Chemistry at The University of Texas at Arlington under the supervision of Prof. Daniel W. Armstrong. His Research focuses on novel applications of paired ion electrospray ionization (PIESI) mass spectrometry in trace analysis of biologically, environmentally, pharmaceutically and clinically challenging anionic compounds. His research also involves in chiral analysis of pharmaceutical drugs at trace levels with LC-MS.